PETROGRAPHIC STUDY OF ELEVEN SAMPLES RECOVERED FROM THE NAHANNI FORMATION AT WELL LOCATION TEXACO BOVIE LAKE J-72 300/J-72-6020-12245/0

Northwest Territories Geological Survey
Work Order No. 20A20309

March, 2020

AGAT Laboratories
3801 – 21st Street N.E.
Calgary, Alberta T2E 6T5

AGAT Laboratories

SERVICE BEYOND ANALYSIS

TABLE OF CONTENTS

EXECUTIVE SUMMARY

The purpose of this study is to describe the observed lithological characteristics, associated reservoir quality and fluid sensitivity of eleven petrographic samples collected from the Nahanni Formation at well location TEXACO BOVIE LAKE J-72 300/J-72-6020-12245/0. Petrographic analyses and interpretations are based on the observation of thin section and SEM samples generated from core, while XRD analyses were also completed and confirm mineralogy and clay types. An overview of general sample information can be found below within **Table A:**

TS/SEM Sample ID	Depth (ft/m)	Formation	Rock Classification	Analysis (*)	Reservoir Quality (*)
Location: Texaco Bovie Lake J-72 300/J-72-6020-12245/0					
X31	9598.70ft/ 2925.68m	Nahanni	N/A	XRD	N/A
X30	9602.80ft/ 2926.93m	Nahanni	N/A	XRD	N/A
T11,S11,X29	9609.75ft/ 2929.05m	Nahanni	Silty Shale	TS; SEM; XRD	VP
X28	9612.60ft/ 2929.92m	Nahanni	N/A	XRD	N/A
X27	9619.10ft/ 2931.90m	Nahanni	N/A	XRD	N/A
X26	9620.50ft/ 2932.33m	Nahanni	N/A	XRD	N/A
T10,S10	9627.60ft/ 2934.49m	Nahanni	Silty Shale	TS; SEM	VP
X25	9628.20ft/ 2934.68m	Nahanni	N/A	XRD	N/A
X24	9744.25ft/ 2970.05m	Nahanni	N/A	XRD	N/A
T9,S9	9745.75ft/ 2970.50m	Nahanni	Limestone (packstone)	TS; SEM	P

X23	9749.50ft/ 2971.65m	Nahanni	N/A	XRD	N/A
X22	9754.50ft/ 2973.17m	Nahanni	N/A	XRD	N/A
X21	9759.60ft/ 2974.73m	Nahanni	N/A	XRD	N/A
T8,S8	9761.50ft/ 2975.31m	Nahanni	Limestone (wackestone)	TS; SEM	P
X20	9764.60ft/ 2976.25m	Nahanni	N/A	XRD	N/A
X19	9769.25ft/ 2977.67m	Nahanni	N/A	XRD	N/A
X18	9774.75ft/ 2979.34m	Nahanni	N/A	XRD	N/A
X17	9779.50ft/ 2980.79m	Nahanni	N/A	XRD	N/A
X16	9784.75ft/ 2982.39m	Nahanni	N/A	XRD	N/A
T7,S7,X15	9785.00ft/ 2982.47m	Nahanni	Limestone (packstone)	TS; SEM; XRD	P
X14	9794.90ft/ 2985.49m	Nahanni	N/A	XRD	N/A
T6,S6	9799.00ft/ 2986.74m	Nahanni	Limestone (wackestone-packstone)	TS; SEM	P
X13	9799.50ft/ 2986.89m	Nahanni	N/A	XRD	N/A
X12	10038.00ft/ 3059.58m	Nahanni	N/A	XRD	N/A
X11	10042.00ft/ 3060.80m	Nahanni	N/A	XRD	N/A
X10	10051.50ft/ 3063.70m	Nahanni	N/A	XRD	N/A
X9	10054.50ft/	Nahanni	N/A	XRD	N/A

	3064.61m				
X8	10061.50ft/ 3066.75m	Nahanni	N/A	XRD	N/A
X7	10067.00ft/ 3068.42m	Nahanni	N/A	XRD	N/A
X6	10124.75ft/ 3086.02m	Nahanni	N/A	XRD	N/A
X5	10130.00ft/ 3087.62m	Nahanni	N/A	XRD	N/A
X4	10133.50ft/ 3088.69m	Nahanni	N/A	XRD	N/A
T5,S5	10134.00ft/ 3088.84m	Nahanni	Dolostone	TS; SEM	M
X3	10138.75ft/ 3090.29m	Nahanni	N/A	XRD	N/A
T4,S4	10164.40ft/ 3098.11m	Nahanni	Dolostone	TS; SEM	P
T3,S3	10191.50ft/ 3106.37m	Nahanni	Dolostone	TS; SEM	P
T2,S2,X2	10246.00ft/ 3122.98m	Nahanni	Dolostone	TS; SEM; XRD	P
T1,S1,X1	10262.70ft/ 3128.07m	Nahanni	Dolostone	TS; SEM; XRD	M

(*) TS- Detailed thin section analysis with images; SEM - Scanning Electron Microscope analysis with images; XRD: Bulk X-Ray Diffraction Analysis; Reservoir Quality: VP – Very Poor; P- Poor; M – Moderate; G- Good.

Samples T1-T5 (10262.70-10134.00ft) recovered from the Nahanni Formation are determined to be dolostones, while samples T6-T9 (9799.00-9745.75ft) are limestones and samples T10-T11 (9627.60-9609.75ft) are considered to be silty shales. Based on petrographic observation, sample T6 (9799.00ft) is classified as a peloidal-bioclastic wackestone-packstone, sample T7 (9785.00ft) is a packstone, T8 (9761.50ft) a wackestone and T9 (9745.75ft) peloidal-bioclastic packstone.

Dolostone Samples T1 (10262.70ft) to T5 (10134.00ft)

Dolostone samples from this well location are comprised mainly of dolomite (87% to 95%). Secondary quartz is present in minor to trace amounts in most samples, while minor calcite was noted in sample T3 (10191.50ft). The samples generally lack the presence of detrital grains; however, trace possible detrital quartz was observed in sample T3 (10191.50ft). The matrix (1% to 6%) is composed of clays and organics, while sample T2 (10246.00ft) contains trace dolomicrite/very fine crystalline dolomite. Pore-filling cement occurs as fracture-fill or occludes microvuggy pore spaces in some samples. Pore-filling cements observed in these samples include trace to common amounts of quartz cement (trace to 7%) which occurs as vein-fill (T1-T5) or has precipitated within microvugs (samples T1 and T2). Calcite (trace to 3%) is observed mainly as calcite spar vein-fill (T3), or as localized occlusion of intercrystalline pore spaces (T4). Trace to minor amounts of pyrite (trace to 1%) acts as a replacement mineral, while minor pyrite (2%) has also precipitated within microvugs and fractures in sample T5 (10134.00ft).

Dolomite within these samples predominately displays non-planar replacement or alteration textures. ‘Saddle’ or baroque dolomite is represented by subhedral coarse dolomite that displays stepped or curved crystal faces, while sweeping or undulatory extinction can be viewed under cross-polarized light. Baroque dolomite is considered to be a high temperature precipitate that often replaces earlier calcite. Using the ‘white card’ technique with the petrographic microscope, a vague mud-supported depositional texture can be inferred in thin section samples T3 and T4, whereas original texture in dolostone samples T1-T3 is poorly preserved. Sample T4 also contains a dolomitic intraclast (~ 3% of the rock volume) that is likely remnant of the original texture before dolomitization.

Samples T5 (10134.00ft) and T4 (10164.40ft), notably sample T4, also consist of significant amounts of planar fine crystalline subhedral dolomite that contains appreciable amounts of clay inclusions, plus interstitial clays and organics. Sub- to Euhedral dolomite rhombs, often displaying compositional zoning, line microvuggy pore spaces or have precipitated within vertical and sub-vertical fractures.

Reservoir quality for these five samples ranges from poor to moderate and is mainly controlled by replacement texture and the precipitation of secondary quartz cement. Compaction and pressure/solution (stylolites) are evident in these dolostones. Low amplitude stylolites are generally horizontal, while relatively high amplitude stylolites, in addition to cemented and partially open fracture systems, are generally subvertical to vertical.

Reservoir quality is considered to be poor for samples T3 (10191.50ft), T2 (10246.00ft) and T4 (10164.40ft) as they generally display only trace amounts of open fracture and intercrystalline porosity, while sample T2 also displays minor amounts of isolated microvuggy porosity (1%). Samples T1 (10262.70ft) and T5 (10134.00ft) are estimated to have moderate reservoir quality. In addition to trace to minor amounts of open fracture (trace to 1%) and intercrystalline (1%) porosity, these dolostones also display minor microvuggy porosity (2% to 5%); however, pore spaces in sample T1 have been predominately occluded by quartz cement and organic matter (probable bitumen). Please see the Petrographic Summary (Table 1B) in the appendix for details regarding mineralogy, texture and porosity.

Limestone Samples T6 (9799.00ft) to T9 (9745.75ft)

The mineralogy of the four limestone samples (wackestone to packstone) consists primarily of calcite (84% to 95%), with minor to moderate amounts of clays and organic matter (3% to 15%) and minor pyrite (1% to 2%). Minor secondary chert (2%) is noted in sample T9 (9745.75ft). Trace detrital quartz grains occur in sample T6 (9799.00ft).

The framework grains consist of various carbonate clasts (15% to 25% - samples T6 and T9 only) and bioclasts (17% to 55%). Micritic peloids comprise carbonate clasts within these samples, while bioclasts have been identified as stromatoporoids, crinoids, sponge spicules, mollusks, brachiopods, bryozoa, ostracods, gastropods and possible forams in various proportions. Indistinct bioclast fragments that are too small to identify, or their structure has been replaced/recrystallized, are also present in trace to moderate amounts. Moderate to abundant amounts of calcite-micrite (10% to 77%), plus minor to moderate amounts of clays and organics (3% to 15%) comprise the matrix. Trace silt-sized detrital quartz grains are noted in sample T6 (9799.00ft).

Intraparticle porosity and micro-fractures are locally filled with trace to minor amounts of calcite spar (trace to 2%) and pyrite (1% - T9 only). Trace dolomite cement also occludes intraparticle porosity in sample T8 (9761.50ft). Trace to minor amounts (trace to 2%) of pyrite replacement (carbonate grains, bioclast and matrix), along with minor calcite (2% to 5% - T6 and T7) and chert (2% - T9) replacement is also noted.

Visible porosity includes trace open fracture porosity in sample T8 (9761.50ft); therefore, overall reservoir quality is considered to be poor for these samples. The reservoir quality appears to be mainly controlled by depositional environment (i.e. abundance and distribution of micritic matrix and micritic framework grains), and to a lesser extent, by diagenetic events (compaction, precipitation of the framework sustaining cements). Stylolites, and cemented microfactures, are generally vertical to subvertical within these samples. Please see the Petrographic Summary (Table 1B) in the appendix for details regarding mineralogy, texture and porosity.

Shale Samples T10 (9627.60ft) to T11 (9609.75ft)

The two silty shale samples are massive to weakly laminated. Laminae are characterized by the parallel alignment of platy micas and elongate chert lenses. Subangular to subrounded framework grains are well sorted and range in size from clay-sized particles to very fine silt. Framework grains visible in thin section are dominated by quartz (6% to 7%), plus lesser amounts of feldspar (trace). Due to the small size of the grains, feldspar content is underestimated in thin section since prominent petrographic features, such as twinning, are difficult to interpret. XRD analysis of sample T11 (9609.75ft) indicates ~1% both plagioclase and potassium feldspar. Accessory components include minor amounts of muscovite mica (3% to 5%). Minor to moderate amounts of chert (2% to 4%) and dolomite (6% to 24%), plus trace pyrite, locally replace matrix clays and minute framework grains. Dolomite is noted as very fine sub- to euhedral rhombs. Pyrite occurs as scattered irregular blebs or framboids.

The matrix (62% to 68%) appears dark brown, which suggests high organic content. Based on optical properties matrix clays are likely detrital. As per XRD analysis, the clays within this sample are dominated by illite. It should be noted that organic content cannot be detected by XRD analysis due to a lack of crystal structure; therefore, quartz content is notably higher within the XRD results in relation to observed thin section mineralogy. These sample lack visible porosity; therefore, overall reservoir quality is considered to be very poor. Please see the Petrographic Summary (Table 1B) in the appendix for details regarding mineralogy, texture and porosity.

The following table summarize the most important factors that control the reservoir quality of the eleven samples recovered from TEXACO BOVIE LAKE J-72 300/J-72-6020-12245/0 location.

Sample ID	Depth (ft/m)	Total Micrite /Matrix (%)	Total Cement (%)	Total Porosity (%)						Main Porosity controlling factors (*)	RQ(*)
				IP	Int.	Ixl	Mv	Fr	M		
Location: Texaco Bovie Lake J-72 300/J-72-6020-12245/0											
11	9609.75ft 2929.05m	68	20	-	-	-	-	-	-	C; Dc	VP
10	9627.60ft 2934.49m	62	29	-	-	-	-	-	-	C; Dc	VP
9	9745.75ft 2970.50m	15	3	-	-	-	-	-	-	Mic; Cc; Com	P
8	9761.50ft 2975.31m	80	1	-	-	-	-	TR	-	Mic; C; Py	P
7	9785.00ft 2982.47m	45	-	-	-	-	-	-	-	Mic; Cc; Com	P
6	9799.00ft 2986.74m	47	2	-	-	-	-	-	-	Mic; Cc; Com	P
5	10134.00ft 3088.84m	3	9	-	-	1	5	1	-	SDol; Qc; Py	M
4	10164.40ft 3098.11m	6	1	-	-	TR	-	TR	-	SDol; C; Dc; Qc; Com	P
3	10191.50ft 3106.37m	3	3	-	-	TR	-	TR	TR	SDol; Cc; C; Qc	P
2	10246.00ft 3122.98m	1	3	-	-	TR	TR	1	-	SDol; Qc; C; Mic	P

1	10262.70ft 3128.07m	3	5	-	-	1	2	TR	TR	SDol; Qc; C	M

Porosity value (%): IP – interparticle porosity; **Int** – intraparticle; **Ixl** – intercrystalline; **Mv** – micro-vuggy; **Fr** – fracture porosity; **M** – micro-intercrystalline porosity
Main Porosity controlling factors: Com – compaction**;** M**ic** – micrite (calcite or dolomite); **Ms** – micro- and/or pseudospar; **SDol** - saddle dolomite; **Cc** – calcite cement (druse and spar); **Dc** – dolomite cement**; Qc -** quartz cement; **C** – clays and organics; **Ov** – quartz overgrowths; **Py** – pyrite (replacement and/or cement); **F** – fabric: [**CC** – concavo-convex orthochem contacts; **S** – sutured orthochem contacts]
RQ (*) - reservoir quality: VP – very poor; **P –** poor; **M –** moderate; **G -** good

Reservoir problems for the samples recovered from the Nahanni Formation at the Texaco Bovie Lake J-72 300/J-72-6020-12245/0 location, may include the following: **(1)** Heterogeneity of the pore system, plus overall poor interconnectivity between pores could restrict the flow of hydrocarbons, **(2)** hydrochloric acid (HCl) treatment of this reservoir has the potential to loosen carbonate fines (dolo-micrite and calcite micrite) that could migrate and block pore throats, plus cause fabric collapse, **(3)** Sensitivity of calcium carbonate to hydrofluoric acid (HF) in regard to precipitation of calcium fluoride scales.

Detailed mineralogical composition of each of the sample are summarized in the tables that can be found in the 'RESULTS' chapter of this report. Following the tabulated data there are images (with descriptions) that show specific features of the samples.

METHODS

Petrographic Microscopy

To prepare the thin section samples, select portions of the core samples were impregnated with blue epoxy, polished and mounted onto a glass slide. After drying of the epoxy the samples were ground down to a total thin section thickness of 30μm. One half of each thin section was then stained with a combination of Alizarin Red (for calcite) and potassium ferricyanide (for ferroan carbonate) to highlight carbonate mineralogy. The dual carbonate stain helps to differentiate the carbonate components within the samples, and affects them as follows: calcite appear pink to red-brown, ferroan calcite shows mauve to blue, ferroan dolomite colors vary from pale blue to turquoise, while non-ferroan dolomite remains unstained. Finally a second glass slide was glued on the samples to protect the polished surface. The prepared thin sections were point counted. The thin sections were examined in plain and cross polarized light conditions and photomicrographs taken at various magnifications (x12.5ppl; x25ppl; x50ppl, x100ppl, and x200ppl) to document structure, porosity, composition and nature of optically resolvable grains and matrix. To determine original texture of dolostone samples, the 'white card' technique has been used. Each sample has been described separately and the important features of it that includes framework mineralogy, diagenetic minerals and cements, textures, grain size range and average, porosity, etc., and the results are provided in the tabulated format. Annotated images of the thin sections with descriptions show the important aspects that were observed during the thin section examination. These images are placed after the tabulated data. A detailed petrographic summary which includes all samples (**Table 1A and 1B**) is provided in the **Tables and Figures** section of this report.

SEM Analysis

A representative portion of each sample was adhered onto an aluminum stub specimen mount. The stubs were then sputter-coated with a conductive gold-palladium alloy for detailed Scanning Electron Microscopy (SEM) analysis and imaging. SEM analysis is useful in identifying lithological characteristics such as pore types, framework mineralogy, clay and cement composition, in addition to the potential deportment of clay constituents in relation to pore spaces and pore throats. Energy dispersive X-ray (EDX) was also used in conjunction with SEM observation in order to determine the elemental composition of the observed clay minerals and overall mineralogy.

<u>Bulk XRD Analysis</u>

Sample Preparation: Each sample, consisting of rock fragments, is manually crushed carefully using a mortar and pestle to reduce the size of the fragments. The sample is then ground with a vibratory disc mill (RS200; Retsch) to further reduce crystallite sizes. Finally, the sample is micronized using a planetary ball mill (PQN04; Across International) and scanned for X-ray diffraction analysis.

X-Ray Data Collection and Analysis:

Diffractometer Name: Bruker D4 Endeavor XRD with a Lynx-Eye detector

Instrumental Parameters: Radiation Source – Cobalt (Co)

Generator settings - 40 mA, 35 kV

Start position [°2θ] - 4

End position [°2θ] - 80

Step size [°2θ] - 0.02

Scan step time [s] - 1

Data Analysis: ICDD PDF-4 Mineral 2020 powder diffraction database

X'PERT HighScore Software for mineral identification

TOPAS Software for quantitative phase analysis

Detection Limit: 0.1 – 0.5 % depending on the type and nature of sample

Quantitative Mineral Phase Analysis: Using the HighScore program, the different mineral phases of the XRD patterns are identified. Once the mineral phases are identified, Rietveld refinements are performed by importing the XRD trace pattern into TOPAS 5. This program (TOPAS 5) is used for Rietveld analysis to quantify the mineralogy. The quantitative mineral phases of all samples are given in Table 2. The refined diffractograms and **Table 2** are placed in the **Tables and Figures** section of this report.

Classification and Grain sizes:

To describe the original texture of the rocks the modified Dunham (1962) classifications for carbonate rocks was used (see the figure below).

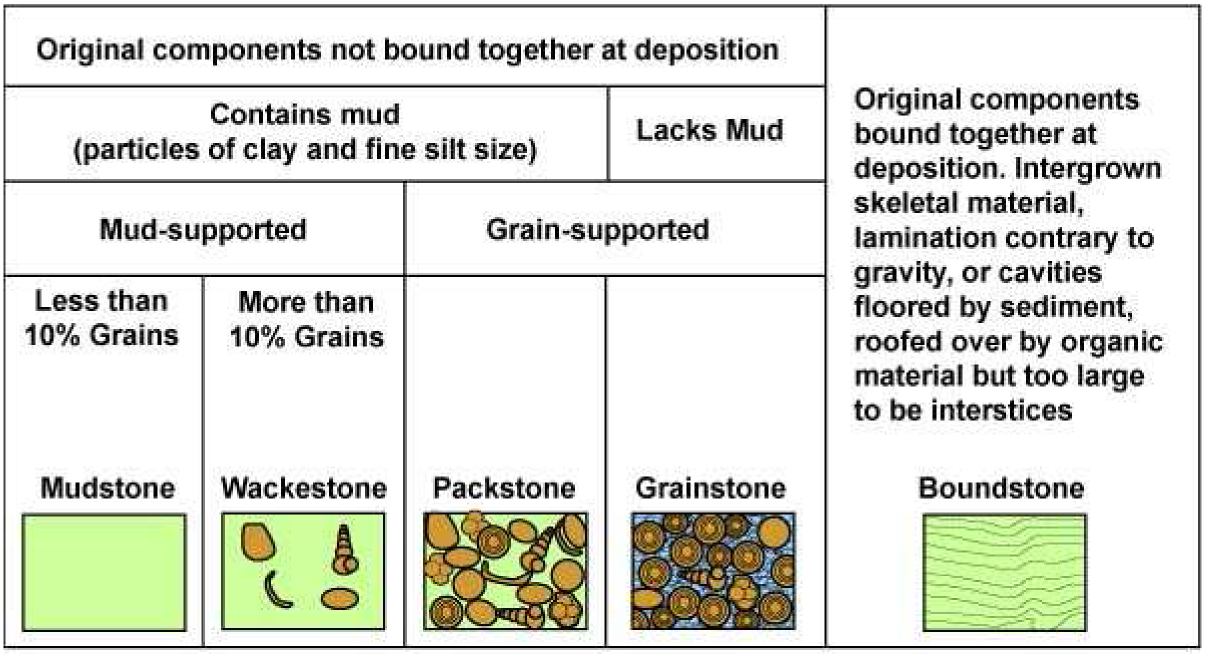

C. G. St. C. Kendall, 2005 (after Dunham, 1962, AAPG Memoir 1)

The scale for authigenic constituents in carbonates follows the Wentworth division, which is the most useful for dolomites, where transported particles are usually obliterated by replacement and crystal size is one of the few describable characteristic. The carbonate crystal sizes ranges are as follows: very fine crystalline (4 to 16μm), fine (16 to 62 μm), medium (62 to 250 μm), coarse (250-1000 μm), and very coarse crystalline (1000 to 4000 μm). The finest authigenic constituents are called cryptocrystalline (less than 1μm) and aphanocrystalline with the crystal size between 1 and 4 μm.

The following describes a division within the carbonate matrix. Micrite term is used for carbonate mud that consists of 1 to 4 μm diameter crystals and forms as an inorganic precipitate or through breakdown of coarser carbonate grains. Micrite is produced within the basin of deposition and shows little or no evidence of transport (Folk, 1959). Microspar is generally 5 to 20 μm sized calcite produced by recrystallization (neomorphism) of micrite and can be as coarse as 30 μm (Folk, 1965). Microspar is restricted to recrystallization products, not primary precipitates. Calcite fabric crystal size larger than 30 to 50 μm is called a <u>pseudospar</u>.

To describe detrital grains sizes, the Wentworth divisions will be used. The following is a list of actual size range for each Wentworth grain size: coarse silt (31 to 62.5μm), very fine (62.5 - 125μm), fine (125 - 250μm), medium (250 - 500μm), coarse (500- 1000μm), very coarse (1000 - 2000μm), plus granule (2000 - 4000μm) and pebble (>4000μm). The suffix 'lower' denotes that the grain size is toward the smaller portion of a specific size range, while the suffix 'upper' denotes that the grain size is toward the larger portion of a specific size range.

For the dolomite crystal fabrics the classification proposed by Sibley and Gregg (1987) was used (see the chart below).

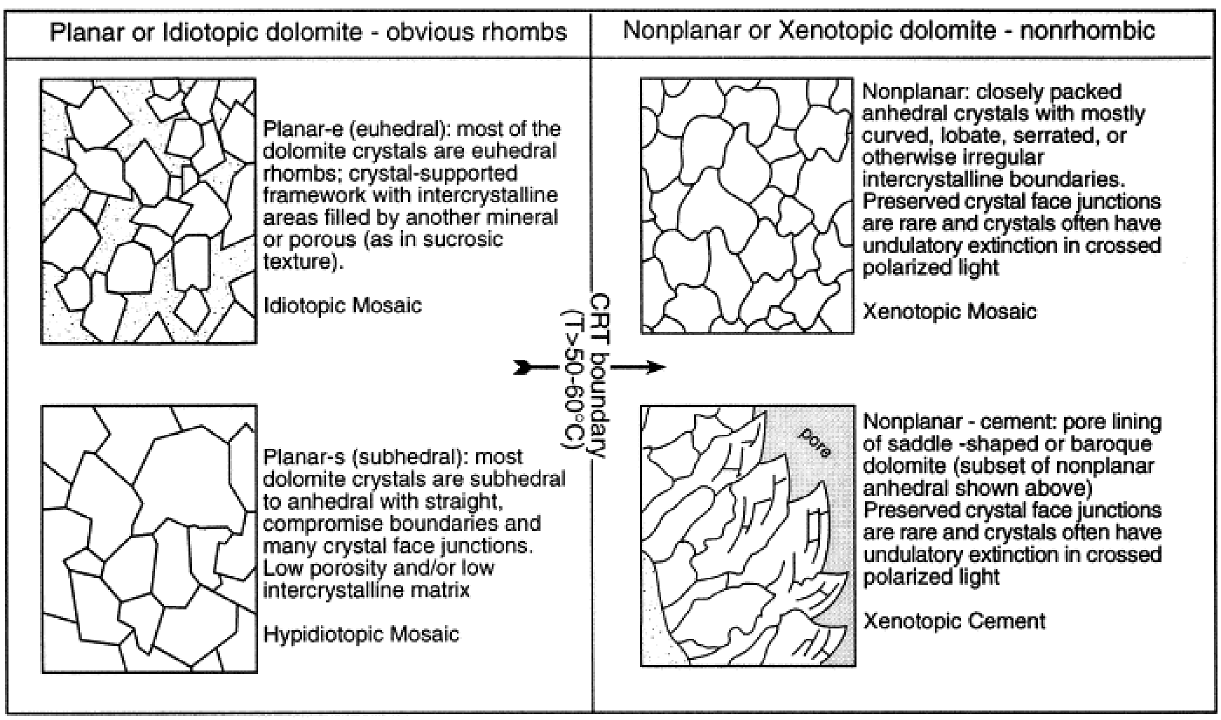

Xenotopic dolomite/Idiotopic dolomite/Hypidiotopic dolomite

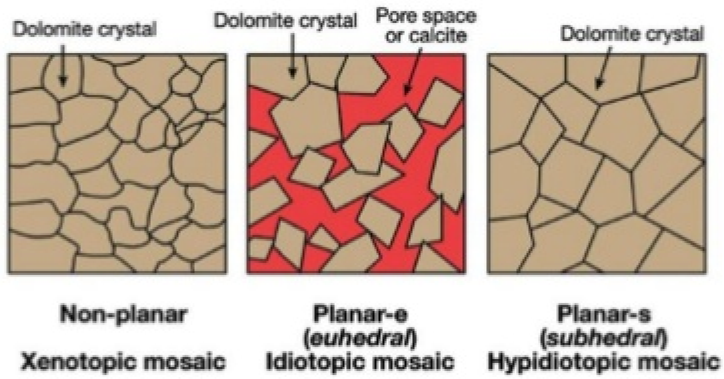

Adapted from Sibley and Gregg (1987)
James & Jones, 2015

10

Abbreviations

The list of common thin section abbreviations in provided in the table below.

NAME	ABBREVIATION	NAME	ABBREVIATION
Anhydrite	Anh	Intragranular Porosity	Intr.
Barite	Ba	Kaolinite	Kao
Biotite	Bio	K-Feldspar	K-Fld
Bioclasts (indistinct)	Biocl	Laminae	Lam
Burrows/Bioturbation	Bur	Metamorphic Rock Frag.	MRF
Bioturbation	Bt	Muscovite	Musc
Calcite	Cal	Matrix	Mtx
Carbonaceous	Carb	Micro-vuggy pore	Mv
Chert	Cht	Organic material	OM
Chlorite	Chl	Phosphate	Phos
Concavo-convex	CC	Plutonic Rock Fragments	PRF
Dolomite	Dol	Polycrystalline quartz	PQ
Detrital Calcite	dC	Pseudo-matrix	P-mtx
Detrital Dolomite	dD	Pyrite	Py
Feldspar	Fld	Quartz	Qtz
Ferroan Dolomite	Fe-Dol	Quartz Cement	Qc
Ferroan Calcite	Fe-Cal	Quartz overgrowths	Ov
Glauconite	Glauc	Sedimentary Rock Frag.	SRF
Grain dissolution pore	GD	Secondary porosity	SP
Heavy minerals	HM	Sutured grain contact	S
Hematite	Hem	Volcanic Rock Fragments	VRF
Illite	Ill	Marcasite	Marc
Intergranular Porosity	IP	Saddle Dolomite	SDol
Intercrystalline Porosity	Ixl	Dolomite Cement	Dc
Intraclast	Intraclast		

RESULTS

In this section of the report, the eleven samples that were recovered from the TEXACO BOVIE LAKE J-72 300/J-72-6020-12245/0 location will be described separately. The images that show specific features of each sample will follow the tabulated sample description.

Sample T11/S11/X29, 9609.75ft/2929.05m

Well Name	Texaco Bovie Lake J-72	**Location**	300/J-72-6020-12245/0
Sample Type	Thin section/SEM grain mount from a core sample	**Depth (m)**	9609.75ft/2929.05m
Stratigraphic Unit	Nahanni Formation	**Reservoir Quality**	Very Poor
Classification	Silty Shale	**Stain type**	½ Dual carbonate stain

MINERALOGY

Thin Section Point counting (%)	Qtz	Fld	K-Fld	Cht	Rock Fragm.	Mica	HM	Glau	OM
	7	TR	TR	-	-	5	-	-	-
	Mtx/ P-mtx	**AC**	**Cht (Cem)**	**Cal**	**F-Cal**	**Dol**	**F-Dol**	**Sid**	**Py**
	68	-	14	-	-	6	-	-	TR

ADDITIONAL FEATURES and OTHER COMMENTS

Depositional	The sample appears weakly laminated as indicated by the parallel alignment of platy micas and elongate chert lenses.
Biogenic structures	No biogenic structures are observed.
Textures	Subangular to subrounded framework grains are well sorted and range in size from clay-sized particles to very fine silt.
Mineralogy (Framework and accessory grains)	Framework grains visible in thin section are dominated by quartz, plus lesser amounts of feldspar. Due to the small size of the grains, feldspar content may be underestimated in thin section since prominent petrographic features, such as twinning, are difficult to interpret. Accessory components include minor amounts of mica. Minor to moderate amounts of chert and dolomite, plus trace pyrite, locally replace matrix clays and minute framework grains.
Matrix/ Pseudo-matrix	The matrix appears dark brown, which suggests high organic content. Based on optical properties, matrix clays are likely detrital. As per XRD analysis, the clays in the clay fraction of this sample are dominated by illite. It should be noted that organic content cannot be detected by XRD analysis due to a lack of crystal structure; therefore, quartz content is notably higher within the XRD results in relation to observed thin section mineralogy.
Authigenic Clays	Clay minerals in this sample are considered to be detrital.
Diagenetic minerals/ Diagenesis	The matrix, in addition to possible detrital silicate grains, has been locally replaced by moderate chert, minor dolomite and trace amounts of pyrite. Chert occurs in elongate, discontinuous lenses that align with the depositional structure. Dolomite is noted as very fine sub- to euhedral rhombs. Pyrite occurs as scattered irregular blebs or framboids.
Porosity	No visible porosity.

Annotated microphotographs with descriptions for the thin section and SEM samples are provided below.

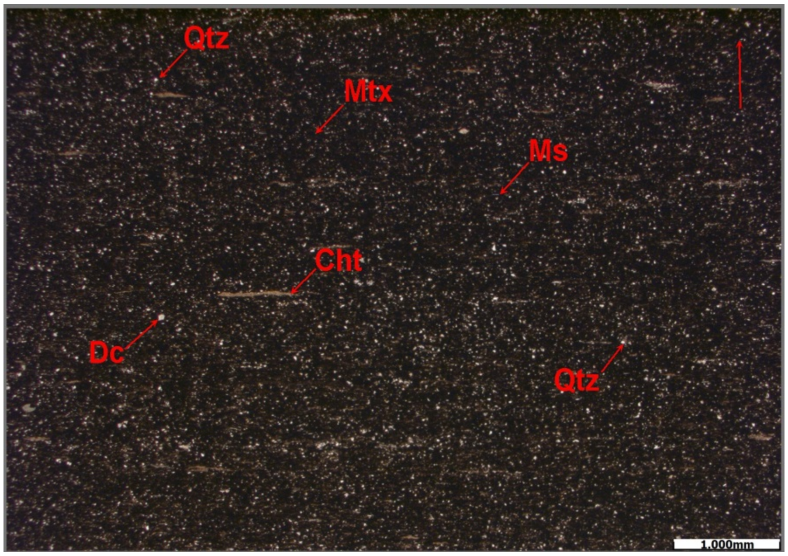

Figure 1.1. Sample T11, 9609.75ft/2929.05m. Low magnification overview image of the massive to weakly laminated mudstone. The overall laminated fabric of the sample is defined by the parallel alignment of chert lenses and platy micas (Ms: muscovite mica). The dark colouration of the matrix (Mtx) combined with moderate illite clay content, as determined by XRD analysis, suggests high organic content. Localized pyrite replacement of the matrix was identified with reflected light observation. Detrital constituents include scattered clay to silt-sized quartz (Qtz) and feldspar grains. Very fine rhombohedral dolomite cement (Dc) locally replaces the matrix, in addition to elongate lenses of chert (Cht). The sample lacks visible porosity; therefore, overall reservoir quality is estimated to be very poor. **x25 ppl**

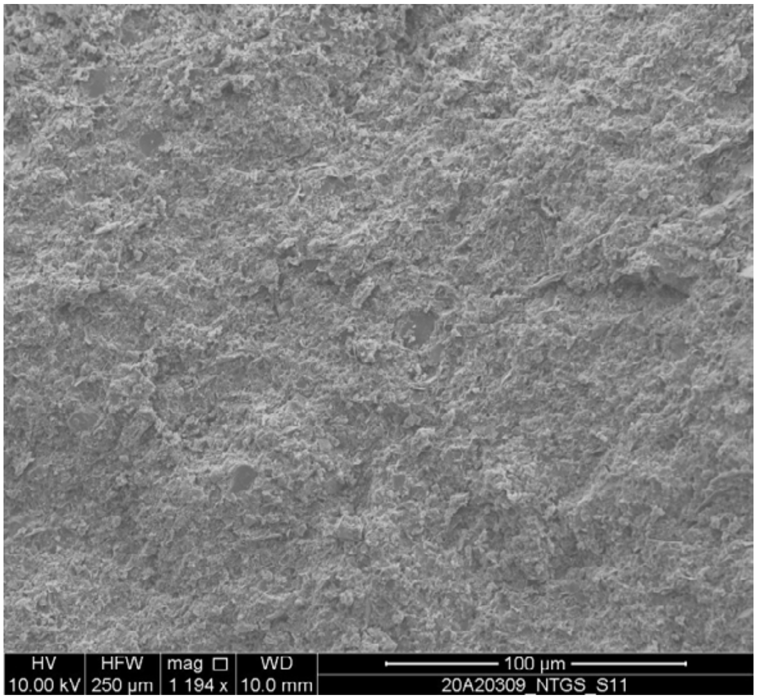

SEM Figure 1.2. Sample S11, 9609.75ft/2929.05m. Low magnification overview showing the overall texture of the massive to weakly laminated silty shale. **x1194**

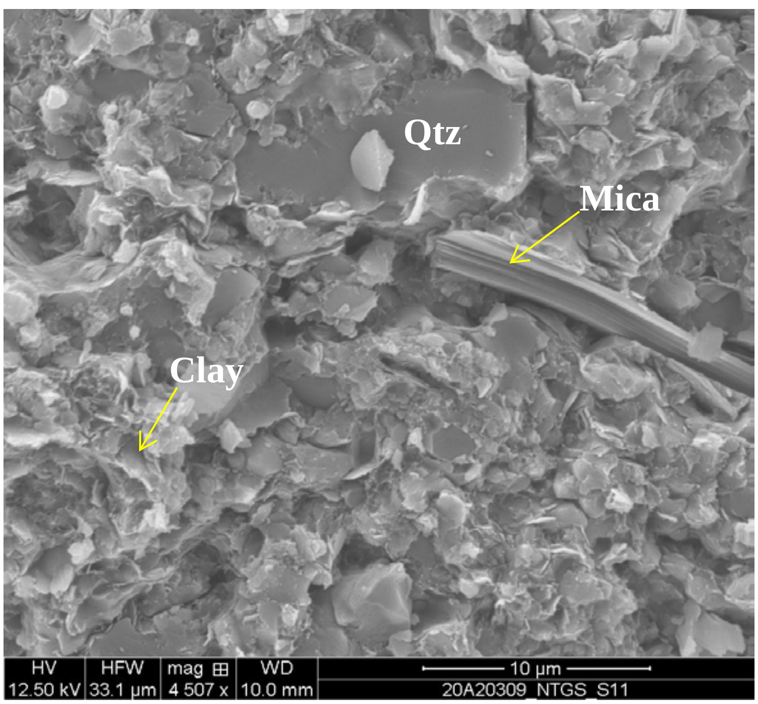

SEM Figure 1.3. Sample S11, 9609.75ft/2929.05m. Moderate magnification SEM image showing an angular silt-sized quartz grain (Qtz), illitic clays (Clay) and a mica booklet (Mica). **x4507**

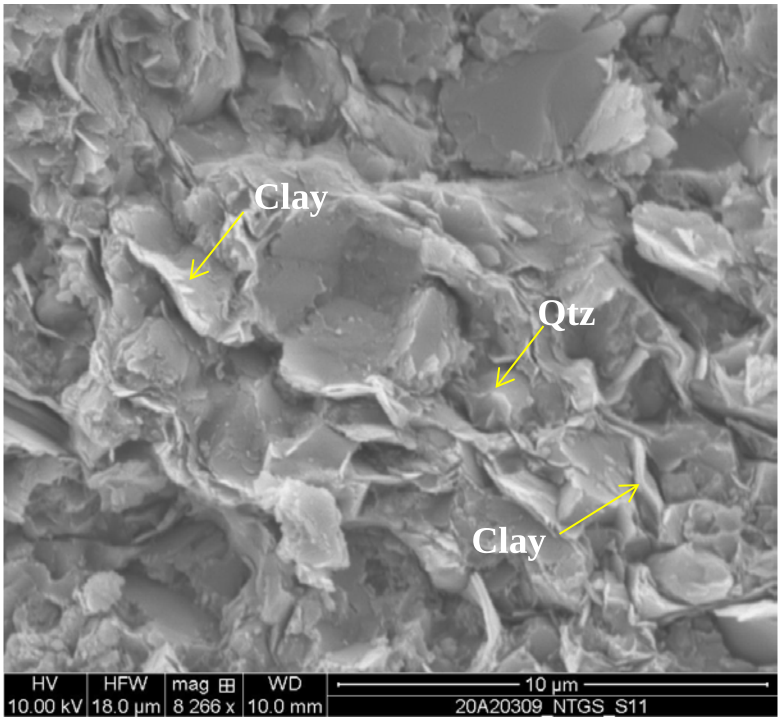

SEM Figure 1.4. Sample S11, 9609.75ft/2929.05m. High magnification image showing clay-sized quartz particles (Qtz) with interstitial illitic clays (Clay). **x8266**

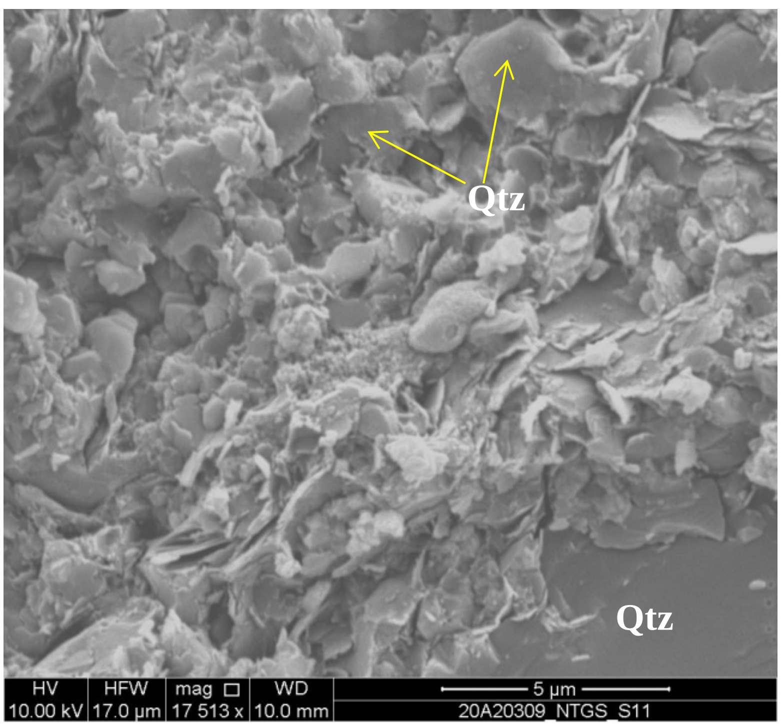

SEM Figure 1.5. Sample S11, 9609.75ft/2929.05m. High magnification image highlighting the localized alignment of platy clay and mica minerals. Quartz (Qtz) occurs both as clay and silt-sized particles. **x17513**

Sample T10/S10, 9627.60ft/2934.49m

Well Name	Texaco Bovie Lake J-72	**Location**	300/J-72-6020-12245/0
Sample Type	Thin section/SEM grain mount from a core sample	**Depth (m)**	9627.60ft/2934.49m
Stratigraphic Unit	Nahanni Formation	**Reservoir Quality**	Very Poor
Classification	Silty Shale	**Stain type**	½ Dual carbonate stain

MINERALOGY

Thin Section Point counting (%)									
	Qtz	**Fld**	**K-Fld**	**Cht**	**Rock Fragm.**	**Mica**	**HM**	**Glau**	**OM**
	6	TR	TR	-	-	3	-	-	-
	Mtx/ P-mtx	**AC**	**Cht (Cem)**	**Cal**	**F-Cal**	**Dol**	**F-Dol**	**Sid**	**Py**
	62	-	2	3	-	24	-	-	TR

ADDITIONAL FEATURES and OTHER COMMENTS

Depositional	The sample appears weakly laminated as indicated by localized concentrations of detrital quartz, plus the parallel alignment of platy micas and elongate chert lenses.
Biogenic structures	Not observed.
Textures	Subangular to subrounded framework grains are well sorted and range in size from clay-sized particles to very fine silt.
Mineralogy (Framework and accessory grains)	Framework grains visible in thin section are dominated by quartz, plus lesser amounts of feldspar. Due to the small size of the grains, feldspar content may be underestimated in thin section since prominent petrographic features, such as twinning, are difficult to interpret. Accessory components include minor amounts of mica. Significant amounts of dolomite, plus minor to trace amounts of chert and pyrite, locally replace matrix clays and minute framework grains. Minor secondary calcite occurs as fracture-fill.
Matrix/ Pseudo-matrix	The matrix appears dark brown, which suggests high organic content. Based on the optical properties it was concluded that the majority of the clay matrix is detrital. Illite is suspected to be the prominent clay variety.
Authigenic Clays	Clay minerals in this sample are considered to be detrital.
Diagenetic minerals/ Diagenesis	The matrix, in addition to possible detrital silicate grains, has been locally replaced by abundant dolomite, minor chert and trace amounts of pyrite. Chert occurs in elongate, discontinuous lenses that align with the depositional structure. Dolomite is noted as very fine sub- to euhedral rhombs. Pyrite occurs as scattered irregular blebs or framboids. A subvertical vein is infilled with calcite cement.
Porosity	No visible porosity.

Annotated microphotographs with descriptions for the thin section and SEM samples are provided below.

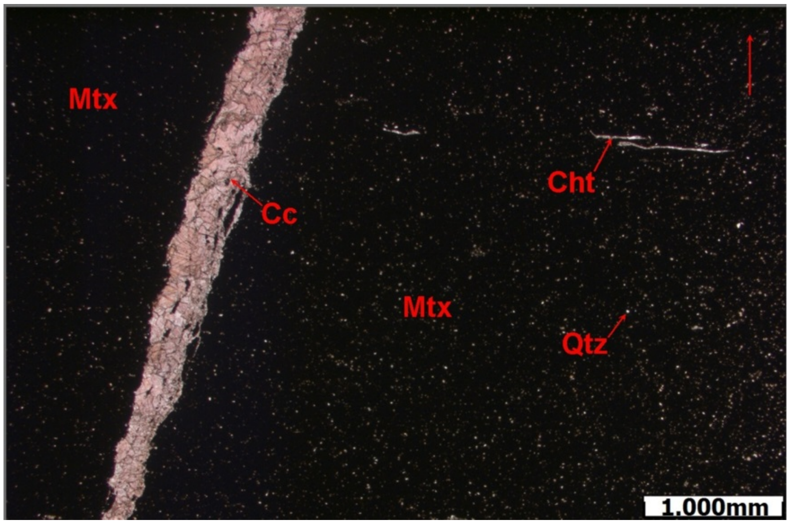

Figure 2.1. Sample T10, 9627.60ft/2934.49m. Low magnification view of the massive to vaugely laminated silty shale. The dark organic-rich matrix (Mtx) shows scattered clay and silt-sized detrital quartz (Qtz), and possibly other silicate grains. Thin lenses of microcrystalline chert (Cht) are noted. As shown in subsequent views, the matrix has been also partly cemented by secondary dolomite (Dc). A subhorizontal fracture is infilled by calcite cement (Cc). Porosity is not visible in thin section. **x25 ppl**

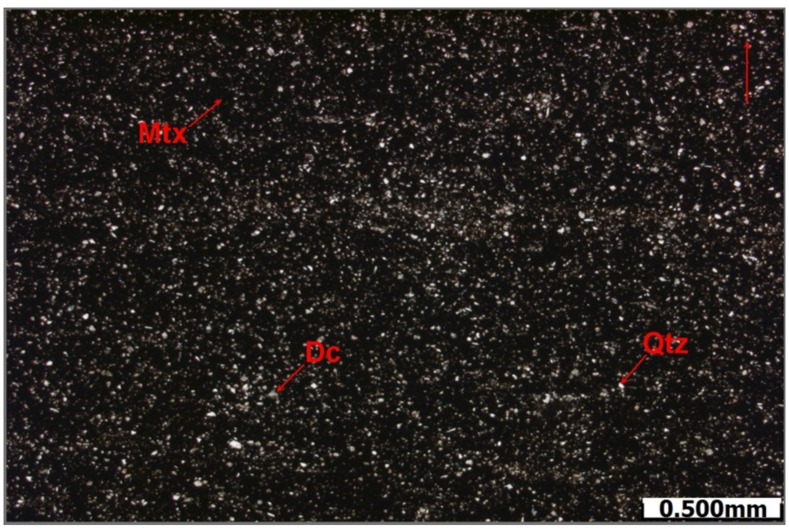

Figure 2.2. Sample T10, 9627.60ft/2934.49m. Moderate magnification view of the silty shale showing vague laminations defined by concentrations of clay and silt-sized detrital quartz grains (Qtz) within a dark organic-rich clay matrix (Mtx) that has been partly cemented by secondary dolomite (Dc). **x50 ppl**

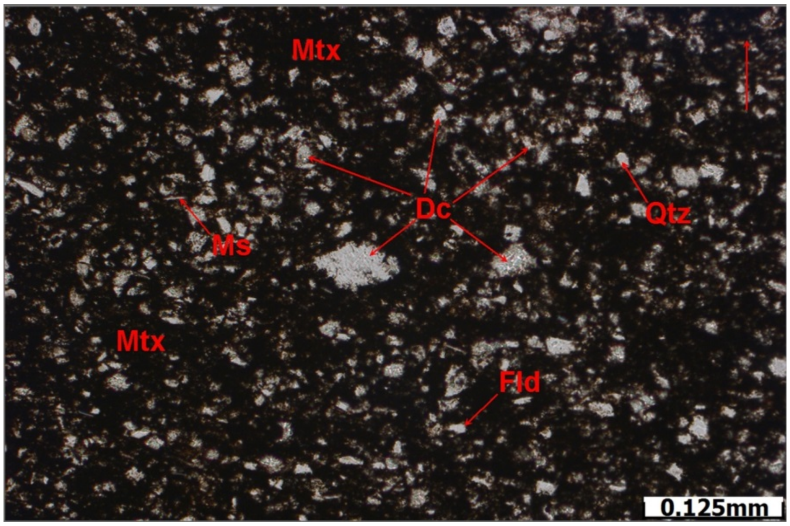

Figure 2.3. Sample T10, 9627.60ft/2934.49m. Very high magnification view highlighting secondary sub- to euhedral dolomite rhombs (Dc) scattered throughout the silty shale. Detrital grains featured within this view include quartz (Qtz), along with possible feldspar (Fld) which shows weak cleavage planes, plus muscovite mica flakes (Ms). Mtx: matrix. **x200 ppl**

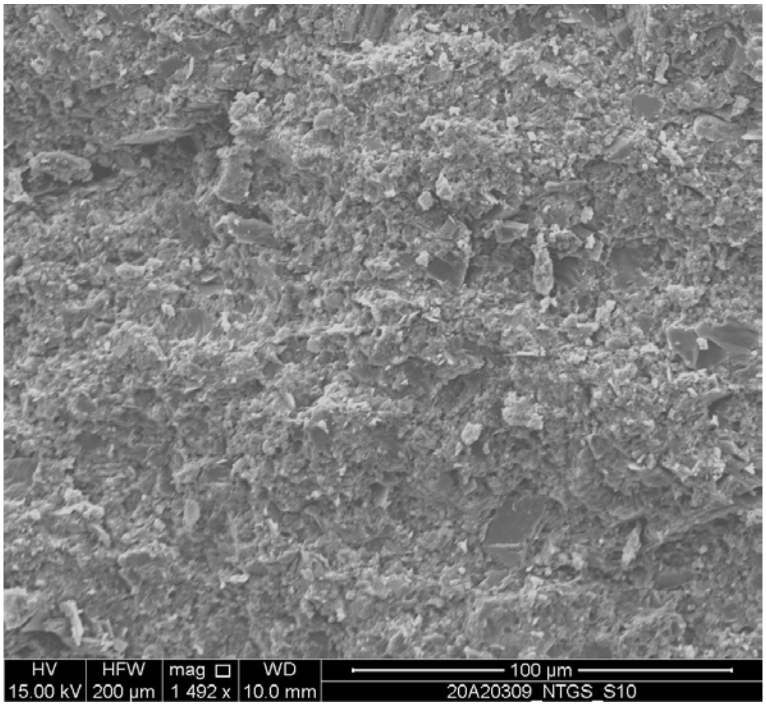

SEM Figure 2.4. Sample S10, 9627.60ft/2934.49m m. Overview image of the silty mudstone showing vague bedding. **x1492**

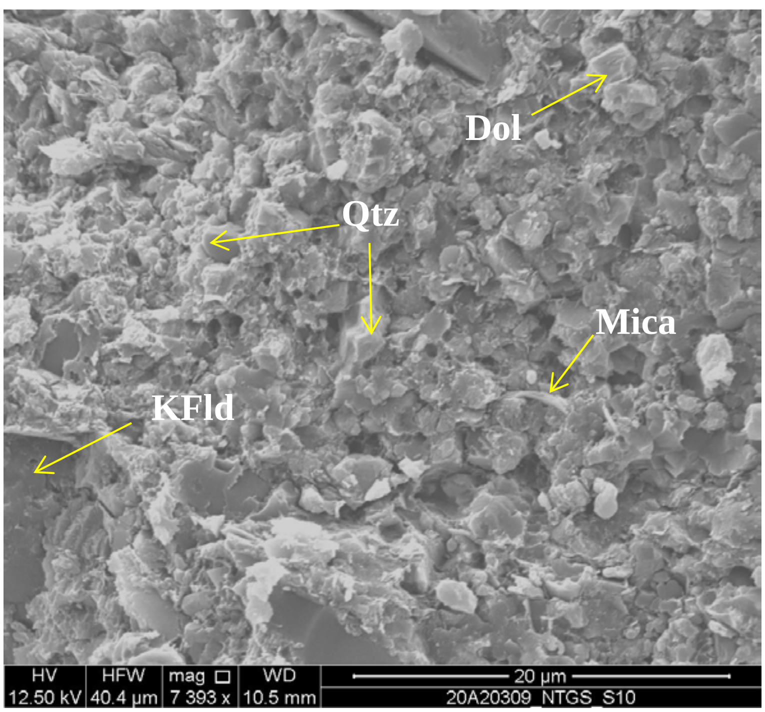

SEM Figure 2.5. Sample S10, 9627.60ft/2934.49m m. High magnification image showing various constituents of the detrital matrix including quartz (Qtz), potassium feldspar (KFld) and mica (Mica). A small dolomite rhomb (Dol) is also noted. Apparent porosity within this view may be artefact porosity generated by grain-plucking. **x7393**

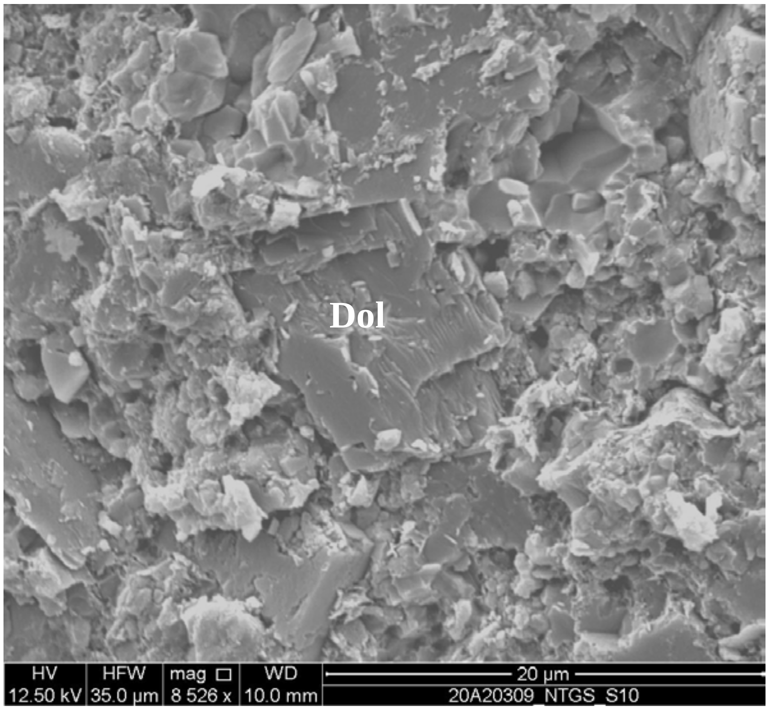

SEM Figure 2.6. Sample S10, 9627.60ft/2934.49m. High magnification image of localized secondary dolomite (Dol). **x8526**

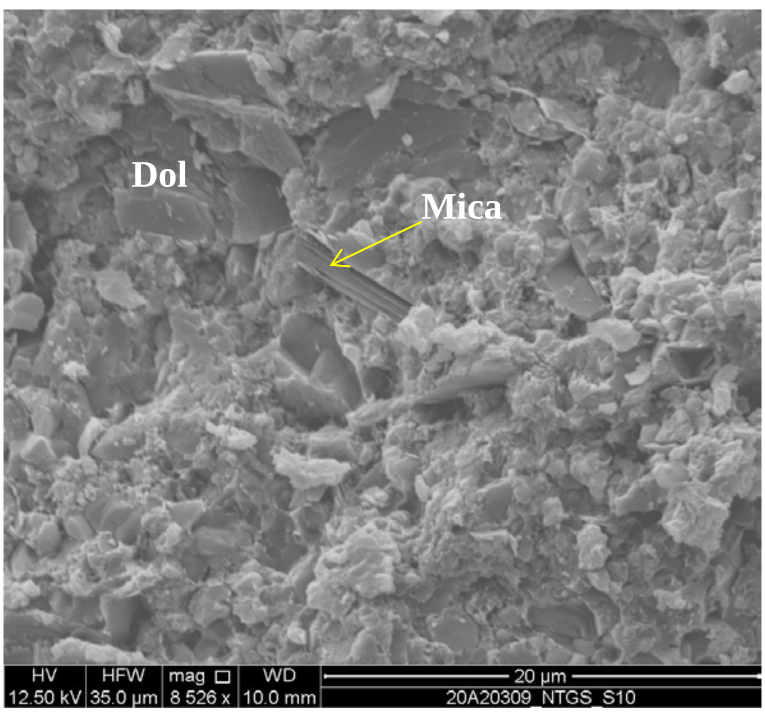

SEM Figure 2.7. Sample S10, 9627.60ft/2934.49m. Alternate high magnification view of secondary dolomite (Dol) in addition to a mica booklet (Mica) showing well-developed parallel cleavage. **x8526**

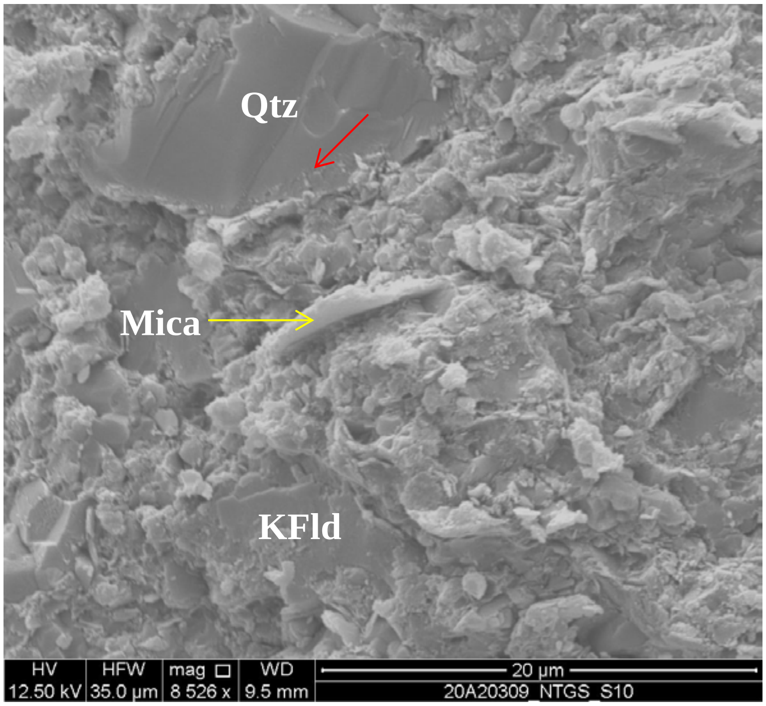

SEM Figure 2.8. Sample S10, 9627.60ft/2934.49m. High magnification view of a detrital quartz grain (Qtz) showing a possible overgrowth surface indicated by clay inclusions (red arrow). KFld: potassium feldspar; Mica: mica. **x8526**

Sample T9/S9, 9745.75ft/2970.50m

Well Name	Texaco Bovie Lake J-72		**Location**	300/J-72-6020-12245/0		
Sample Type	Thin section/SEM grain mount from a core sample		**Depth (m)**	9745.75ft/2970.50m		
Stratigraphic Unit	Nahanni Formation		**Reservoir Quality**	Poor		
Classification	Limestone (Packstone)		**Stain type**	½ Dual carbonate stain		
MINERALOGY						
	Total Bulk mineralogy					
Thin Section Point counting (%)	**Calcite**	**Dolomite**	**Anhydrite**	**Quartz/Cht**	**Pyrite**	**Clays & organics**
	92	-	-	2	1	5
	Framework, Matrix, Cement, and Replacement					
	Carbonate clasts	**Bioclasts**	**Detrital grains**	**Matrix**	**Pore filling cement**	**Replacement**
	25	55	-	15	3	2

ADDITIONAL FEATURES and OTHER COMMENTS

Depositional	At the time of deposition, the sample was most likely massive. Fracturing of the sediment typically happens during burial diagenesis, but may also be associated with later hydrothermal events. Micro-fractures within the sample have been healed by sparry calcite cement and pyrite.
Textures	Based on the mineralogy and proportion between framework components (carbonate clasts and bioclasts) and matrix, the sample was classified as a packstone. For the matrix, the crystal texture is generally anhedral, while cement shows subhedral to euhedral crystal texture. Some bioclasts have been micritized, while crinoid fragments often show single-crystal extinction and well-developed calcite twinning.
Framework (Carbonate clasts, Bioclasts)	Petrographic Summary Table 1B shows detailed mineralogy of the sample. This sample contains 92% calcite. Other minerals include clays and organics (5%), pyrite (1%) and chert (2%). In regards to the framework components, calcite occurs mainly as bioclasts [crinoids 20%, stromatoporoids 20%, mollusks 10%, indistinct 5%, plus trace brachiopod, coral and bryozoa fragments]. Abundant carbonate clasts [peloids - 25%] were also observed.
Detrital Grains & Other Non-Carbonate Grains	There are no detrital grains in this sample.
Matrix	Calcite is the main component of the matrix (10% of the total rock volume), while clays and organics are estimated to occur in minor amounts (5%).
Pore Filling Cements	The pore filling cements within this sample are associated with healed micro-fractures. The fractures have been infilled by sparry calcite cement (2%) and pyrite (1%).
Replacement Minerals	Minor amounts of chert (2%), plus trace pyrite, locally replaced bioclasts within the sample.
Porosity	The collected sample lacks visible porosity.

Annotated microphotographs with descriptions for the thin section and SEM samples are provided below.

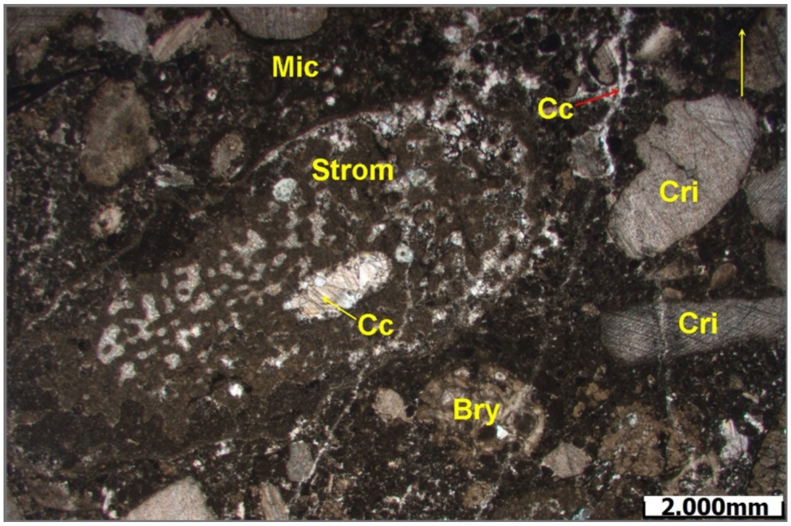

Figure 3.1. Sample T9, 9745.75ft/2970.50m. Low magnification overview image of the limestone (packstone). Crinoids (Cri) and stromatoporoids (Strom) are the dominant bioclasts, along with lesser amounts of mollusk, bryozoan (Bry), coral and indistinct skeletal fragments. Trace sponge spicules were also identified. Abundant micrite, including micritized peloids, plus minor clay and organics, comprise the matrix. A stromatoporoid fragment in this view shows an overall irregular structure, however local replacement by calcite spar cement (Cc) highlights the probable location of the original axial canal. Some fragments have also been replaced by minor amounts of chert, while trace framboidal pyrite has replaced matrix content. This sample lacks visible porosity. Closed fractures have been filled by minor calcite cement and secondary pyrite. **x12.5 ppl**

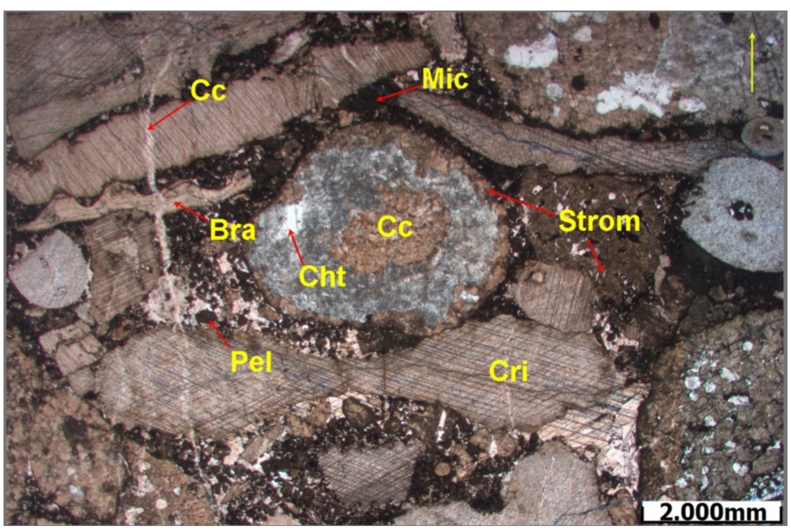

Figure 3.2. Sample T9, 9745.75ft/2970.50m. Alternate overview image of the grainstone. A healed vertical fracture is visible in the left-hand portion of the image. The fracture has been infilled by calcite cement (Cc), which in addition to chert (Cht), has also partially replaced a possible stromatoporoid (Strom) fragment. This view also shows a discoidal crinoid plate (Cri) which has a relatively thin interior and appears thickest towards its margin. The skeletal plate has been replaced by crystalline calcite which displays well-formed lamellar twinning. Rounded pellets (Pel) of unknown, possible fecal, origin locally comprise the micritic matrix (Mic). Bra: brachiopod fragment. **x12.5 ppl**

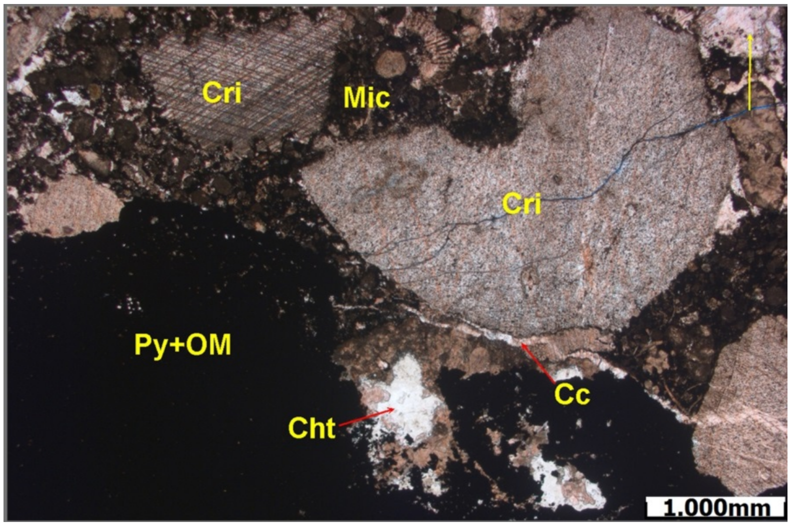

Figure 3.3. Sample T9, 9745.75ft/2970.50m. Low magnification view highlighting localized pyrite replacement of organic material (Py+Om). Minor chert (Cht) replacement of indistinct bioclasts is also shown. A subhorizontal fracture is infilled by calcite cement (Cc). Crinoid fragments (Cri) display characteristic uniform extinction under cross-polarized light. Mic: micritic matrix. **x25 ppl**

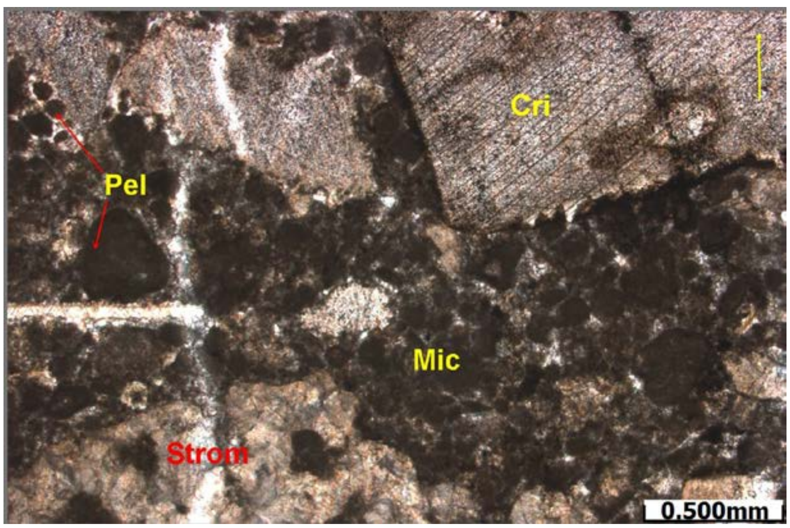

Figure 3.4. Sample T9, 9745.75ft/2970.50m. Moderate magnification view highlighting peloids (Pel) which comprise portions of the micritic matrix (Mic). Strom: stromatoporoid; Cri: crinoid fragment. **x50 ppl**

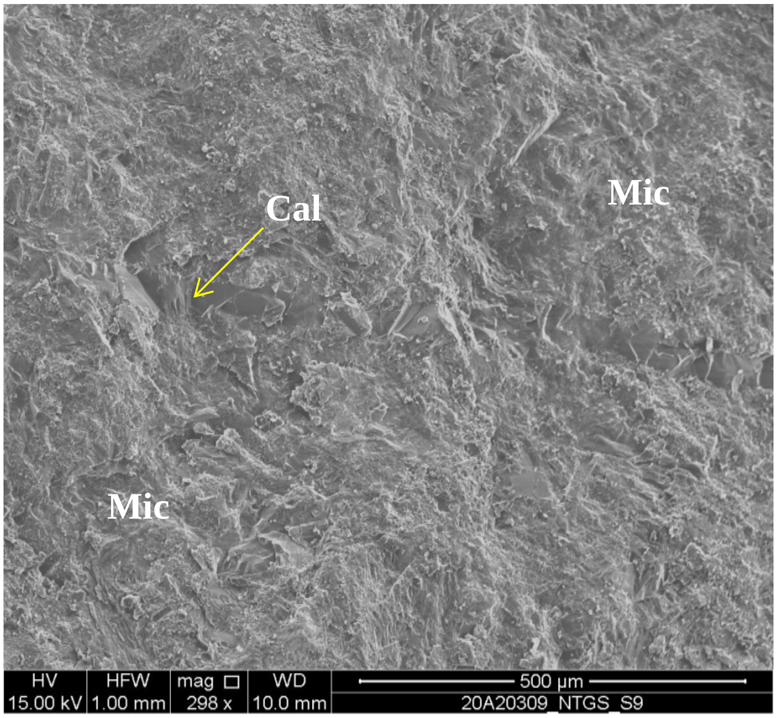

SEM Figure 3.5. Sample S9, 9745.75ft/2970.50m. Low magnification overview image of a calcite veinlet (Cal) within a micritic matrix (Mic). **x298**

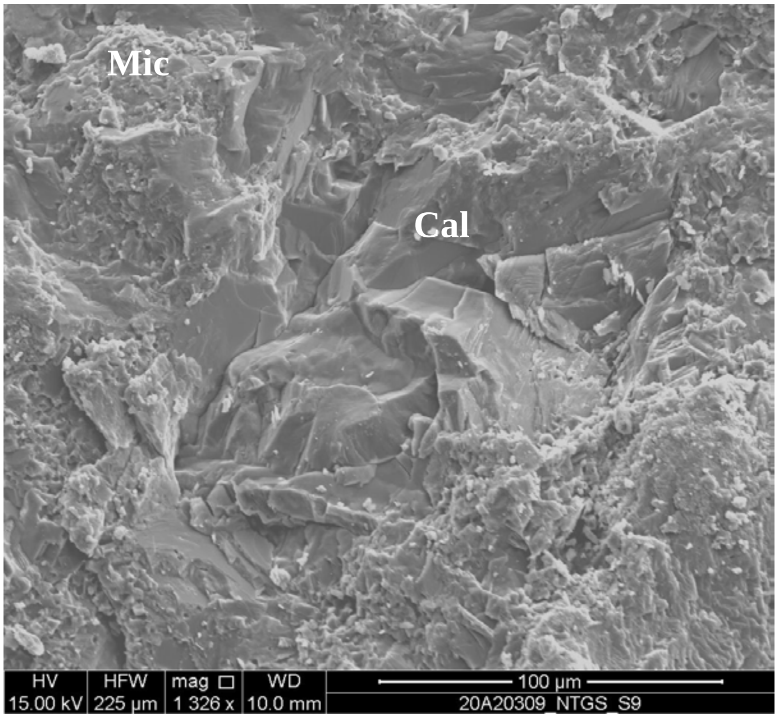

SEM Figure 3.6. Sample S9, 9745.75ft/2970.50m. Moderate magnification view showing subhedral calcite (Cal) within a micritic matrix (Mic). Porosity is poor. **x1326**

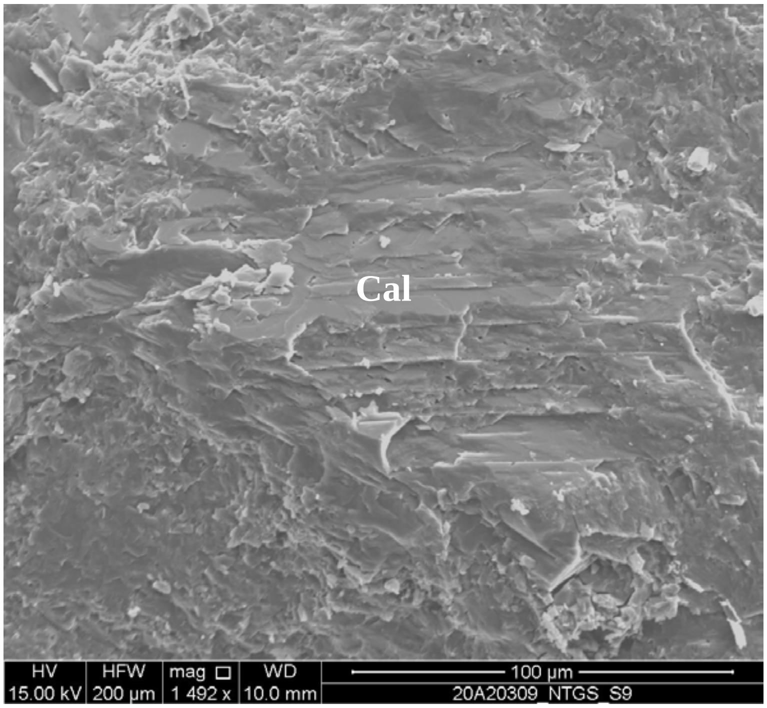

SEM Figure 3.7. Sample S9, 9745.75ft/2970.50m. Moderate magnification view of calcite (Cal) with well-developed cleavage. **x1492**

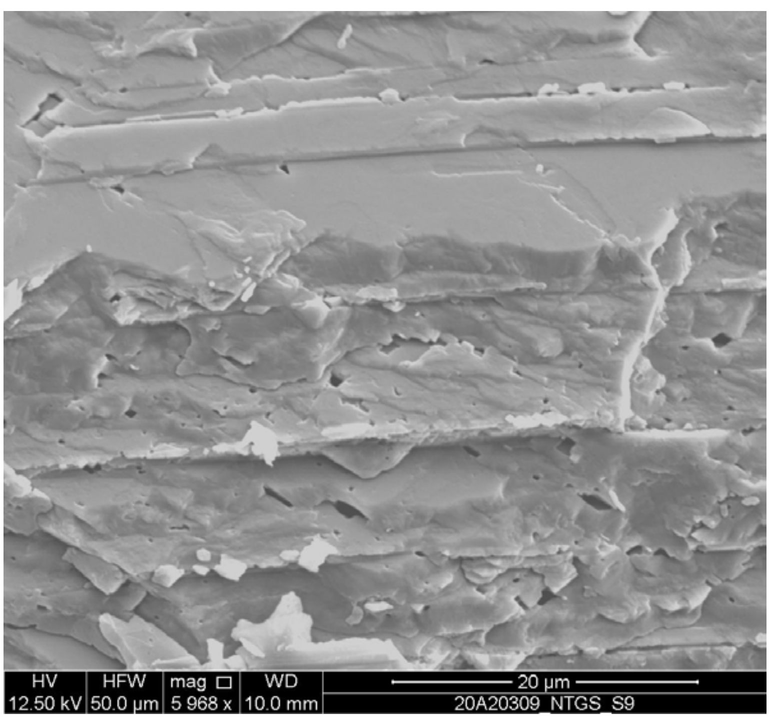

SEM Figure 3.8. Sample S9, 9745.75ft/2970.50m. Higher magnification view of calcite in **Figure 3.7** showing pinpoint micropores within the crystal. **x5968**

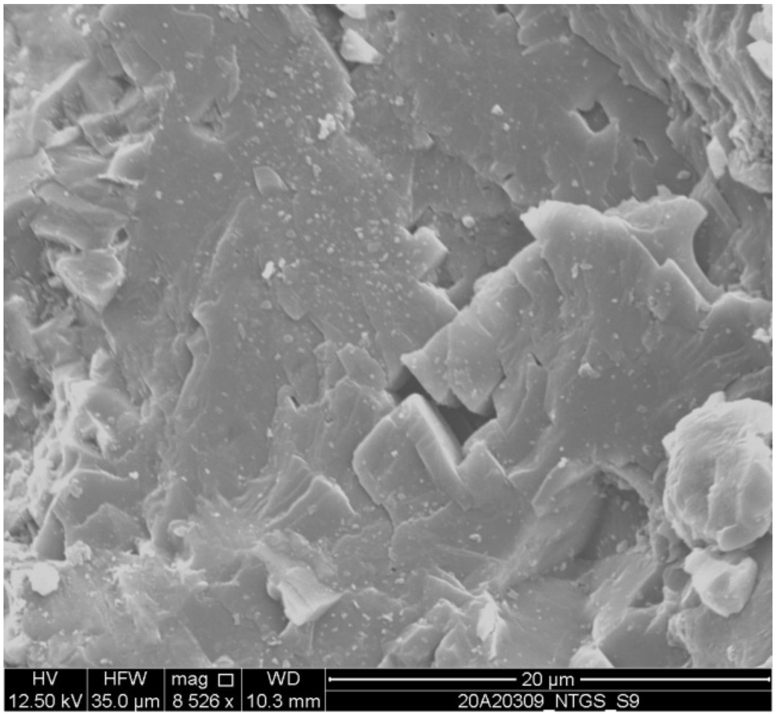

SEM Figure 3.9. Sample S9, 9745.75ft/2970.50m. Slightly higher magnification view of micropores in **Figures 3.7 and 3.8**. These pores likely represent interrupted growth within the crystal structure, or possible recrystallization. **x8526**

Sample T8/S8, 9761.50ft/2975.31m

Well Name	Texaco Bovie Lake J-72	**Location**	300/J-72-6020-12245/0
Sample Type	Thin section/SEM grain mount from a core sample	**Depth (m)**	9761.50ft/2975.31m
Stratigraphic Unit	Nahanni Formation	**Reservoir Quality**	Poor
Classification	Limestone (Wackestone)	**Stain type**	½ Dual carbonate stain

MINERALOGY

	Total Bulk mineralogy					
Thin Section Point counting (%)	**Calcite**	**Dolomite**	**Anhydrite**	**Quartz/Cht**	**Pyrite**	**Clays & organics**
	95	-	-	-	2	3
	Framework, Matrix, Cement, and Replacement					
	Carbonate clasts	**Bioclasts**	**Detrital grains**	**Matrix**	**Pore filling cement**	**Replacement**
	-	17	-	80	1	2

ADDITIONAL FEATURES and OTHER COMMENTS

Depositional	At the time of deposition the sample most likely had a massive structure. The sample displays trace calcite healed fractures. Fracturing occurred during burial diagenesis likely as a result of collapse associated with solution or tectonic deformation.
Textures	Based on the mineralogy and proportion of framework components in relation to matrix (micrite, clays and organics) the sample is classified as a limestone (wackestone). The texture of the micritic matrix (microcrystalline calcite) is anhedral, while local calcite spar cement has a sub- to euhedral texture.
Framework (Carbonate clasts, Bioclasts)	Petrographic summary Table 1 shows the detailed mineralogy of the sample. This sample is composed of calcite (95%), along with minor clays/organics (3%) and pyrite (2%). In regards to the framework components calcite occurs as various bioclasts including common to minor amounts of crinoid (7%), brachiopod (5%), coral (1%) and ostracod (1%) fragments, along with trace sponge spicules, stromatoporoid and bryozoa fragments, plus trace amounts of indistinct recrystallized skeletal grains.
Detrital Grains & Other Non-Carbonate Grains	There are no detrital grains in this sample.
Matrix	Calcite is the main component of the matrix (77%), while clays and organics (3%) make up the remaining portion of the matrix; however, this may be underestimated as the matrix appears dark and may have higher volumes of finely disseminated organic debris. SEM analysis shows clay particles are often distributed between micro-crystallines, while thin section observation shows clays and organics are also concentrated in thin laminae and/or low amplitude stylolites.
Pore Filling Cements	Minor amounts of sub- to euhedral calcite spar (1%), plus trace euhedral dolomite cement, has occluded intraparticle porosity associated with some bioclasts within the sample.
Replacement Minerals	Minor pyrite (2%) replacement of matrix constituents (micrite, clay and organics) were observed under reflected light.
Porosity	Trace porosity associated with open sub-vertical micro-fractures occur in this sample. However, the fracture may also have been generated during the coring process.

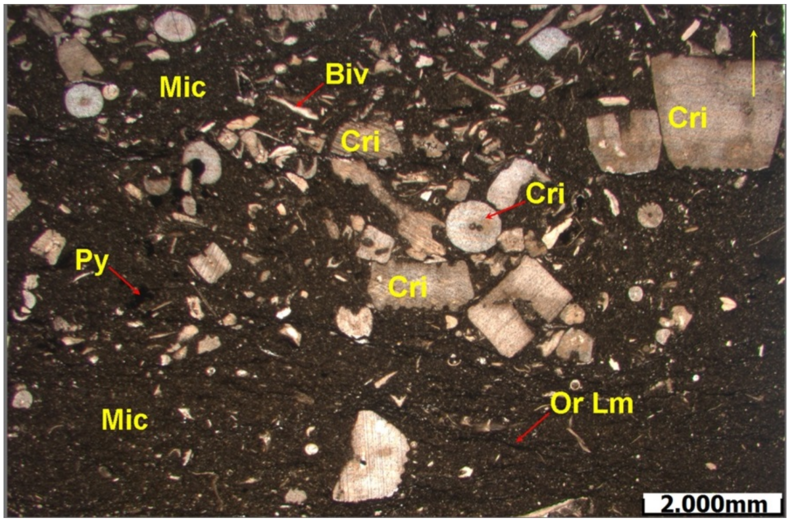

Figure 4.1. Sample T8, 9761.50ft/2975.31m. Overview image of the wackestone/packstone. Crinoid fragments appear to be the predominant faunal constituent, while bivalve (Biv) and brachiopod fragments were also noted in lesser amounts. Discontinuous wavy organic laminations (Or Lm) cross-cut the micritic matrix (Mic). Py: pyrite. **x12.5 ppl**

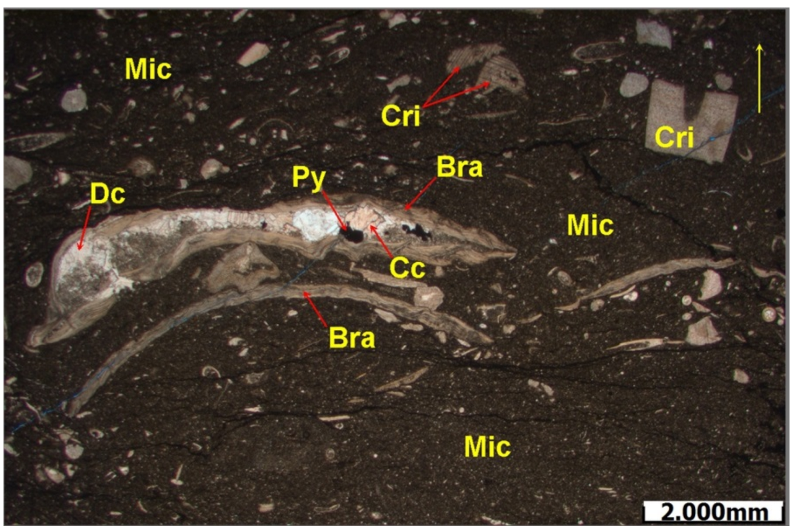

Figure 4.2. Sample T8, 9761.50ft/2975.31m. Low magnification image showing a probable compacted pseudopunctate brachiopod shell (Bra). Intraparticle porosity within the bioclast has been occluded by secondary dolomite (Dc), calcite (Cc) and pyrite (Py) cements. Crinoid fragments (Cri), along with other scattered bioclasts (as outlined in the summary table), are suspended in the micritic matrix (Mic). **x12.5 ppl**

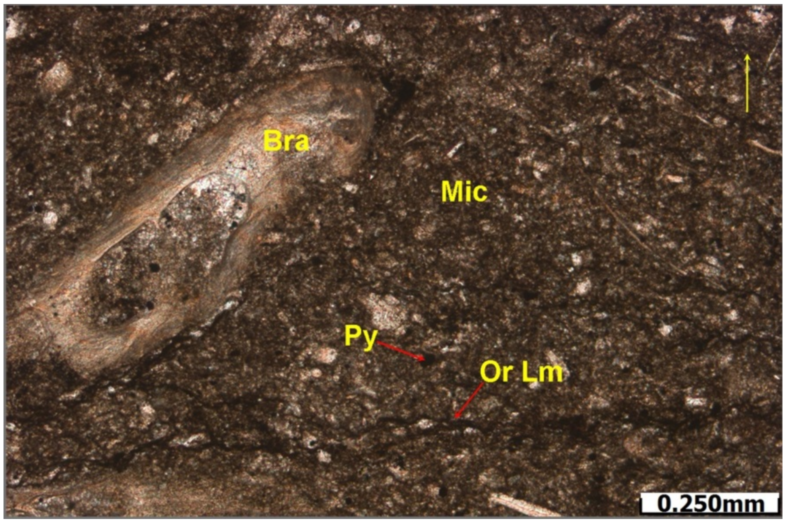

Figure 4.3. Sample T8, 9761.50ft/2975.31m. Close-up view of the micrite (microcrystalline calcite) matrix with organic laminae (Or Lm) or low amplitude stylolites. Scattered pyrite cubes and framboids are noted throughout the sample. A brachiopod shell fragment and possible cross-section showing where the spine attached to the shell.

x100 ppl

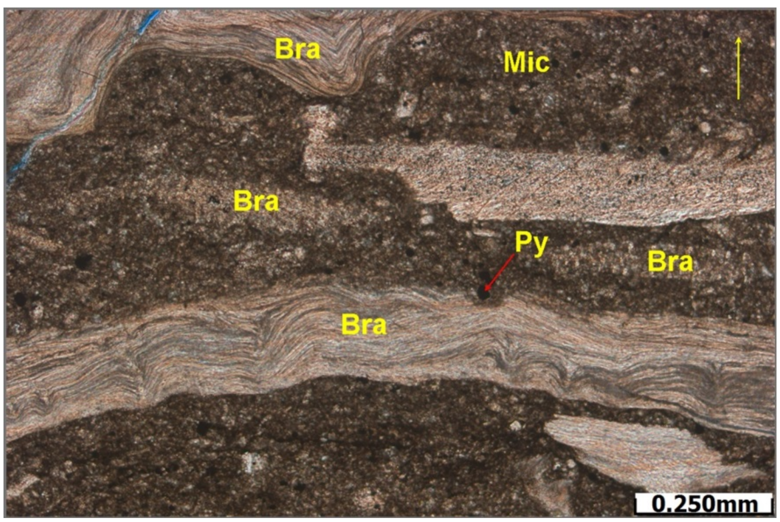

Figure 4.4. Sample T8, 9761.50ft/2975.31m. Alternate close-up view of pseudopunctuate brachiopod shell fragments (Bra) within a micritic matrix (Mic). These brachiopod shell fragments display a wavy fibrous structure. Possible punctate brachiopod shell fragments are noted towards the center of the image, but internal structure has been poorly preserved. Scattered pyrite cubes (Py) are noted throughout.

x100 ppl

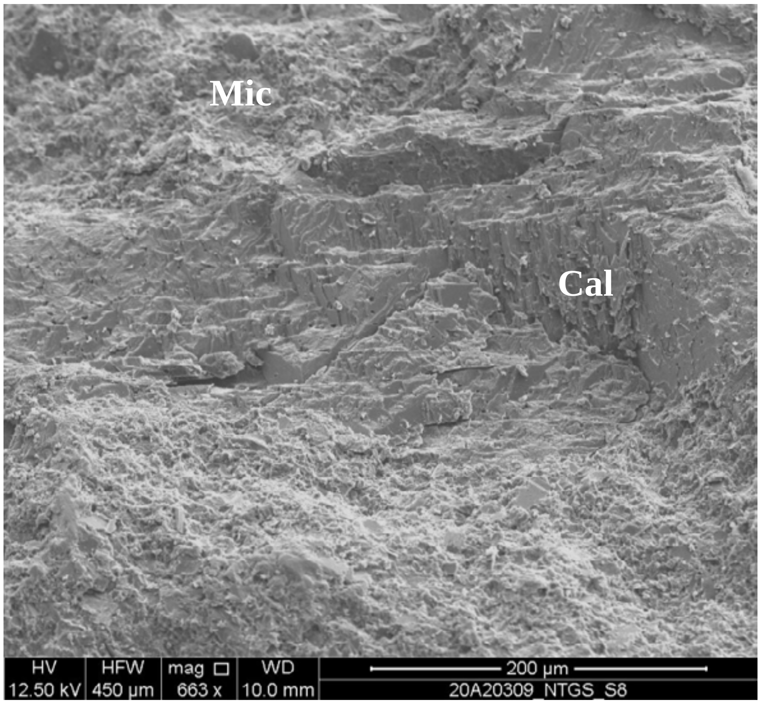

SEM Figure 4.5. Sample S8, 9761.50ft/2975.31m. Low magnification overview image showing medium to coarse crystalline calcite (Cal) within a relatively fine micritic matrix (Mic). Larger crystals within this sample are likely associated with scattered bioclasts. **x663**

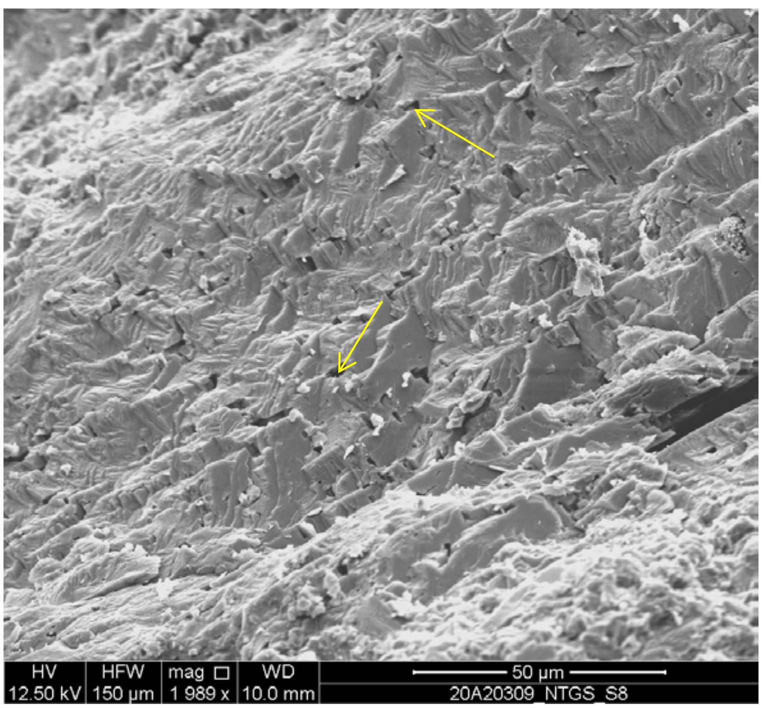

SEM Figure 4.6. Sample S8, 9761.50ft/2975.31m. Moderate magnification image showing intraparticle porosity (yellow arrows) associated with medium to coarse calcite crystals shown in **Figure 4.5**. **x1989**

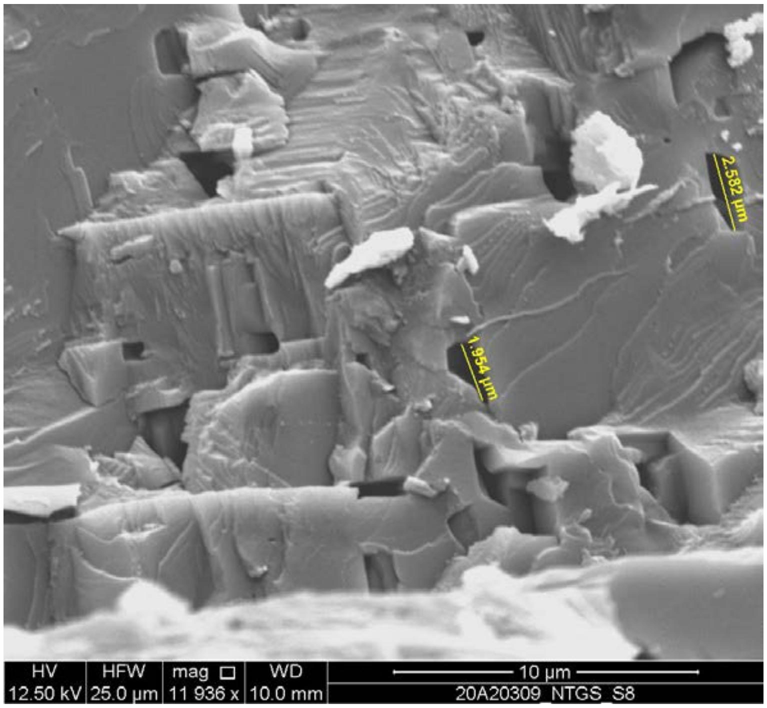

SEM Figure 4.7. Sample S8, 9761.50ft/2975.31m. Higher magnification image of **Figure 4.6** showing scattered angular micropores (<3µm). **x11936**

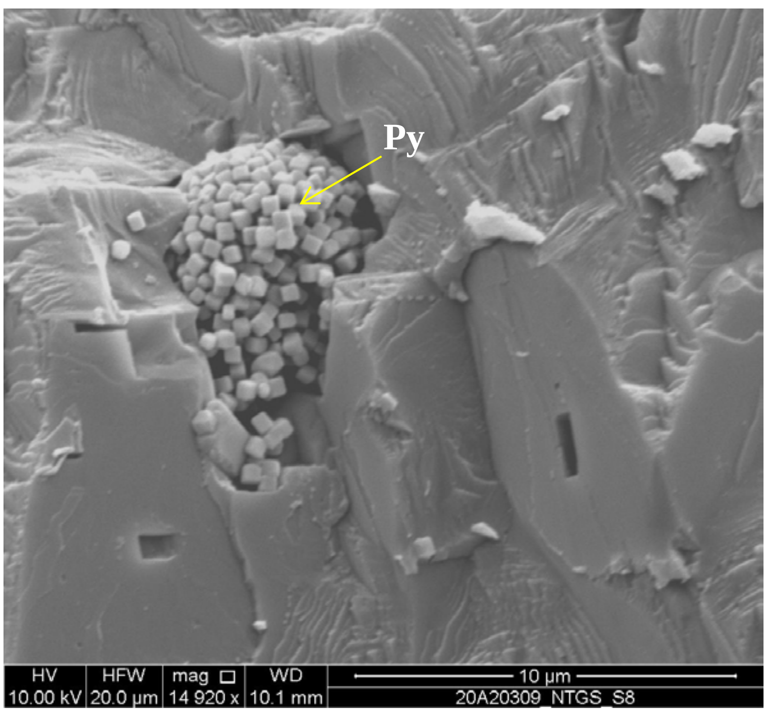

SEM Figure 4.8. Sample S8, 9761.50ft/2975.31m. High magnification image of a pyrite framboid (Py), with some scattering of individual crystallites. **x14920**

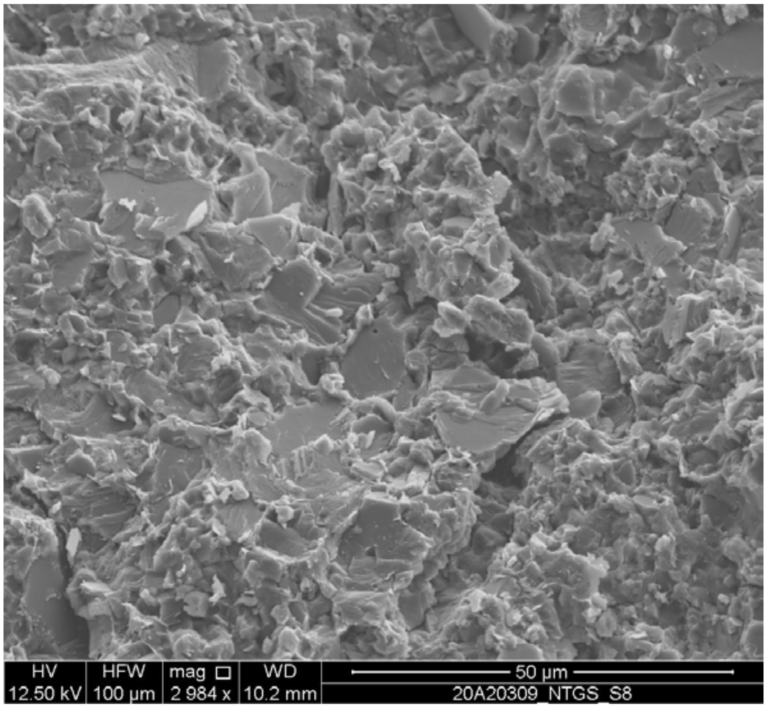

SEM Figure 4.9. Sample S8, 9761.50ft/2975.31m. Moderate magnification view of a portion of the matrix, which consists predominately of calcite, plus clays. See **Figure 4.10** for a more detailed view of the matrix. **x2984**

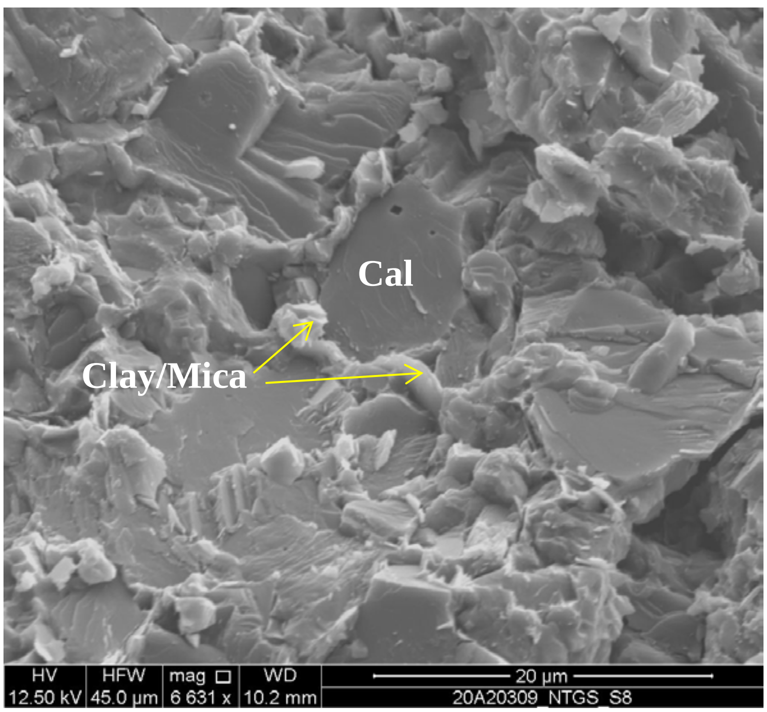

SEM Figure 4.10. Sample S8, 9761.50ft/2975.31m. High magnification view showing platy interstitial clays and/or micas (Clay/Mica). See **Figure 4.10a** for elemental composition as determined by EDX analysis. Cal: calcite. **x6631**

Sample T7/S7/X15, 9785.00ft/2982.47m

Well Name	Texaco Bovie Lake J-72	**Location**	300/J-72-6020-12245/0
Sample Type	Thin section/SEM grain mount from a core sample	**Depth (m)**	9785.00ft/2982.47m
Stratigraphic Unit	Nahanni Formation	**Reservoir Quality**	Poor
Classification	Limestone (Packstone)	**Stain type**	½ Dual carbonate stain

MINERALOGY

	Total Bulk mineralogy					
Thin Section Point counting (%)	**Calcite**	**Dolomite**	**Anhydrite**	**Quartz/Cht**	**Pyrite**	**Clays & organics**
	84	-	-	1	-	15
	Framework, Matrix, Cement, and Replacement					
	Carbonate clasts	**Bioclasts**	**Detrital grains**	**Matrix**	**Pore filling cement**	**Replacement**
	-	52	-	45	-	3

ADDITIONAL FEATURES and OTHER COMMENTS

Depositional	At the time of deposition, the sample was most likely massive. Formation of low amplitude stylolites and fracturing of the sediment typically happens during burial diagenesis (mechanical and chemical compaction).
Textures	Based on the mineralogy and proportion of framework components in relation to matrix (micrite, clays and organics) the sample is classified as a limestone (packstone). The texture of the micrite (microcrystalline calcite) matrix is anhedral, while local calcite spar cement has a sub- to euhedral texture.
Framework (Carbonate clasts, Bioclasts)	Petrographic summary Table 1B shows the detailed mineralogy of the sample. This sample is composed of abundant calcite (84%), along with moderate amounts of clays/organics (15%), plus minor pyrite (1%). In regards to the framework components, calcite occurs as various bioclasts moderate amounts of indistinct bioclasts (20%) and sponge spicules (15%), plus common to minor amounts of mollusk (8%), stromatoporoid (5%), brachiopod (3%) and gastropod (1%) fragments.
Detrital Grains & Other Non-Carbonate Grains	There are no detrital grains in this sample.
Matrix	Calcite is the main component of the matrix (30%), while clays and organics (15%) make up the remaining portion of the matrix.
Pore Filling Cements	Trace sub- to euhedral calcite spar occludes rare intraparticle porosity associated with some bioclasts within the sample.
Replacement Minerals	Minor sparry calcite (2%) has locally overprinted the original grain fabric and occludes rare intraparticle pores. Minor pyrite (1%) replacement of matrix constituents (micrite, clay and organics) can be observed under reflected light.
Porosity	This sample lacks visible porosity; however, the micritic matrix may be a source of microporosity.

Annotated microphotographs with descriptions for the thin section and SEM samples are provided below.

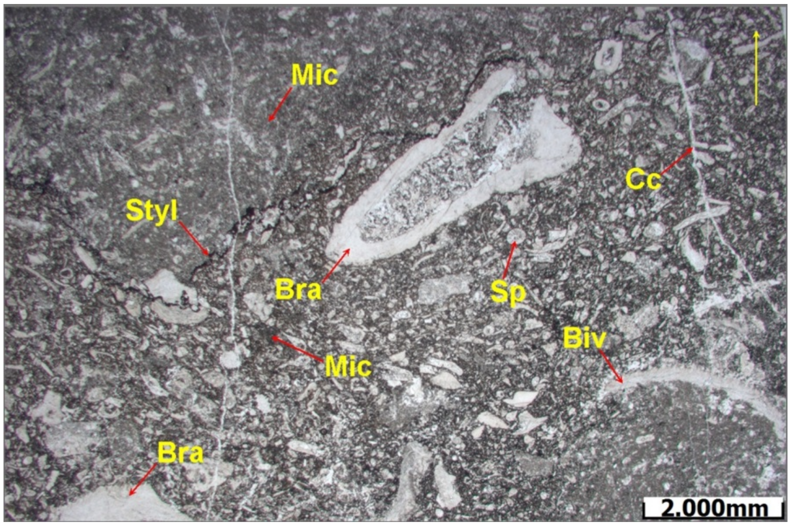

Figure 5.1. Sample T7, 9785.00ft/2982.47m. Overview image of the packstone/grainstone which lacks applied dual carbonate stain. Abundant bioclast fragments identified include sponge spicules (Sp), bivalves (Biv), brachiopods (Bra), ostracods, gastropods and stomatoporoids. The micritic matrix (Mic) is cross-cut by stylolites (Styl), defined by concentrations of insoluble organic residue, and calcite-healed (Cc) vertical microfractures. **x12.5 ppl**

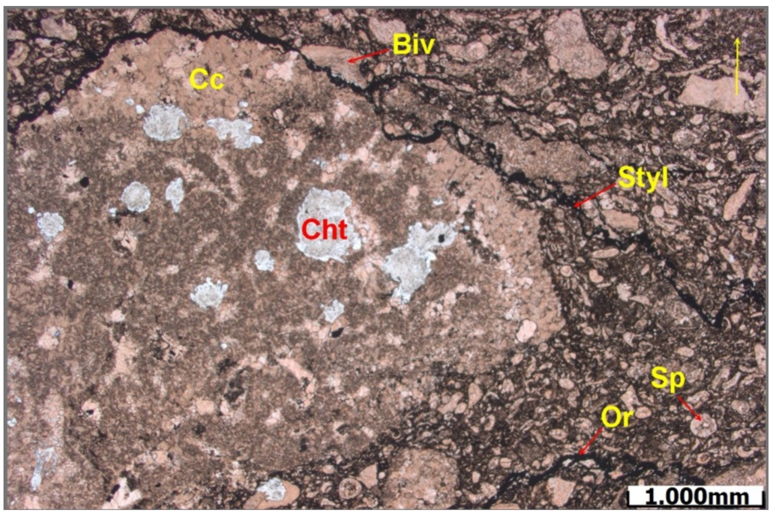

Figure 5.2. Sample T7, 9785.00ft/2982.47m. Low magnification view featuring a relatively large stromatoporoid fragment. Possible relicts of the clinoreticular microstructure are poorly preserved due to replacement by calcite (Cc) and chert (Cht) cements. Calcite cement appears pink within this view due to the applied dual carbonate stain. Abundant skeletal fragments within the surrounding matrix consist mainly of sponge spicules (Sp) and lesser amounts of bivalve (Biv) fragments. Styl: stylolites. **x25 ppl**

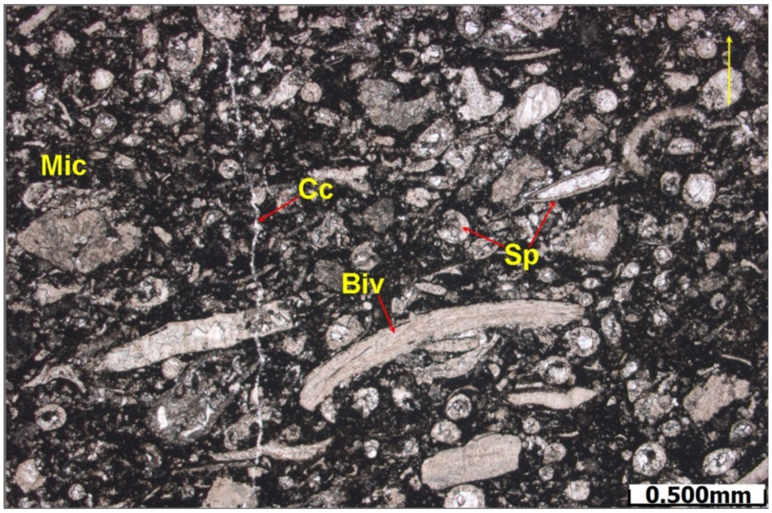

Figure 5.3. Sample T7, 9785.00ft/2982.47m. Moderate magnification view of an unstained portion of the thin section displaying dominantly longitudinal and transverse sections through calcite replaced sponge spicules (Sp). A single central canal has been preserved within many of the fragments. A bivalve fragment (Biv) displaying a fibrous lamallar crystal structure is also featured. A vertical microfracture cross-cuts some of the skeletal fragments and appears to be infilled by calcite cement (Cc). Mic: micrite. **x50 ppl**

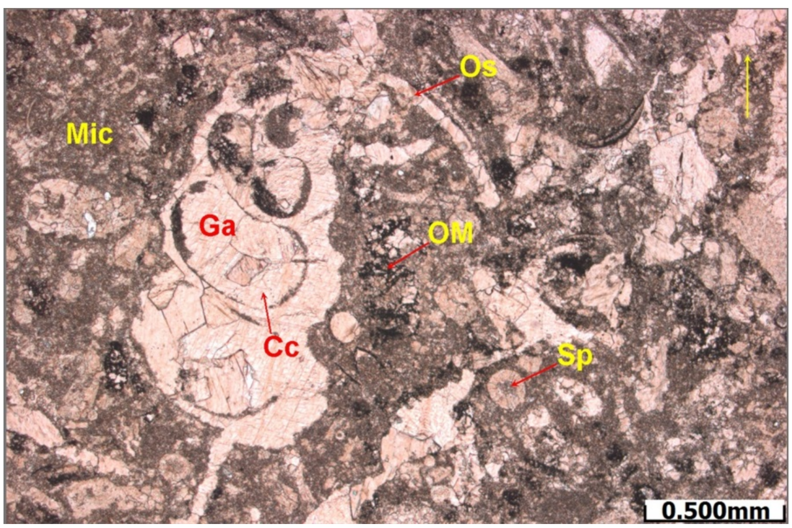

Figure 5.4. Sample T7, 9785.00ft/2982.47m. Alternate moderate magnification image highlighting a gastropod shell (Ga). Both the shell and internal cavities have mostly been replaced by very fine crystalline calcite (Cc). A partial ostracode carapace (Os) and sponge spicules (Sp) are also visible within this view. Mic: micrite; Py: pyrite. **x50 ppl**

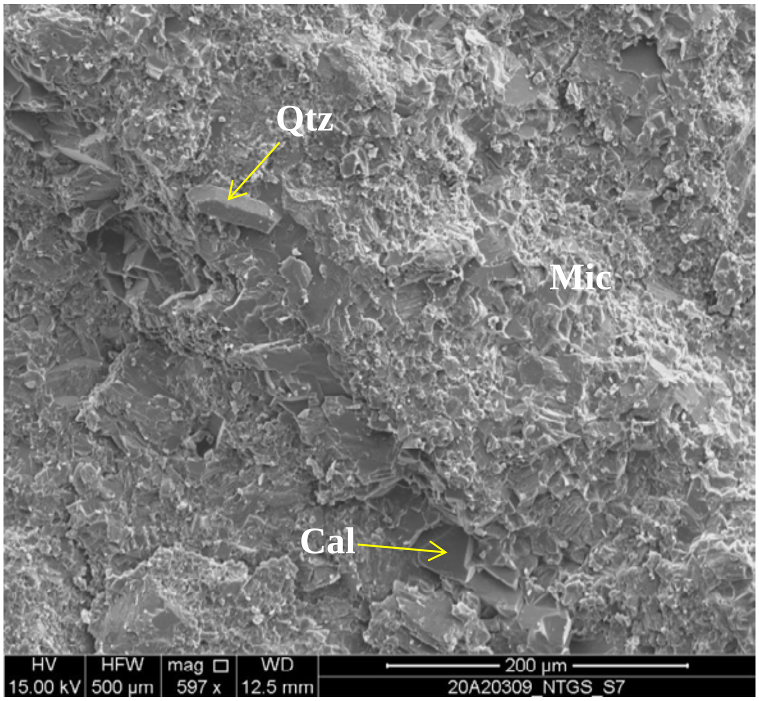

SEM Figure 5.5. Sample S7, 9785.00ft/2982.47m. Low magnification overview of the limestone. A calcite vein (Cal) is shown within a calcite micrite (Mic). A trace euhedral quartz crystal (Qtz) is noted in proximity to the vein. **x597**

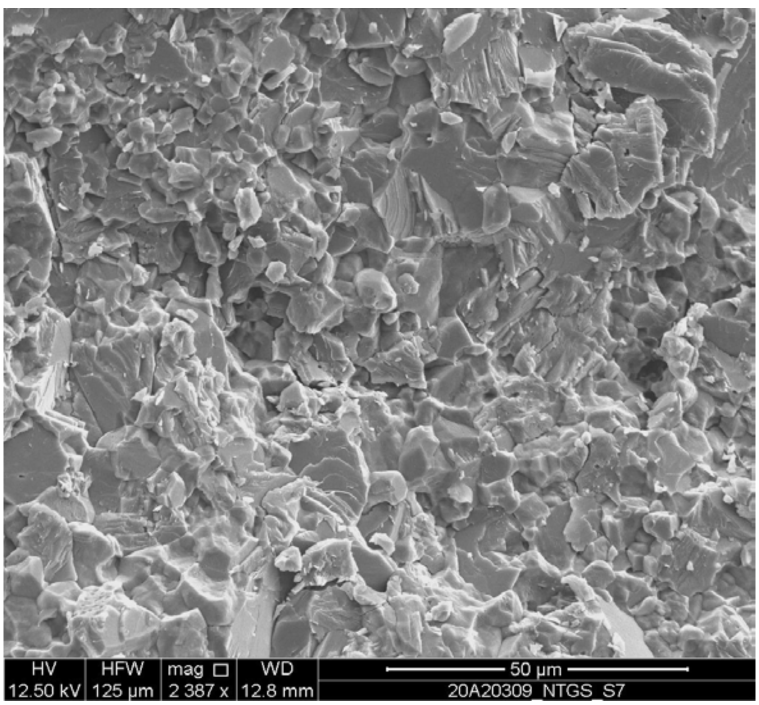

SEM Figure 5.6. Sample S7, 9785.00ft/2982.47m. Moderate magnification image showing details of the very fine to fine crystalline calcite matrix shown in **Figure 5.5**. Surface topography and grain plucking along the broken sample surface has resulted in artefact porosity. Overall porosity for this sample is estimated to be poor. **x2387**

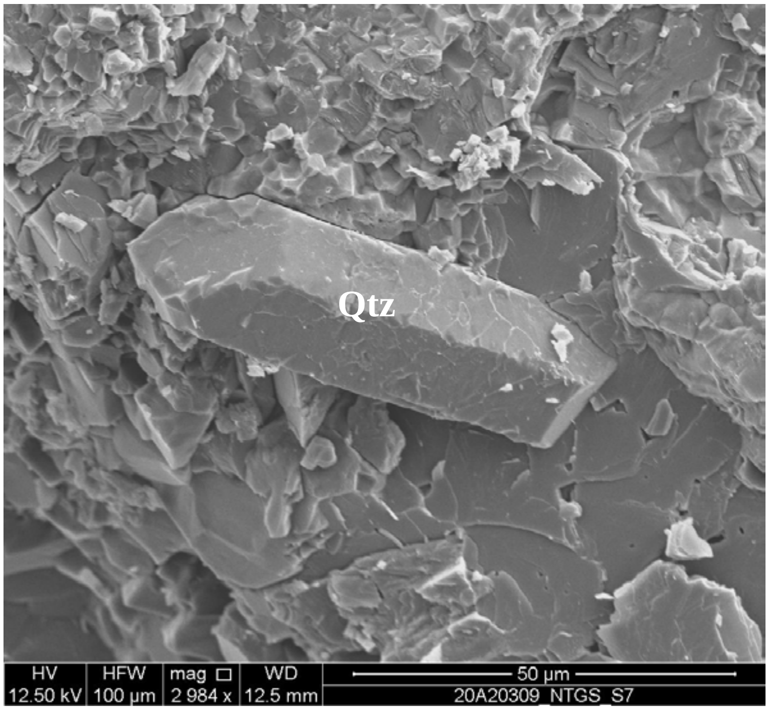

SEM Figure 5.7. Sample S7, 9785.00ft/2982.47m. Moderate magnification view of secondary euhedral quartz (Qtz), as shown in **Figure 5.5**. **x2984**

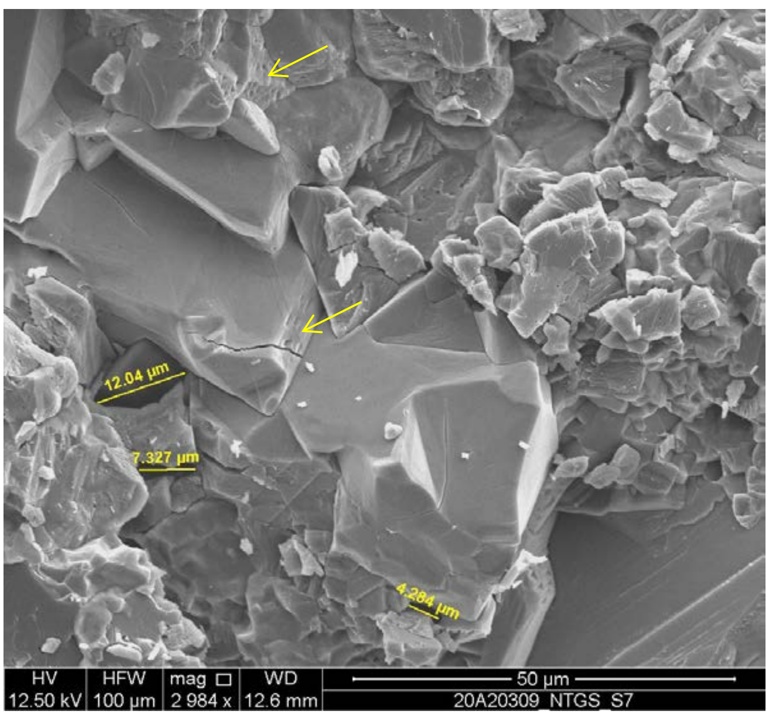

SEM Figure 5.8. Sample S7, 9785.00ft/2982.47m. Moderate magnification view highlighting a portion of the calcite vein-fill shown in **Figure 5.5**. Elongate intercrystalline pores ranging in size from ~5-12µm are shown along the vein contact. Dissolution pitting, or etching, is noted on some crystal surfaces (yellow arrows). **x2984**

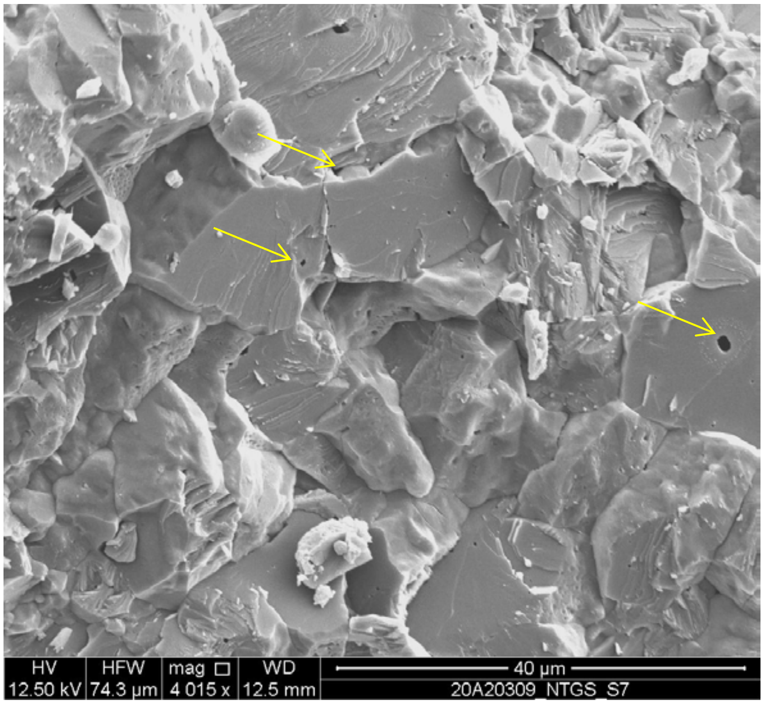

SEM Figure 5.9. Sample S7, 9785.00ft/2982.47m. Moderate magnification image of fine crystalline calcite. Scattered visible inter- and intracrystalline micropores (yellow arrows) are shown in more detail in the subsequent images. **x4015**

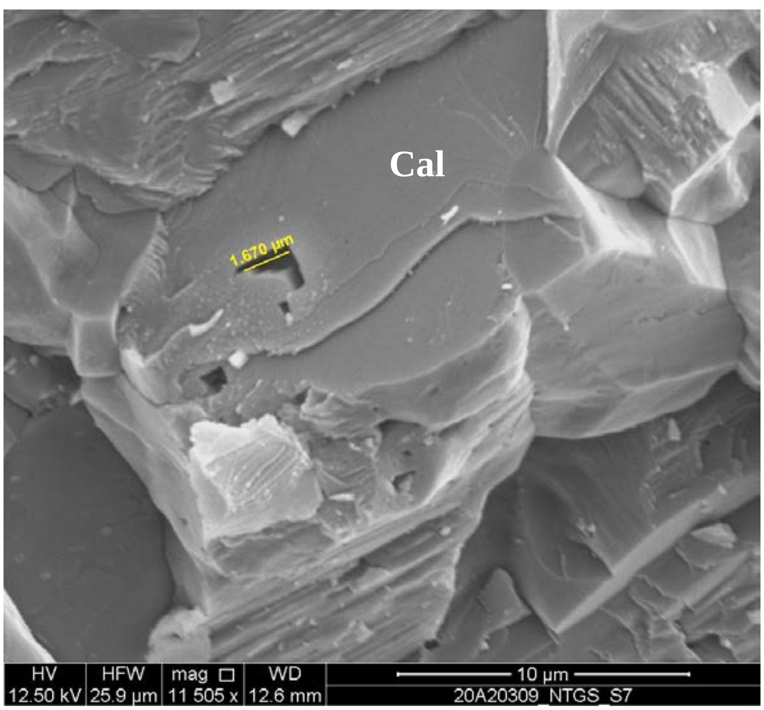

SEM Figure 5.10. Sample S7, 9785.00ft/2982.47m. High magnification image of an intracrystalline micropore (~1.6µm) with minute secondary crystal growth surrounding the pore opening. Cal: calcite **x4015**

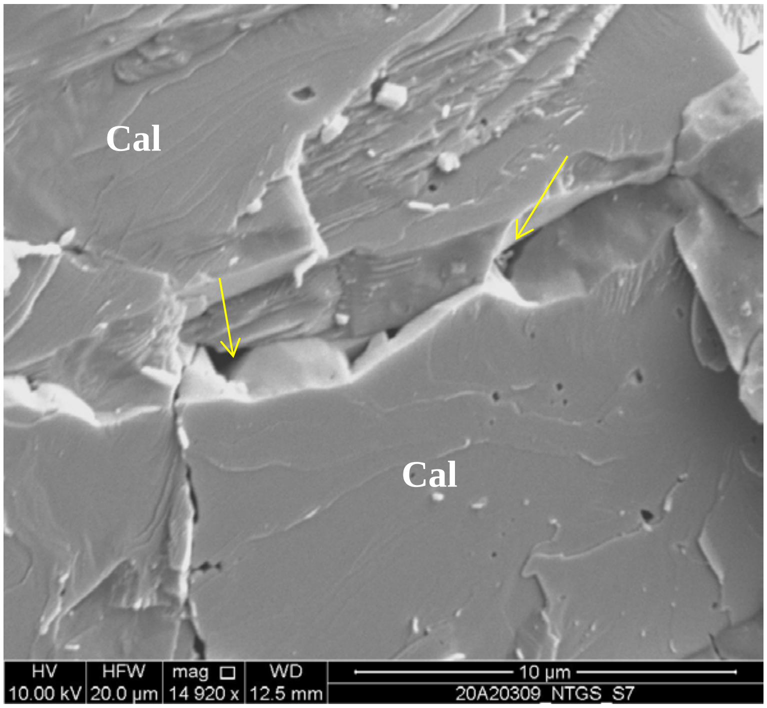

SEM Figure 5.11. Sample S7, 9785.00ft/2982.47m. Very high magnification image highlighting trace intercrystalline microporosity (yellow arrows) as shown in **Figure 5.9**. Cal: calcite. **x14920**

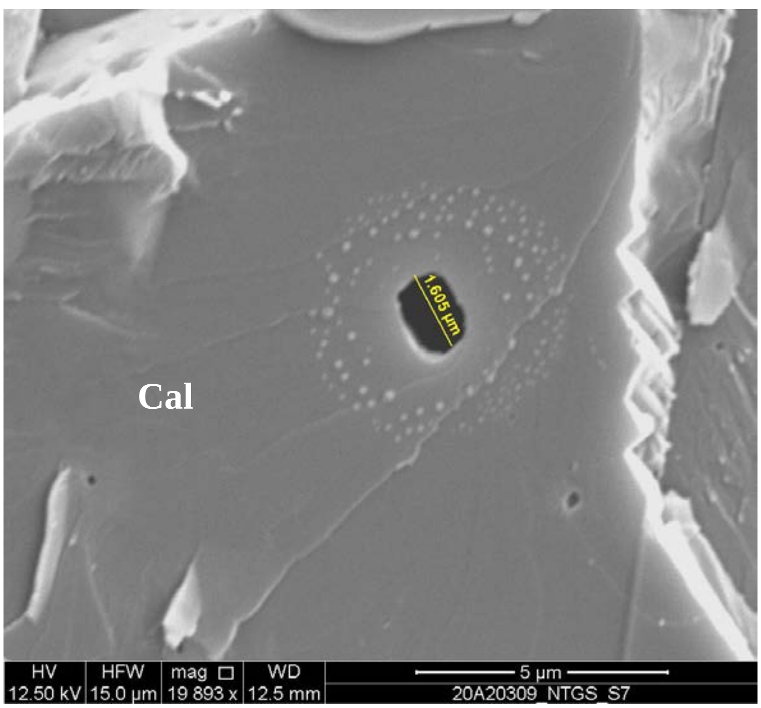

SEM Figure 5.12. Sample S7, 9785.00ft/2982.47m. Alternate very high magnification image showing an intracrystalline micropore (~1.6µm), as featured in **Figure 5.9**, with minute secondary crystal growth surrounding the pore opening. Cal: calcite. **x19893**

Sample T6/S6, 9799.00ft/2986.74m

Well Name	Texaco Bovie Lake J-72	**Location**	300/J-72-6020-12245/0
Sample Type	Thin section/SEM grain mount from a core sample	**Depth (m)**	9799.00ft/2986.74m
Stratigraphic Unit	Nahanni Formation	**Reservoir Quality**	Poor
Classification	Limestone (wackestone/packstone)	**Stain type**	½ Dual carbonate stain

MINERALOGY

	Total Bulk mineralogy					
Thin Section Point counting (%)	Calcite	Dolomite	Anhydrite	Quartz/Cht	Pyrite	Clays & organics
	94	-	-	TR	1	5
	Framework, Matrix, Cement, and Replacement					
	Carbonate clasts	Bioclasts	Detrital grains	Matrix	Pore filling cement	Replacement
	15	30	TR	47	2	6

ADDITIONAL FEATURES and OTHER COMMENTS

Depositional	At the time of deposition, the sample was most likely massive. Formation of low amplitude stylolites and fracturing of the sediment typically happens during burial diagenesis (mechanical and chemical compaction).
Textures	Based on the mineralogy and proportion between framework components (carbonate clasts and bioclasts) and matrix, the sample was classified as a wackestone-packstone. For the matrix, the crystal texture has been determined as anhedral, while cement shows subhedral to euhedral crystal texture. Majority of bioclasts have been replaced by calcite spar; therefore, internal structure is poorly preserved.
Framework (Carbonate clasts, Bioclasts)	Petrographic Summary Table 1B shows detailed mineralogy of the sample. This sample contains 94% calcite. Other minerals include clays and organics (5%), pyrite (1%), plus trace amounts of detrital quartz. In regards to the framework components, calcite occurs mainly as bioclasts (sponge spicules 10%, stromatoporoids 10%, indistinct 5%, bryozoa 3%, echinoderm 1%, plus trace ostracode and foraminifer fragments). Carbonate clasts (peloids 15%) are commonly observed in the collected sample.
Detrital Grains & Other Non-Carbonate Grains	Trace amounts of detrital quartz grains.
Matrix	Calcite is the main component of the matrix (42%), while clays and organics (5%) make up the remaining portion of the matrix; however, this may be underestimated as the matrix appears dark and may have higher volumes of finely disseminated organic debris.
Pore Filling Cements	Vertical and subhorizontal fractures are infilled by minor calcite spar (2%).
Replacement Minerals	Minor patchy calcite spar (5%) has overprinted the original grain fabric. Minor replacement of matrix constituents (micrite, clay and organics) by pyrite (1%) can be observed under reflected light.
Porosity	This sample lacks visible porosity. Under SEM, the micritic matrix shows tightly packed crystallites, with only trace amounts of scattered micropores.

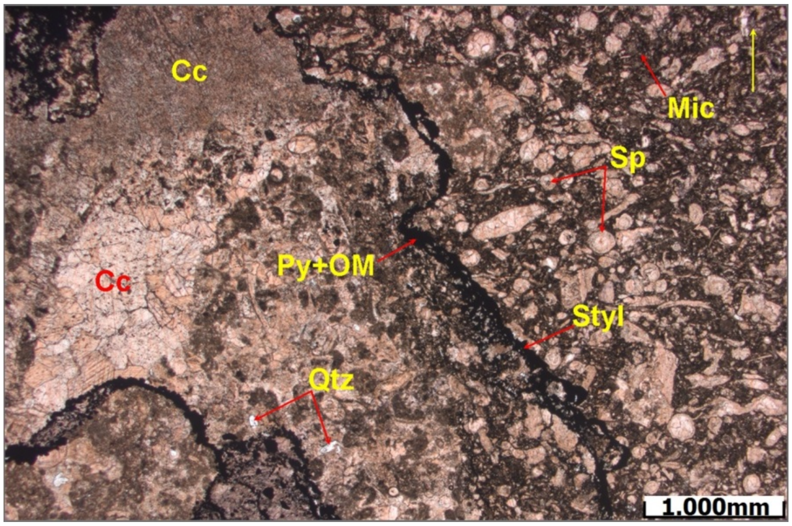

Figure 6.1. Sample T6, 9799.00ft/2986.74m. Low magnification view of the limestone (wackestone-packstone). Bioclasts have been recrystallized and therefore morphological features have generally been poorly preserved. Rounded to elongate skeletal fragments within this view are interpreted to be transverse and longitudinal sections of sponge spicules (SP). Patchy calcite cement (Cc) is noted. Rare scattered quartz grains (Qtz) are noted within the crystalline to micritic (Mic) matrix. This view shows stylolites (Styl) that consist of insoluble organic residue that has been partly replaced by pyrite (Py+OM). **x25 ppl**

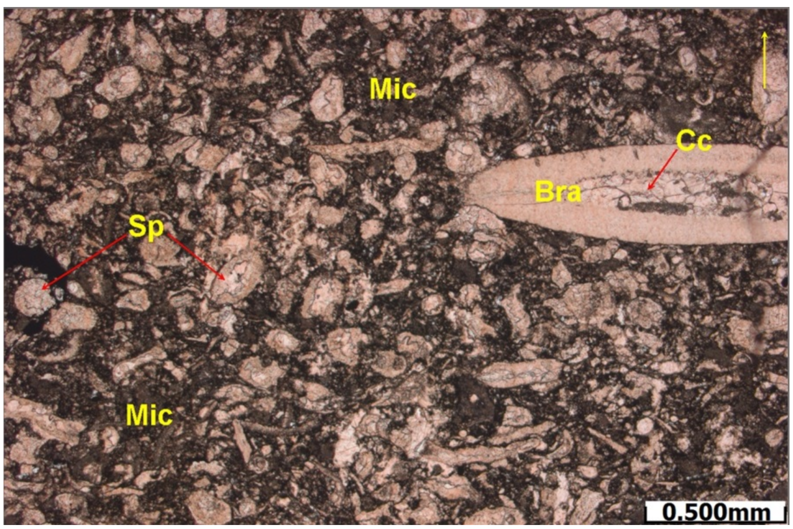

Figure 6.2. Sample T6, 9799.00ft/2986.74m. Moderate magnification view of a brachiopod shell fragment, or possible echinoderm, displaying relict punctae. Sponge spicules (Sp) and scattered indistinct bioclasts are also shown. Mic: micrite; Cc: calcite cement. **x50 ppl**

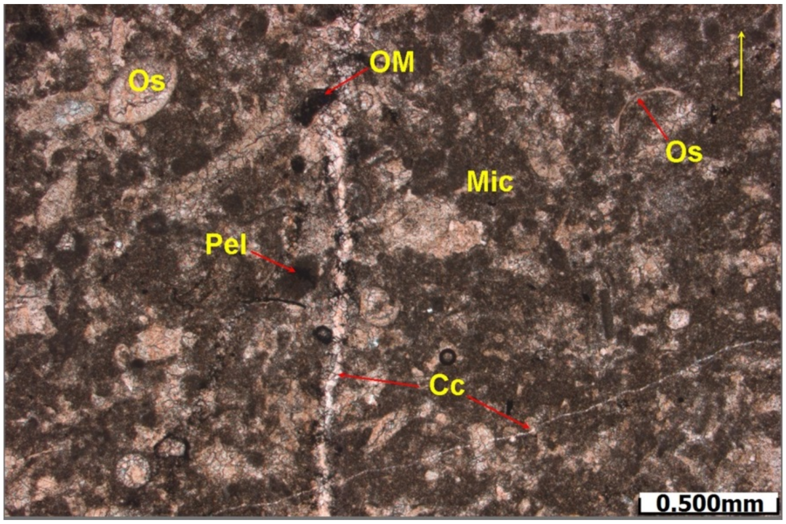

Figure 6.3. Sample T6, 9799.00ft/2986.74m. Alternate moderate magnification view showing both vertical and subhorizontal microfractures that have been infilled by calcite cement (Cc). At higher magnifications the micritic matrix (Mic) displays an overall peloidal texture (Pel). OM: organic matter; Os: ostracod. **x50 ppl**

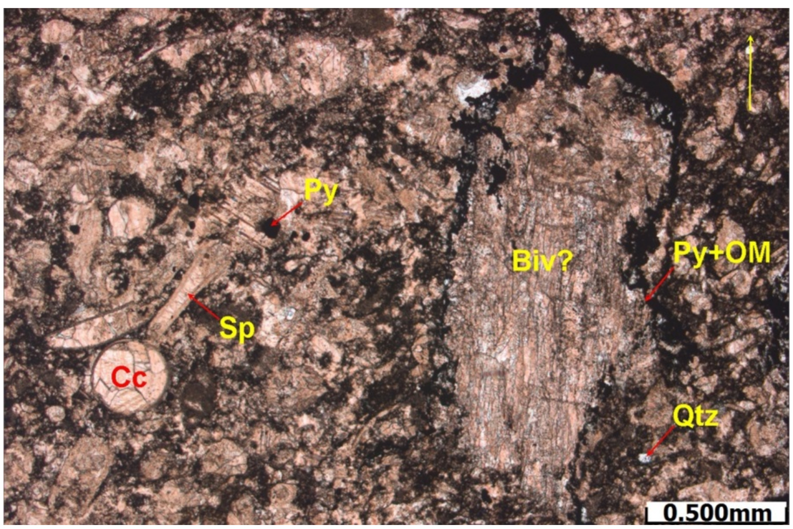

Figure 6.4. Sample T6, 9799.00ft/2986.74m. Moderate magnification view showing a possible bivalve shell fragment displaying a fibrous structure (Biv?). Many of the bioclasts within the sample have been extensively replaced by calcite spar (Cc) and are therefore classified as 'unidentified' within the petrographic summary. A sponge spicule (Sp) displaying a preserved central canal is shown within this view. A rare silt-sized detrital quartz grain is noted (Qtz). Py: framboidal pyrite; Py+OM: pyrite and organics. **x50 ppl**

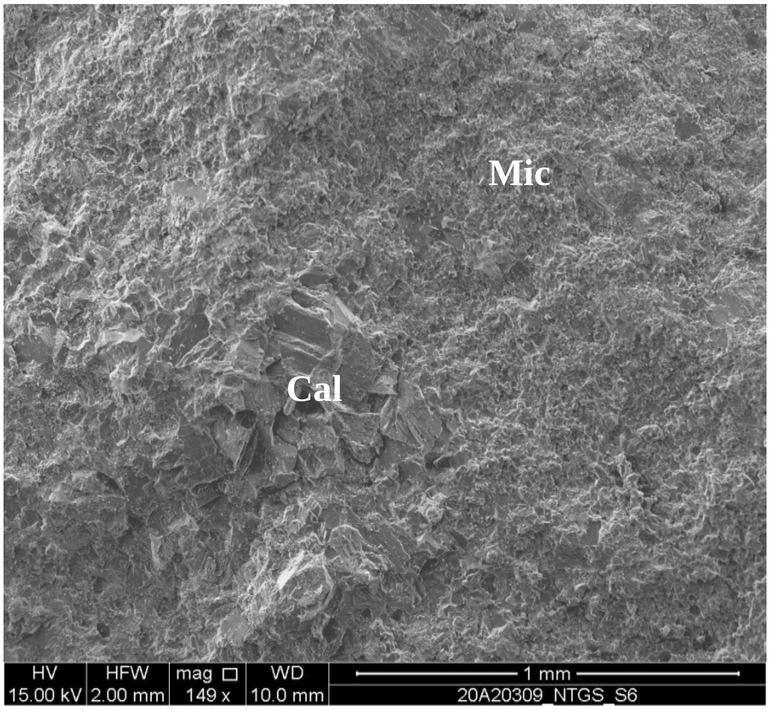

SEM Figure 6.5. Sample S6, 9799.00ft/2986.74m. Low magnification overview of the limestone highlighting the calcite micrite matrix (Mtx) with patchy medium crystalline calcite (Cal). Porosity is estimated to be poor within this sample. **x149**

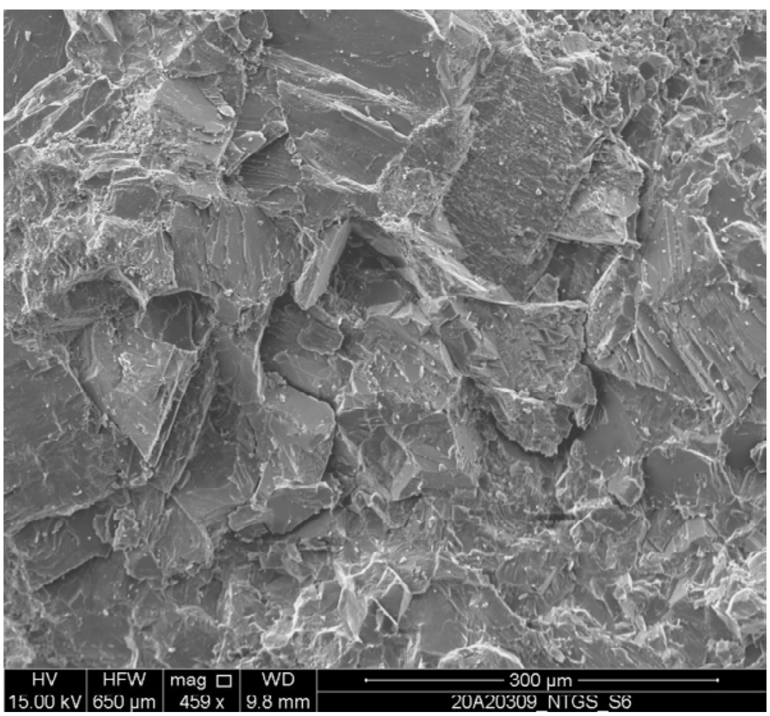

SEM Figure 6.6. Sample S6, 9799.00ft/2986.74m. Slightly higher magnification image showing details of the patchy medium crystalline calcite highlighted in **Figure 6.5**. There is no visible porosity associated with the interlocking crystal texture, while some minor visible fractures are considered to be an artefact of sample preparation. **x459**

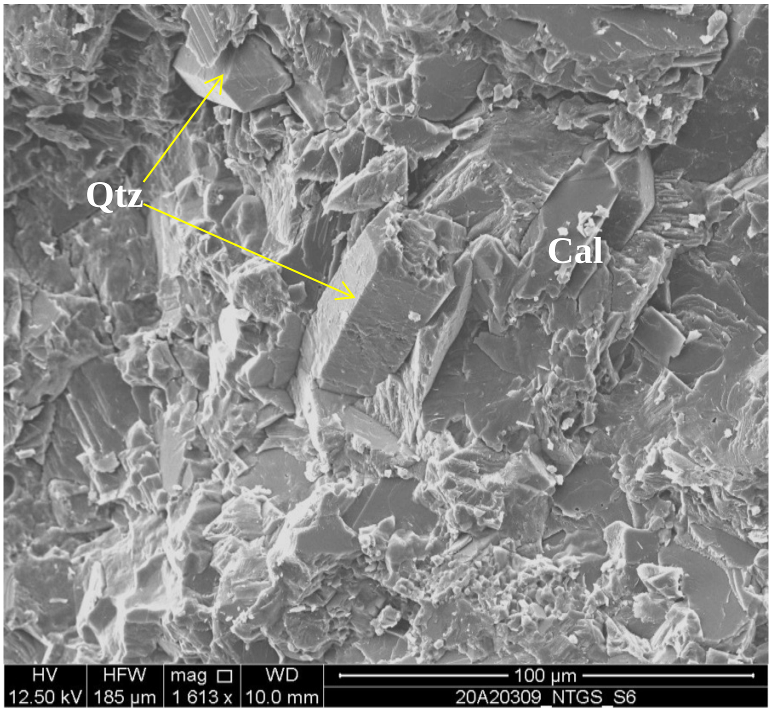

SEM Figure 6.7. Sample S6, 9799.00ft/2986.74m. Moderate magnification image showing trace authigenic quartz (Qtz). Cal: calcite. **x1613**

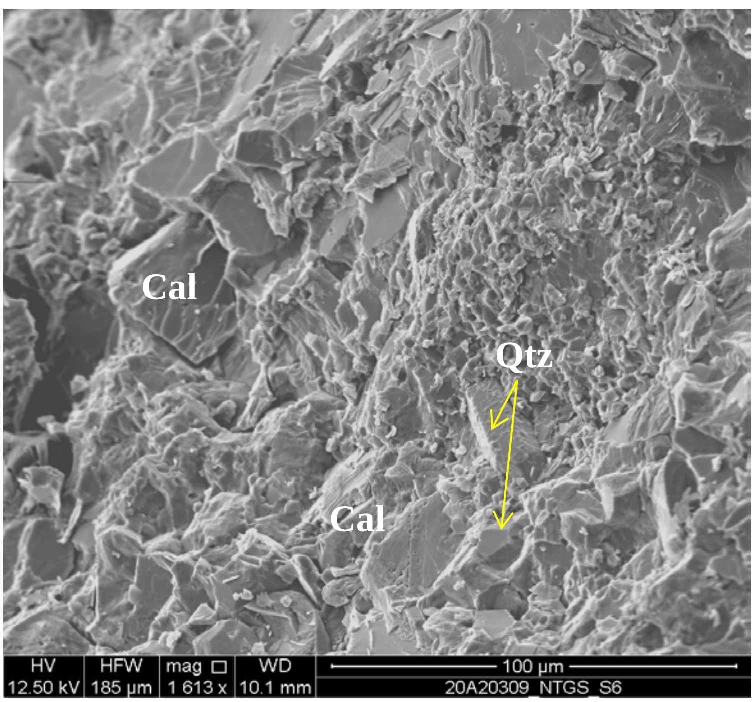

SEM Figure 6.8. Sample S6, 9799.00ft/2986.74m. Additional image of authigenic quartz (Qtz) within the sample. Cal: calcite. **x1613**

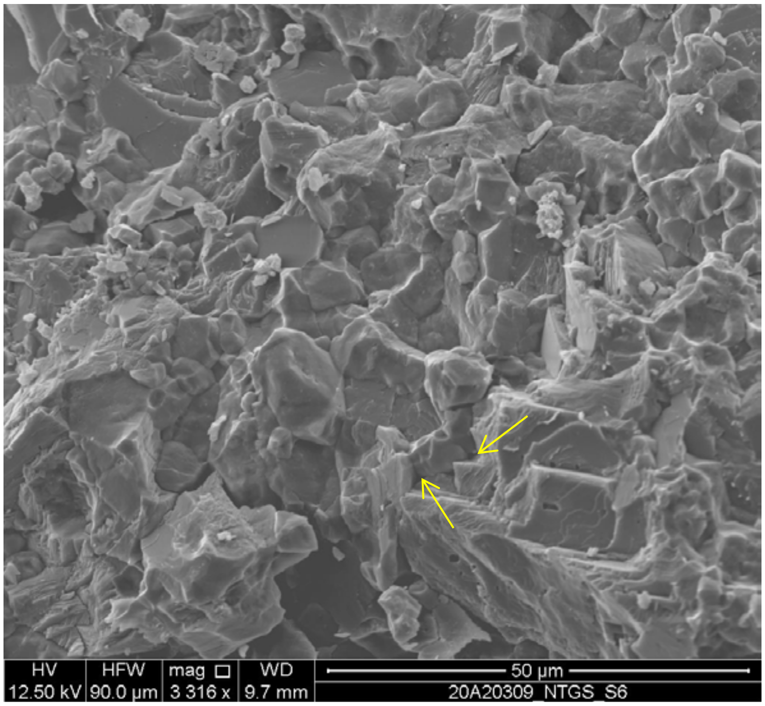

SEM Figure 6.9. Sample S6, 9799.00ft/2986.74m. High magnification image showing details of the calcite matrix. Only trace micropores (highlighted by yellow arrows) are visible within the generally tightly interlocking crystal fabric. **x3316**

Sample T5/S5, 10134.00ft/3088.84m

Well Name	Texaco Bovie Lake J-72	**Location**	300/J-72-6020-12245/0
Sample Type	Thin section/SEM grain mount from a core sample	**Depth (m)**	10134.00ft/3088.84m
Stratigraphic Unit	Nahanni Formation	**Reservoir Quality**	Moderate
Classification	Dolostone	**Stain type**	½ Dual carbonate stain

MINERALOGY

	Total Bulk mineralogy					
Thin Section Point counting (%)	Calcite	Dolomite	Anhydrite	Quartz/Cht	Pyrite	Clays & organics
	-	87	-	7	3	3
	Framework, Matrix, Cement, and Replacement					
	Carbonate clasts	Bioclasts	Detrital grains	Matrix	Pore filling cement	Replacement
	3	-	-	3	9	84

ADDITIONAL FEATURES and OTHER COMMENTS

Depositional	At the time of deposition, the sample was most likely massive. Generation of low amplitude stylolites and fracturing of the sediment typically occurs during burial diagenesis (mechanical and chemical compaction). The presence of sub-vertical stylolites may have subsequently formed as a result of folding or compressional stresses. Saddle dolomite within the sample is a common product of late-stage diagenesis and hydrothermal activity.
Textures	Dolomite within this sample predominately displays replacement or alteration textures. 'Saddle' or baroque dolomite is represented by subhedral coarse dolomite that displays stepped or curved crystal faces, while sweeping or undulatory extinction can be viewed under cross-polarized light. Euhedral dolomite rhombs, often displaying compositional zoning, line microvuggy pore spaces or have precipitated within vertical and sub-vertical fractures.
Framework (Carbonate clasts, Bioclasts)	Dolomitization and recrystallization fabrics have mainly overprinted any original framework clasts/bioclasts within this sample. Using the 'white card' technique with the petrographic microscope, a vague mud-supported depositional texture can be inferred.
Detrital Grains & Other Non-Carbonate Grains	There are no detrital grains in this sample.
Matrix	Minor clay and organics (3%) are observed predominately in association with stylolites which contain insoluble material that accumulates along the irregular dissolution surface. Trace dolomicrite identified in the SEM is found to line some of the vuggy pore spaces.
Pore Filling Cements	Well-formed secondary sub- to euhedral quartz cement (7%) is common and has partly occluded micro-vug and fracture porosity along with minor amounts of dolomite (4%) and pyrite (2%). Minor well-formed rhombic dolomite lines micro-vugs and infills vertical and sub-vertical fractures along with quartz.
Replacement Minerals	In addition to saddle dolomite (80%), which dominates the sample, minor pyrite (1%) replacement is also noted.
Porosity	The sample contains minor amounts of isolated microvugs (5%), along with lesser amounts of

	scattered intercrystalline porosity (1%). Connectivity of the pore system may be locally enhanced due to partly open vertical fracture systems. Visible fracture porosity within the sample is estimated to be minor (1%).

Annotated microphotographs with descriptions for the thin section and SEM samples are provided below.

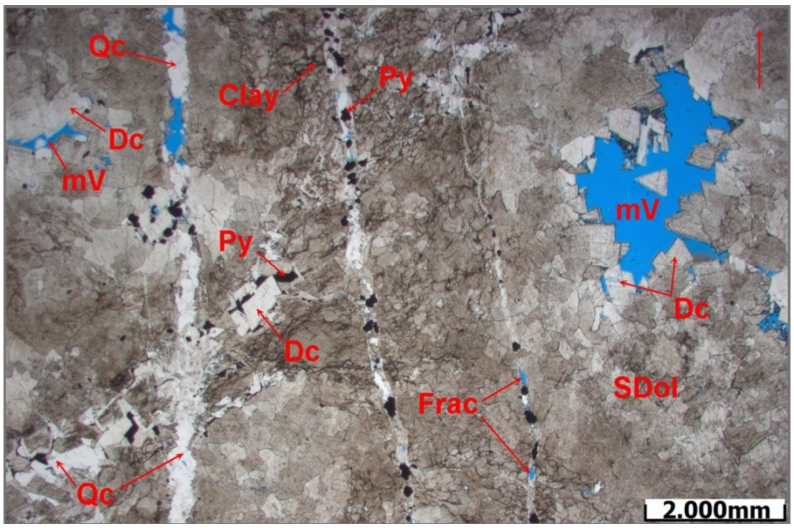

Figure 7.1. Sample T5, 10134.00ft/3088.84m. Overview image of a dolostone that consists predominately of saddle (or baroque) dolomite (SDol). This type of dolomite generally forms from recrystallization of early dolomite through hydrothermal processes. The pore system consists of microvuggy porosity (mV), scattered intercrystalline porosity and partially open fracture porosity (Frac). Vertical and subhorizontal fractures have been partially occluded by secondary quartz (Qtz), pyrite (Py) and dolomite cements. Microvugs are also lined with a subsequent generation of dolomite cement (Dc) that consists of medium crystalline dolomite rhombs that are relatively free of clay inclusions. Clay: interstitial clays. **x12.5 ppl**

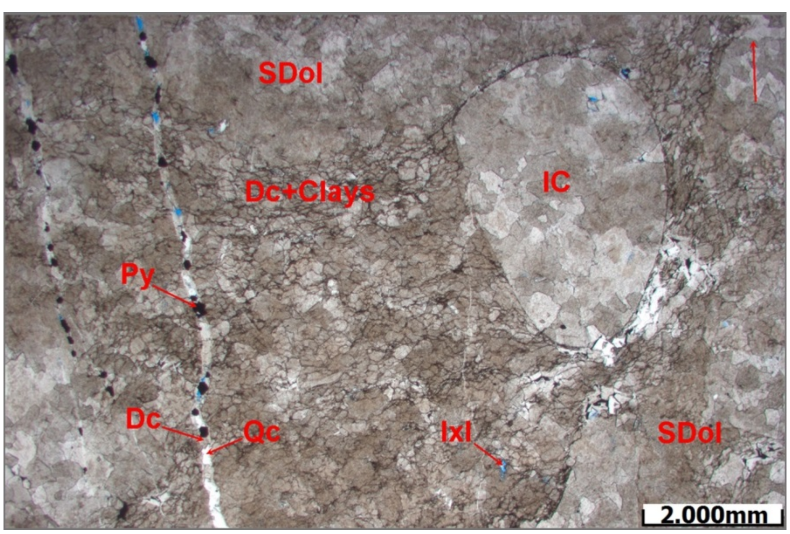

Figure 7.2. Sample T5, 10134.00ft/3088.84m. Alternate overview image of a rounded dolomitic intraclast (IC). The dolomite crystal fabric that surrounds the intraclast appears relatively finer and contains more interstitial clays than the overall coarse crystalline fabric that consists of recrystallized saddle (or baroque) dolomite (SDol). A vertical fracture has been infilled with pyrite (Py), quartz (Qc) and dolomite cements (Dc). Ixl: intercrystalline porosity. **x12.5 ppl**

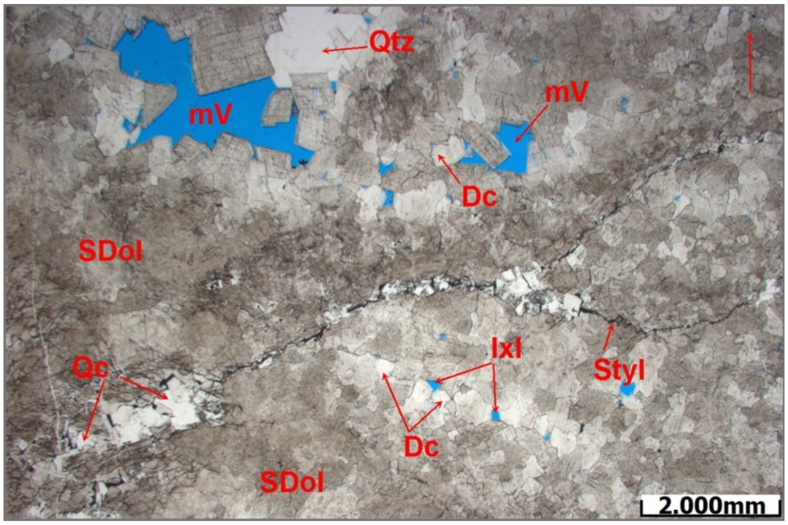

Figure 7.3. Sample T5, 10134.00ft/3088.84m. Alternate overview image showing microvuggy porosity (mV). Subhorizontal fractures/stylolites (Styl) appear to contain insoluble organic residue, plus variably distributed authigenic quartz (Qc). Ixl: intercrystalline porosity; SDol: saddle dolomite; Dc: dolomite cement. **x12.5 ppl**

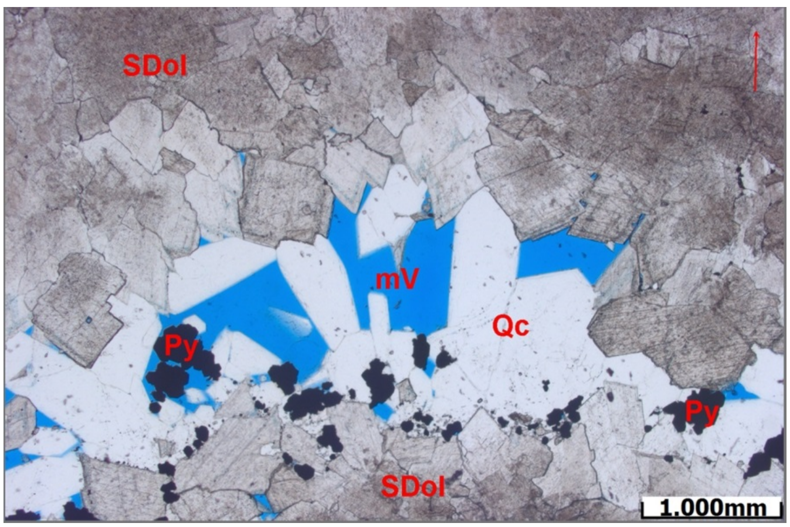

Figure 7.4. Sample T5, 10134.00ft/3088.84m. Low magnification view of a microvuggy pore space that has been partially occluded by euhedral authigenic quartz (Qc) and pyrite (Py). SDol: saddle dolomite. **x25 ppl**

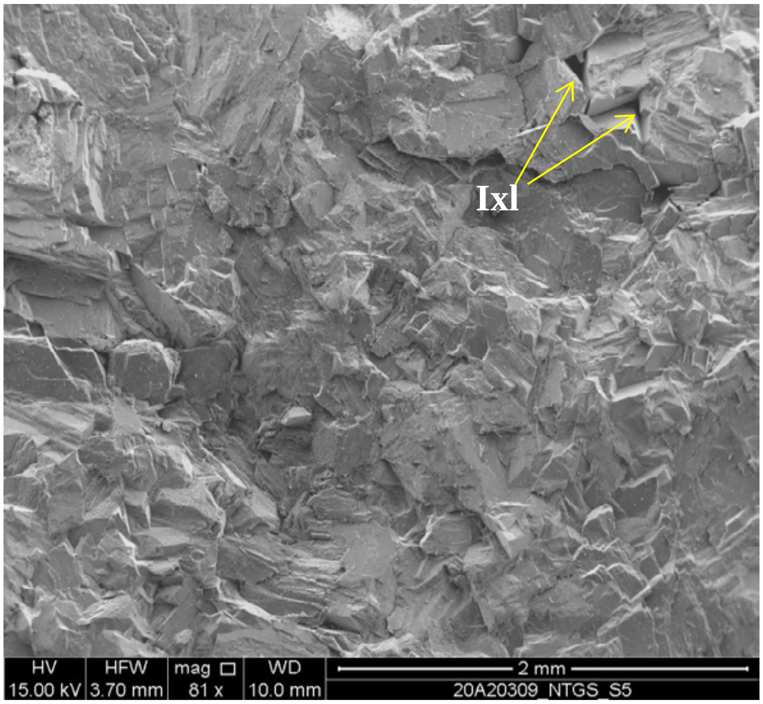

SEM Figure 7.5. Sample S5, 10134.00ft/3088.84m. Low magnification overview of the dolostone. The pore system within this subsample is predominated by intercrystalline (Ixl) and vuggy macropores. **x81**

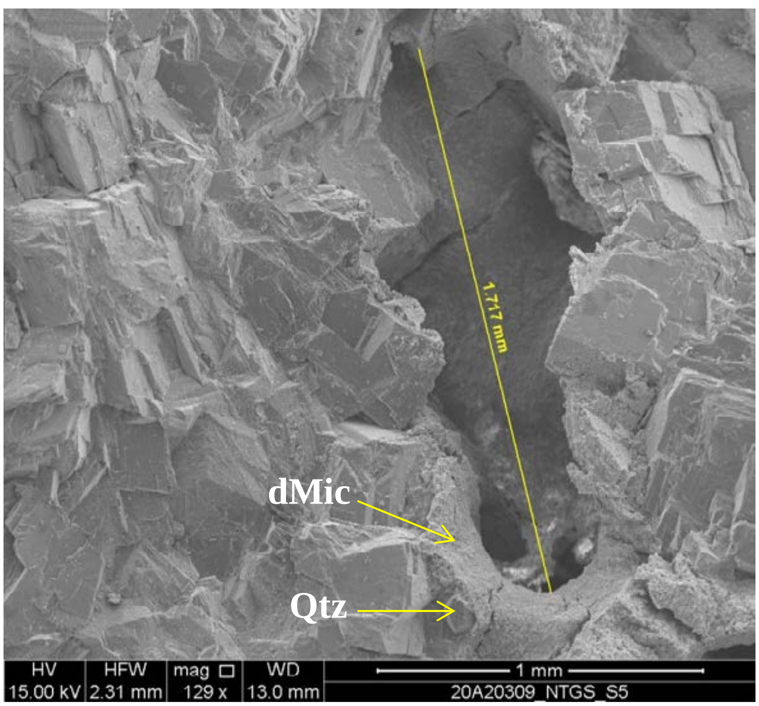

SEM Figure 7.6. Sample S5, 10134.00ft/3088.84m. Low magnification image of a vuggy pore lined with fine euhedral dolomite, dolomicrite (dMic) and authigenic quartz (Qtz). **x129**

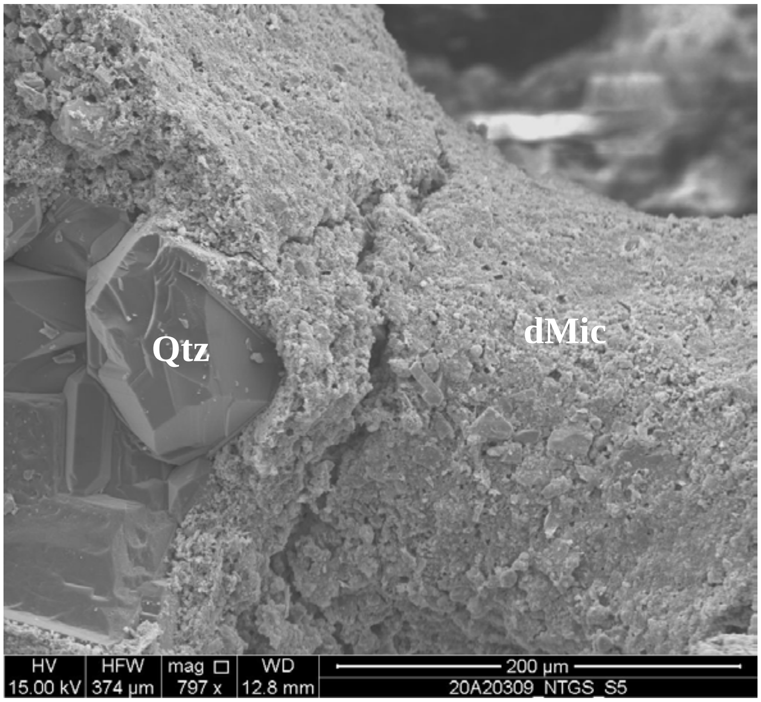

SEM Figure 7.7. Sample S5, 10134.00ft/3088.84m. Higher magnification view of the vuggy pore space represented in **Figure 7.6** highlighting pore-lining dolomicrite (dMic) and authigenic quartz (Qtz). **x797**

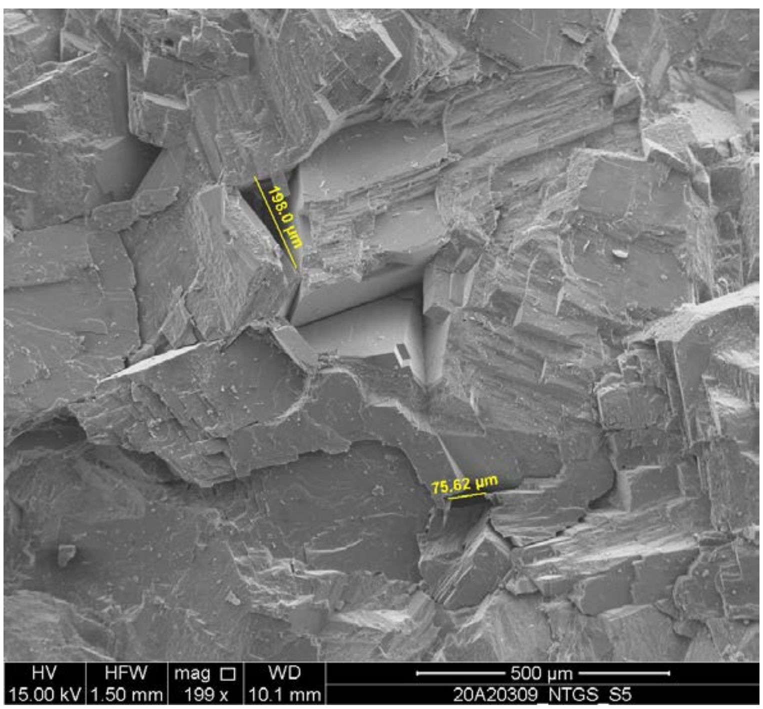

SEM Figure 7.8. Sample S5, 10134.00ft/3088.84m. Additional image of open macropores (~75-200µm). **x199**

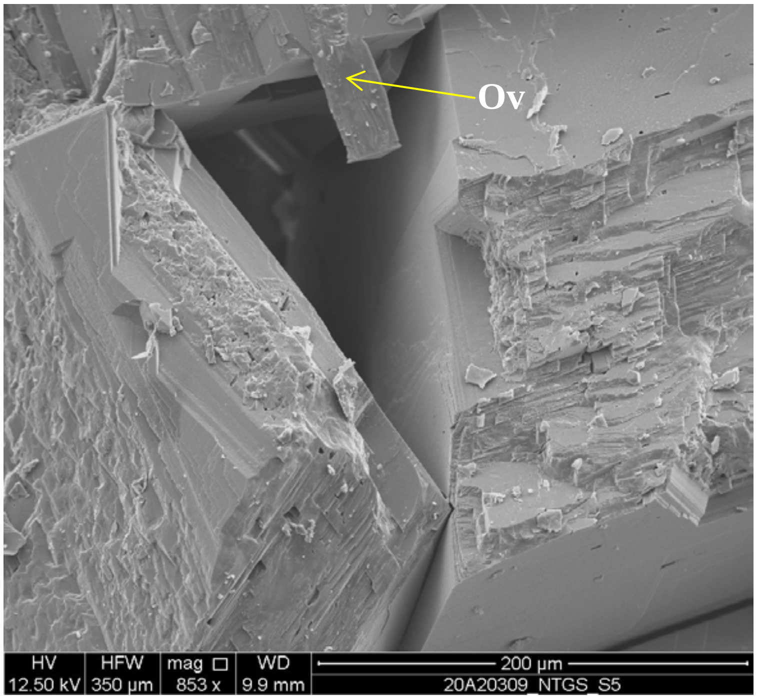

SEM Figure 7.9. Sample S5, 10134.00ft/3088.84m. Higher magnification view showing details of intercrystalline pore shown in the upper right of **Figure 7.8**. The pore is mostly open, with only partial obstruction due to crystal overgrowths (Ov). **x853**

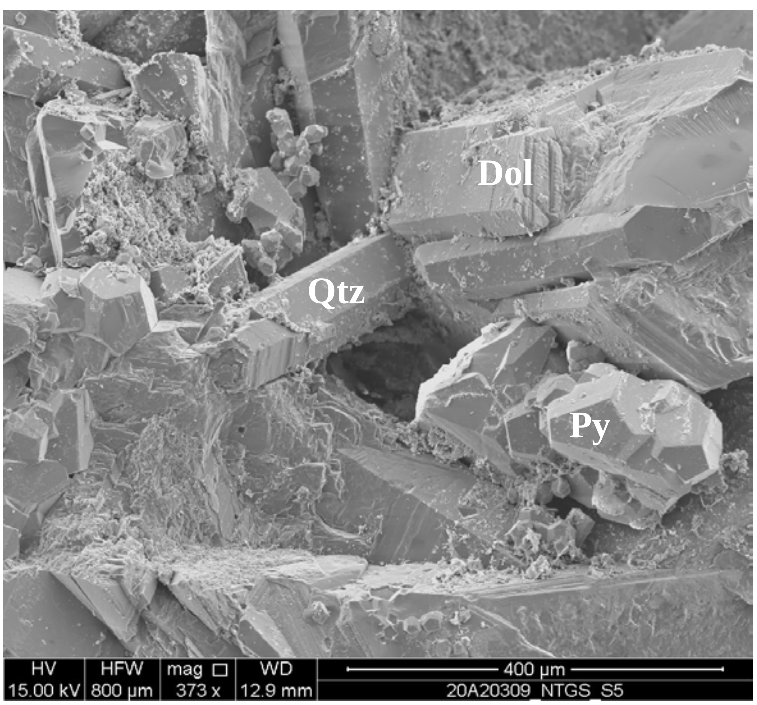

SEM Figure 7.10. Sample S5, 10134.00ft/3088.84m. Low magnification image of well-formed euhedral dolomite (Dol), quartz (Qtz) and pyrite (Py) crystals which line a vuggy pore space. **x373**

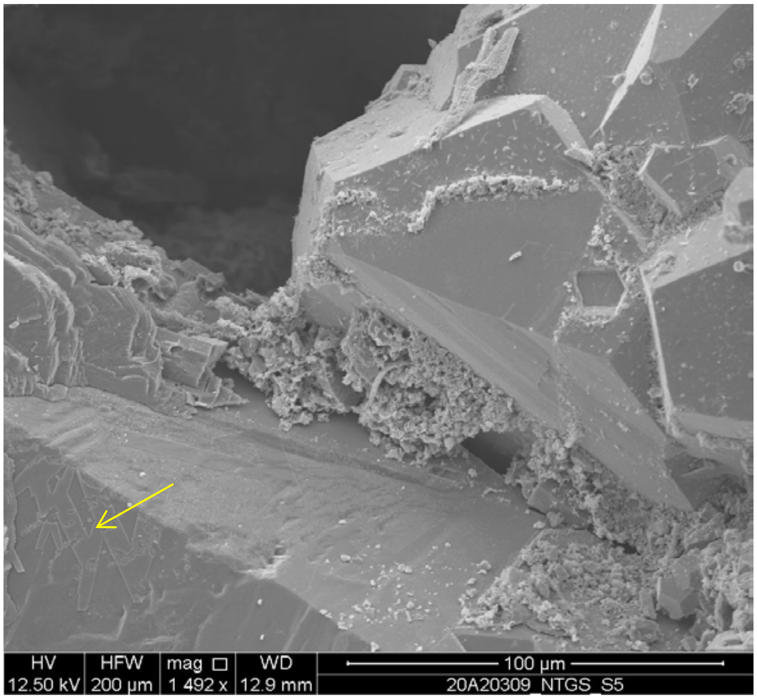

SEM Figure 7.11. Sample S5, 10134.00ft/3088.84m. High magnification view of authigenic quartz showing interesting overgrowth patterns (highlighted by yellow arrow). **x1492**

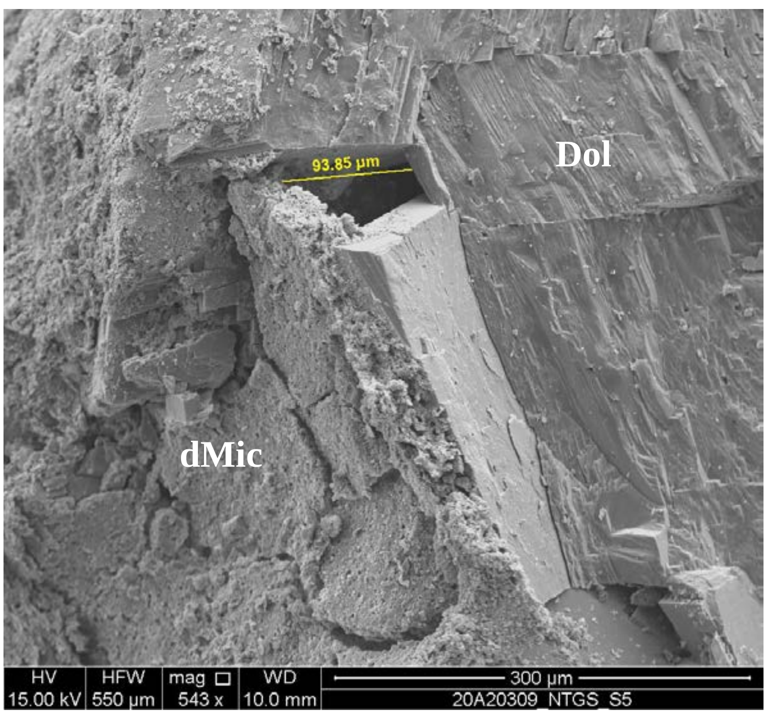

SEM Figure 7.12. Sample S5, 10134.00ft/3088.84m. SEM photomicrograph of an angular macropore measuring ~94µm. Dol: dolomite; dMic: dolomicrite. **x543**

Sample T4/S4, 10164.40ft/3098.11m

Well Name	Texaco Bovie Lake J-72	**Location**	300/J-72-6020-12245/0
Sample Type	Thin section/SEM grain mount from a core sample	**Depth (m)**	10164.40ft/3098.11m
Stratigraphic Unit	Nahanni Formation	**Reservoir Quality**	Poor
Classification	Dolostone	**Stain type**	½ Dual carbonate stain

MINERALOGY

	Total Bulk mineralogy					
Thin Section Point counting (%)	**Calcite**	**Dolomite**	**Anhydrite**	**Quartz/Cht**	**Pyrite**	**Clays & organics**
	-	93	-	1	TR	6
	Framework, Matrix, Cement, and Replacement					
	Carbonate clasts	**Bioclasts**	**Detrital grains**	**Matrix**	**Pore filling cement**	**Replacement**
	-	-	-	6	1	93

ADDITIONAL FEATURES and OTHER COMMENTS

Depositional	At the time of deposition, the sample was most likely massive. Formation of low amplitude stylolites and fracturing of the sediment typically happens during burial diagenesis (mechanical and chemical compaction).
Textures	Dolomite within this sample ranges from fine to very coarse crystalline. Coarse to very coarse dolomite predominately displays replacement or alteration textures. ‘Saddle’ or baroque dolomite is represented by subhedral dolomite that displays stepped or curved crystal faces, while sweeping or undulatory extinction can be viewed under cross-polarized light. Veins of altered saddle dolomite cross-cut the dominant fabric of microcrystalline, plus subhedral fine crystalline, dolomite which appears to contain appreciable amounts of clay inclusions or interstitial clays and organics. This dolostone displays multiple generations of cemented fractures with subhorizontal veins of saddle dolomite cross-cut by veinlets of quartz and relatively fine rhombic dolomite.
Framework (Carbonate clasts, Bioclasts)	Dolomitization and recrystallization fabrics have mainly overprinted any original framework clasts/bioclasts within this sample. Using the ‘white card’ technique with the petrographic microscope, a vague mud-supported depositional texture can be inferred.
Detrital Grains & Other Non-Carbonate Grains	There are no detrital grains in this sample.
Matrix	Minor clay and organics (6%) are observed as cloudy inclusions within the dolomite and as pore-filling matrix notably in association with fine crystalline dolomite.
Pore Filling Cements	Minor dolomite (1%) and quartz (1%) occur as relatively late-stage vein/fracture fill, while trace calcite cement locally occludes intercrystalline porosity associated with saddle dolomite.
Replacement Minerals	In addition to saddle dolomite (80%), which dominates the sample, trace pyrite and marcasite replacement is also noted.
Porosity	Trace amounts of scattered intercrystalline and open fracture porosity.

Annotated microphotographs with descriptions for the thin section and SEM samples are provided below.

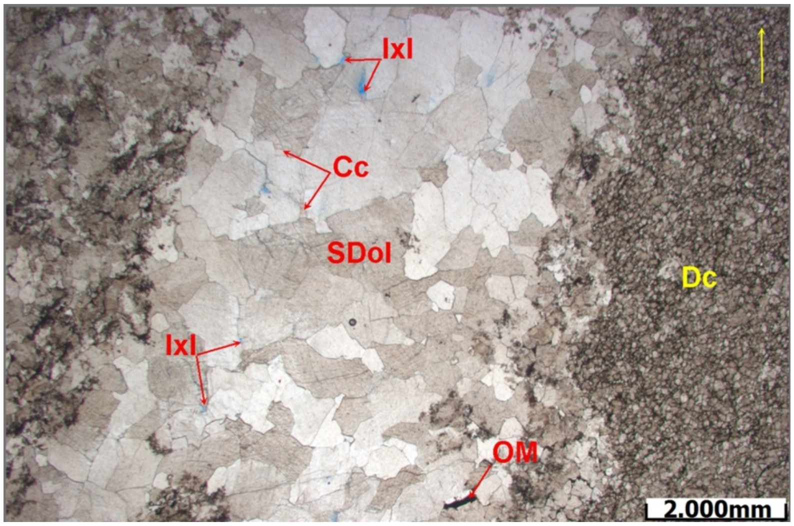

Figure 8.1. Sample T4, 10164.40ft/3098.11m. Low magnification overview of the dolostone highlighting the two prominent crystal fabrics within this sample. Veins of coarse to very coarse altered saddle dolomite (SDol) cross-cut the dominant fabric of microcrystalline, plus subhedral fine crystalline, dolomite (Dol) which appears to contain appreciable amounts of clay inclusions and/or interstitial clays and organics. Visible porosity within this sample includes trace amounts of intercrystalline porosity (Ixl) and open fracture porosity. Porosity is locally occluded by trace calcite cement and organic matter (OM - probable bitumen). **X12.5 ppl**

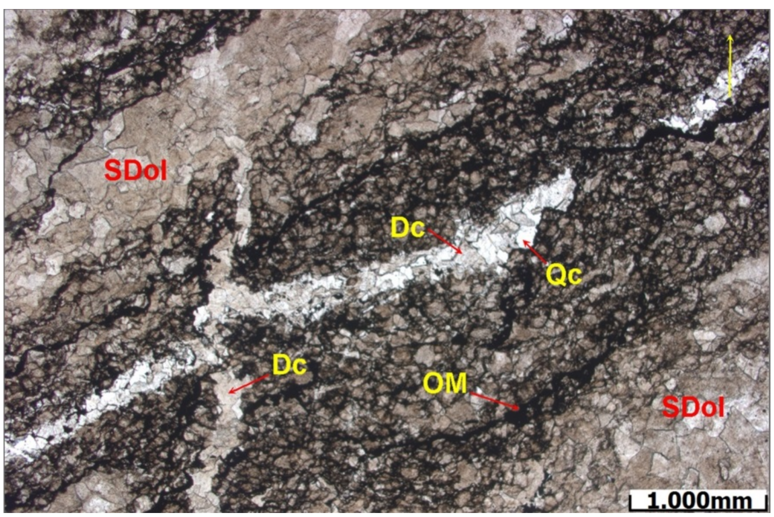

Figure 8.2. Sample T4, 10164.40ft/3098.11m. Low magnification view highlighting multiple generations of veins/cemented fractures. Sub-horizontal veins of saddle dolomite (SDol) are cross-cut by veinlets of quartz (Qc) and relatively fine rhombic dolomite (Dc). Styl: stylolite. **x25 ppl**

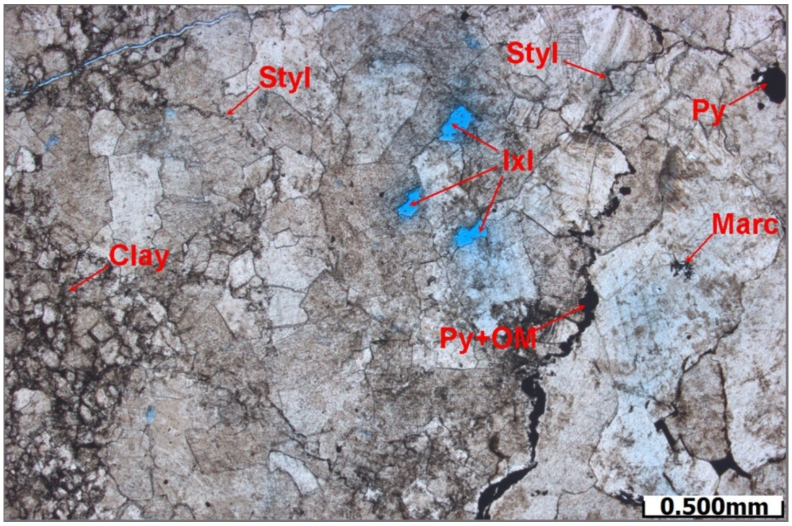

Figure 8.3. Sample T4, 10164.40ft/3098.11m. Moderate magnification view highlighting trace intercrystalline pore spaces (Ixl). The presence of vertical to sub-vertical stylolites (Styl) represent pressure-solution surfaces lined with insoluble organic material and secondary pyrite (Py+OM) that were likely influenced by folding or compressional tectonic stresses. Trace aggregates of framboidal pyrite (Py) and needle-like marcasite (Marc) crystals are also noted. Interstitial clays, probable illite, occur in association with subhedral fine crystalline dolomite. **x50 ppl**

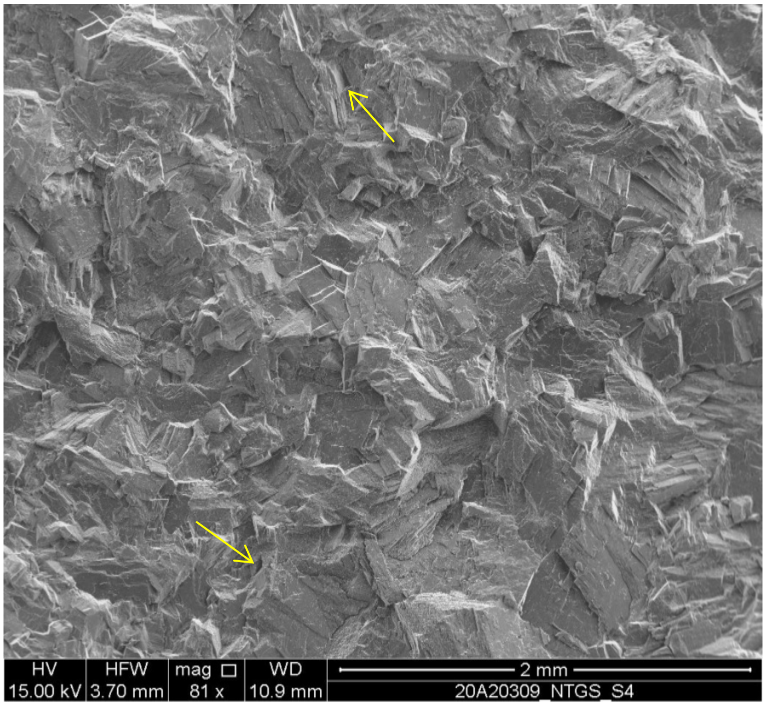

SEM Figure 8.5. Sample S4, 10164.40ft/3098.11m. Low magnification overview of the dolostone. Only isolated pores (highlighted by arrows), measuring ~10-15µm, have been preserved between interlocking subhedral to euhedral dolomite rhombs. **x81**

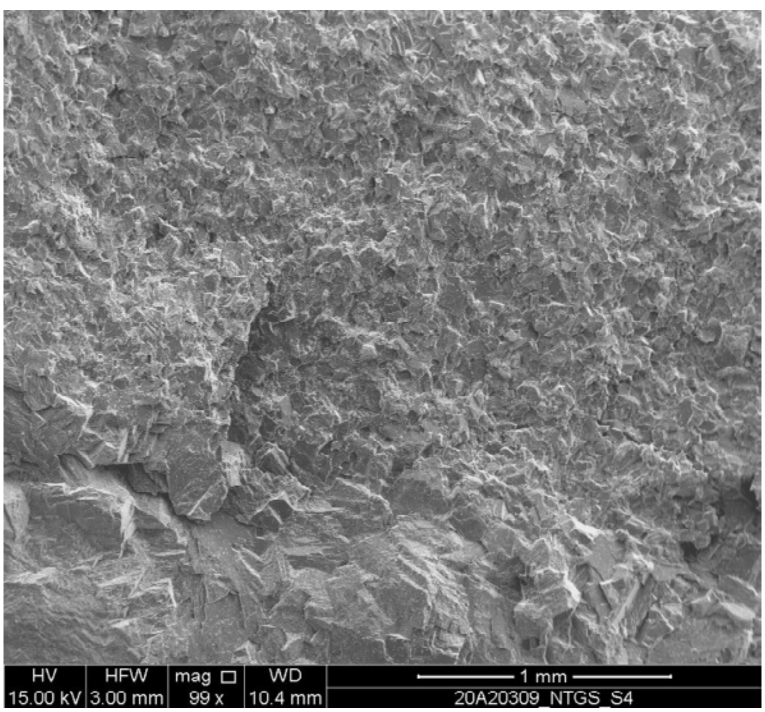

SEM Figure 8.6. Sample S4, 10164.40ft/3098.11m. High magnification image highlighting the boundary between patchy very fine to fine crystalline dolomite and medium to coarse crystalline dolomite rhombs. Scattered micropores are visible within the relatively fine dolomite; however, the uneven surface topography generally creates depressions which are not true pores. **x99**

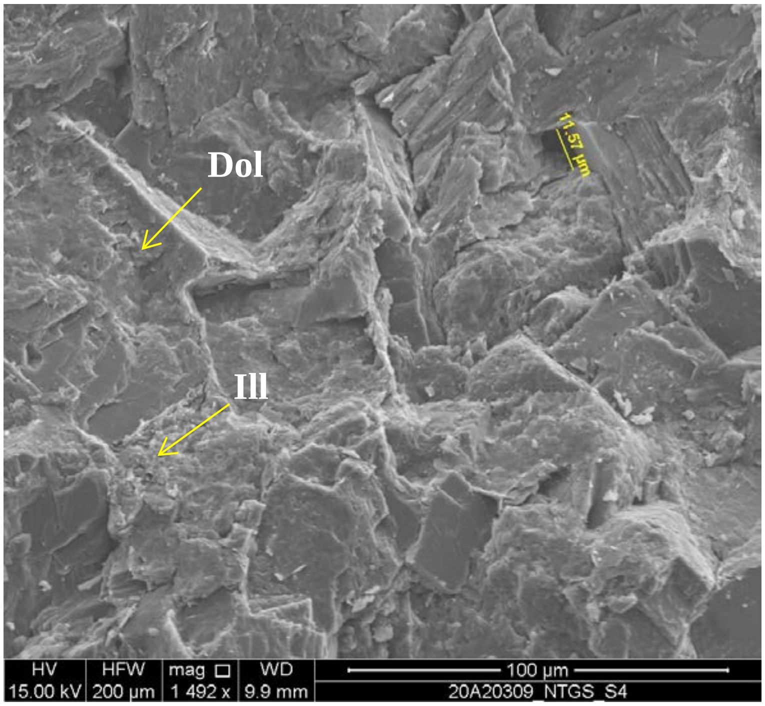

SEM Figure 8.7. Sample S4, 10164.40ft/3098.11m. Moderate magnification view of an isolated pore, measuring ~11µm, within fine to medium crystalline dolomite (Dol). Localized interstitial illitic (Ill) clays are also visible. **x1492**

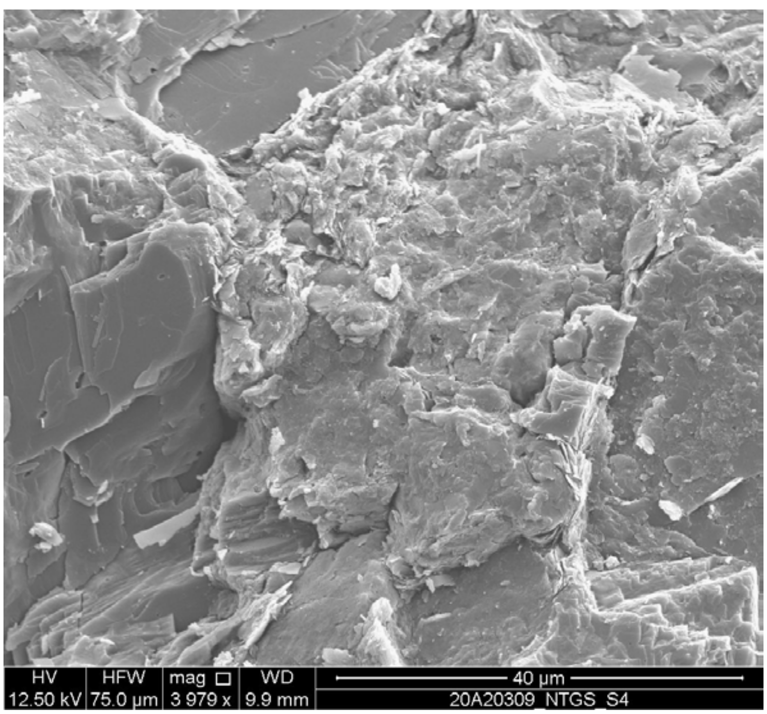

SEM Figure 8.8. Sample S4, 10164.40ft/3098.11m. A very high magnification image of interstitial clays. See **Figure 8.8a** for EDX data representing clay composition. **x3979**

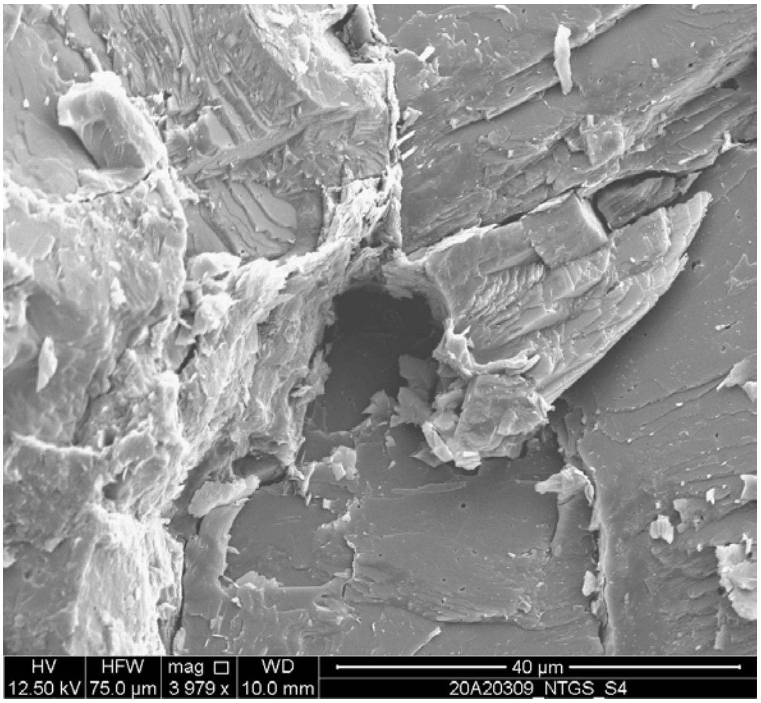

SEM Figure 8.9. Sample S4, 10164.40ft/3098.11m. A very high magnification image of pore-filling platy clays and/or micas. Clays are also noted to locally coat the crystal surfaces. **x3979**

Results	Figure 8.8a - Clay/Mica	
Element	series	[norm. wt.%]
Oxygen (O)	K-series	41.49368
Magnesium (Mg)	K-series	TR
Aluminium (Al)	K-series	17.67275
Silicon (Si)	K-series	33.90791
Potassium (K)	K-series	6.925657
Calcium (Ca)	K-series	TR
	Sum:	100

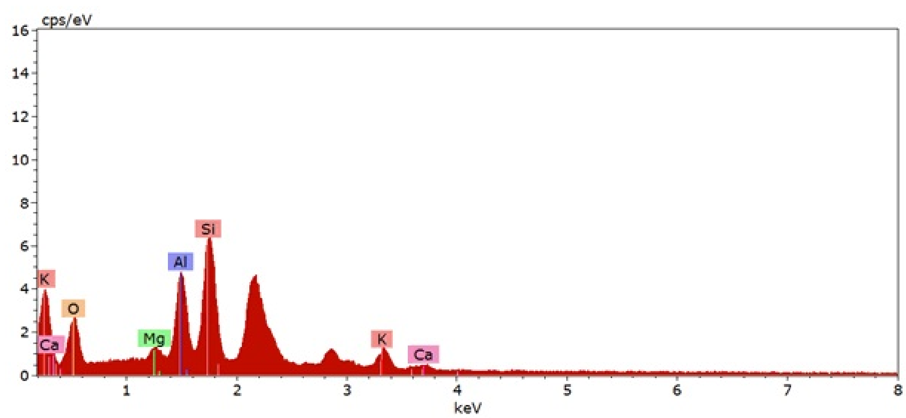

Sample T3/S3, 10191.50ft/3106.37m

Well Name	Texaco Bovie Lake J-72	**Location**	300/J-72-6020-12245/0
Sample Type	Thin section/SEM grain mount from a core sample	**Depth (m)**	10191.50ft/3106.37m
Stratigraphic Unit	Nahanni Formation	**Reservoir Quality**	Poor
Classification	Dolostone	**Stain type**	½ Dual carbonate stain

MINERALOGY

	Total Bulk mineralogy					
Thin Section Point counting (%)	**Calcite**	**Dolomite**	**Anhydrite**	**Quartz/Cht**	**Pyrite**	**Clays & organics**
	3	94	-	TR	-	3
	Framework, Matrix, Cement, and Replacement					
	Carbonate clasts	**Bioclasts**	**Detrital grains**	**Matrix**	**Pore filling cement**	**Replacement**
	-	-	TR	3	3	94

ADDITIONAL FEATURES and OTHER COMMENTS

Depositional	At the time of deposition, the sample was most likely massive. Generation of low-amplitude stylolites and fracturing of the sediment typically occurs during burial diagenesis (mechanical and chemical compaction). Saddle dolomite within the sample is a common product of late-stage diagenesis and hydrothermal activity.
Textures	Dolomite within this sample ranges from fine to very coarse crystalline. Coarse to very coarse dolomite predominately displays replacement or alteration textures. 'Saddle' or baroque dolomite is represented by subhedral dolomite that displays stepped or curved crystal faces, while sweeping or undulatory extinction can be viewed under cross-polarized light. Healed fractures are infilled with subhedral calcite and quartz cements, while minute euhedral dolomite rhombs locally overprint calcite.
Framework (Carbonate clasts, Bioclasts)	Dolomitization and recrystallization fabrics have overprinted any original framework clasts/bioclasts within this sample.
Detrital Grains & Other Non-Carbonate Grains	Trace detrital quartz grains are noted in this sample.
Matrix	Minor clay and organics (3%) are observed as cloudy inclusions within the dolomite and interstitial to dolomite, and is also concentrated in stylolites. SEM observation shows trace amounts of well-formed illite ribbons, suggesting some clay content may be authigenic or has been recrystallized from detrital precursors.
Pore Filling Cements	Minor calcite (3%), along with trace quartz, occur as vertical fracture fill.
Replacement Minerals	Saddle dolomite (94%) comprises replacement minerals.
Porosity	Trace amounts of scattered intercrystalline/micro-intercrystalline porosity, in addition to trace open fracture porosity is observed in this sample.

Annotated microphotographs with descriptions for the thin section and SEM samples are provided below.

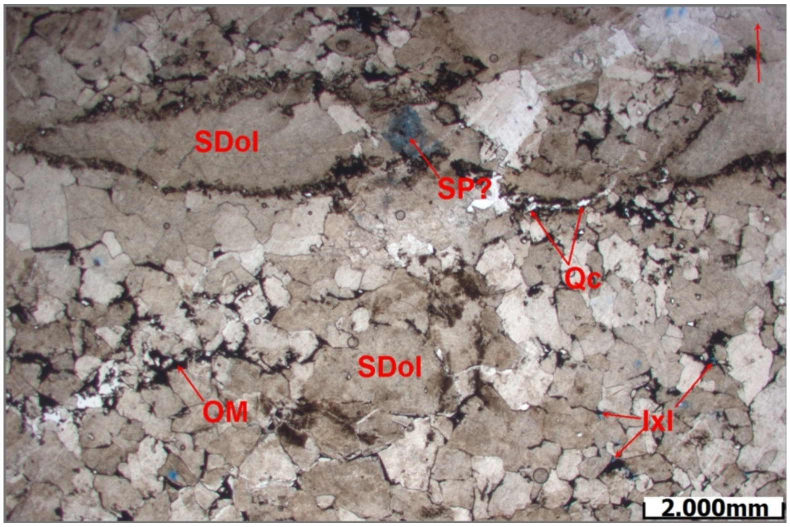

Figure 9.1. Sample T3, 10191.50ft/3106.37m. Overview image of the dolostone which consists of abundant coarse to very coarse 'saddle' or baroque dolomite (SDol), plus trace to minor amounts of calcite and quartz (Qtz) cements which occur as fracture fill. Trace to minor amounts of intercrystalline porosity (Ixl) is visible within the sample; however, the majority of porosity within the sample has been occluded by organic matter, such as bitumen/pyrobitumen (OM). A possible secondary dissolution pore (SP?) is also noted. **x12.5 ppl**

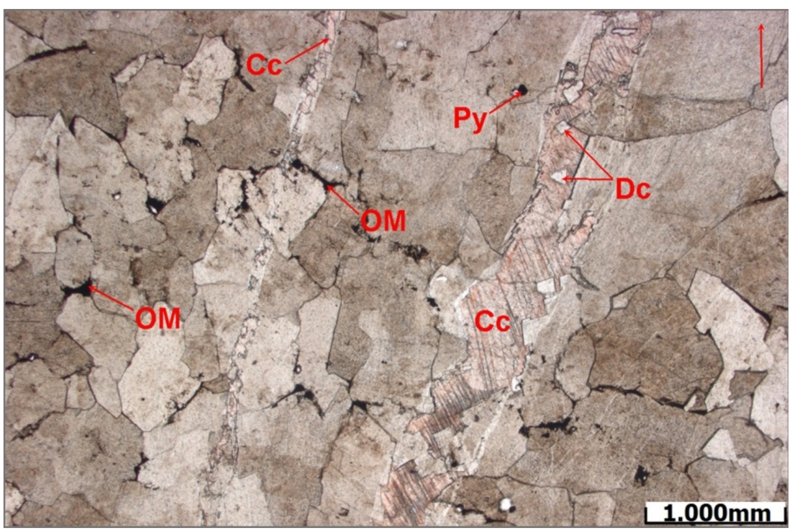

Figure 9.2. Sample T3, 10191.50ft/3106.37m. Low magnification view of subvertical calcite veins which cross-cut coarse crystalline saddle dolomite (SDol). Calcite cement (Cc) has been locally overprinted by relatively late stage dolomite rhombs (Dc). OM: organic matter; Py: pyrite. **x25 ppl**

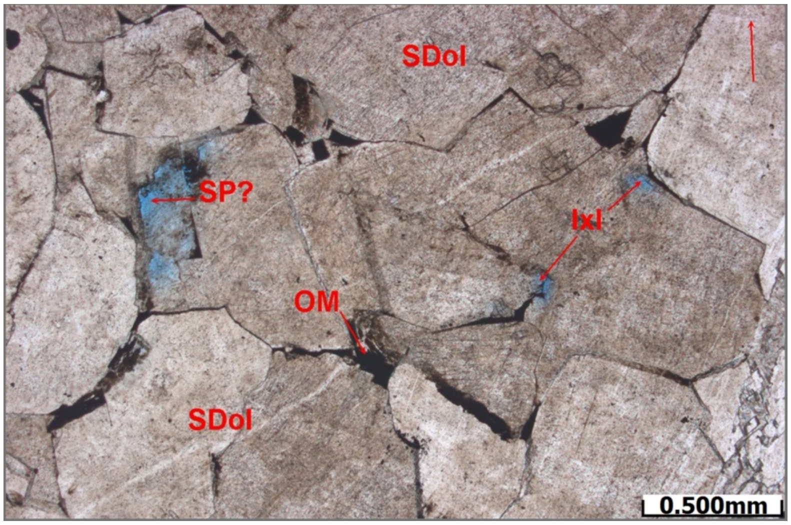

Figure 9.3. Sample T3, 10191.50ft/3106.37m. Moderate magnification image of coarse to very coarse saddle (or baroque) dolomite (SDol) defined by sweeping extinction and irregularly curved crystal boundaries. Trace intercrystalline pores (Ixl) are shown, while the majority of interstitial pores are plugged by organic material such as bitumen (OM). A cloudy intercrystalline pore space is partially occluded by possible microcrystalline chert which appears to have been partly dissolved resulting is secondary microporosity (SP?). **x50 ppl**

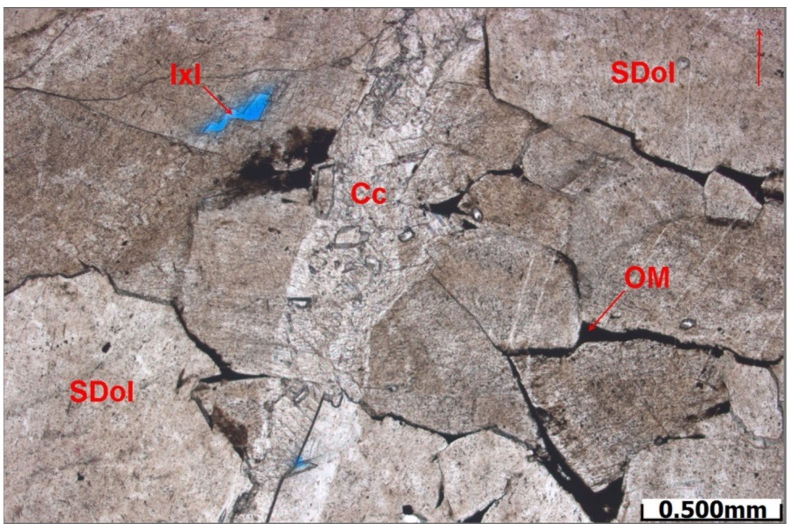

Figure 9.4. Sample T3, 10191.50ft/3106.37m. Alternate moderate magnification view of showing an isolated open intercrystalline pore space (Ixl). The majority of crystal boundaries and pore spaces are lined with organic material such as bitumen (OM). Calcite cement (Cc), which lacks applied stain, is noted as vein-fill. Dolomite crystals within close proximity to the hydrothermal vein appear leached. SDol: saddle dolomite. **x50 ppl**

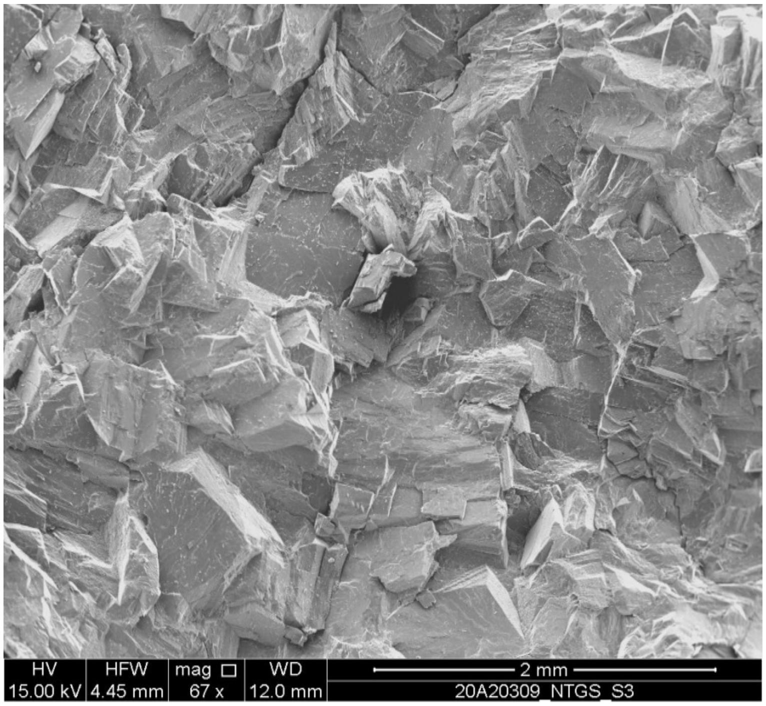

SEM Figure 9.5. Sample S3, 10191.50ft/3106.37m. Low magnification overview of the medium to very coarse crystalline dolostone. The freshly broken surface shows tightly interlocking subhedral to euhedral dolomite crystals. Visible fractures are likely induced by sample preparation. **x67**

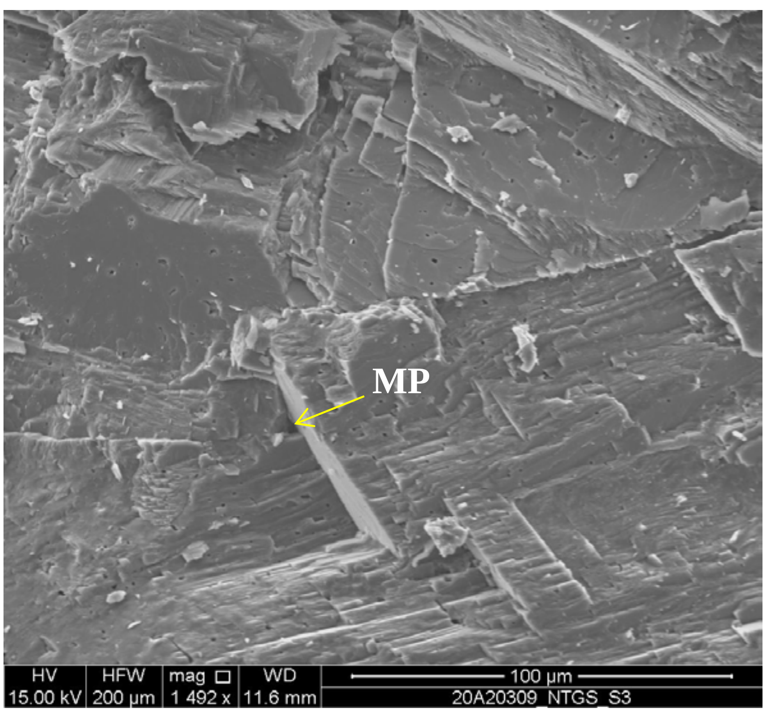

SEM Figure 9.6. Sample S3, 10191.50ft/3106.37m. Moderate magnification SEM image showing tightly interlocking dolomite crystals with a rare intercrystalline micropore (MP). Pinpoint micropores are commonly noted on the crystal surfaces throughout. **x1492**

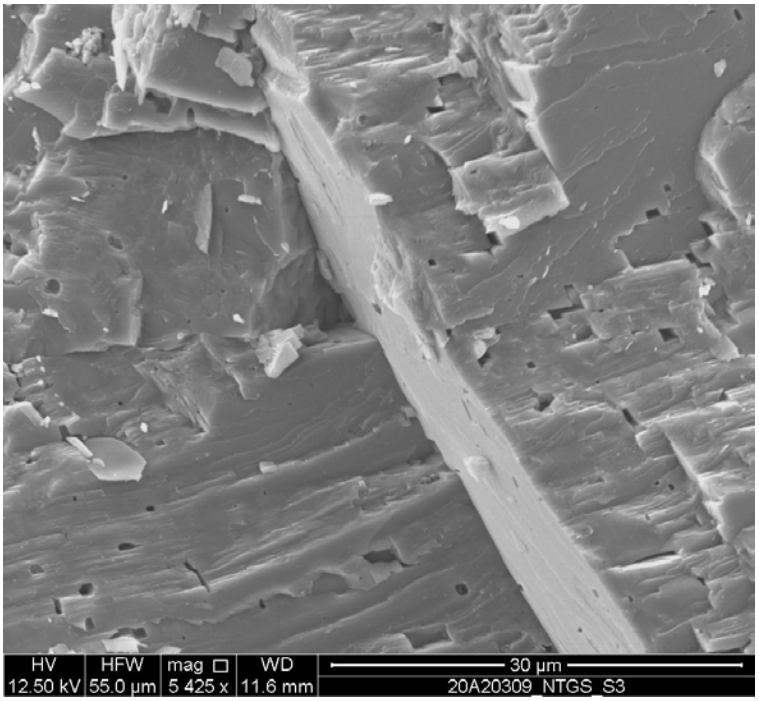

SEM Figure 9.7. Sample S3, 10191.50ft/3106.37m. High magnification image highlighting features in **Figure 9.6**. **x5425**

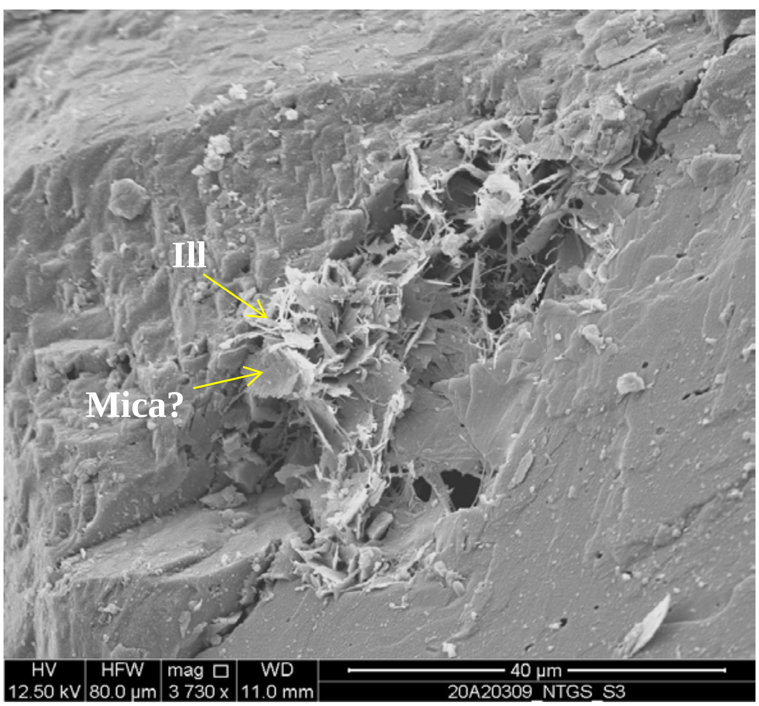

SEM Figure 9.8. Sample S3, 10191.50ft/3106.37m. A very high magnification image showing interwoven illite filaments (Ill), plus possible platy micas (Mica?), that are bridging an intercrystalline pore space. **x3730**

Sample T2/S2/X2, 10246.00ft/3122.98m

Well Name	Texaco Bovie Lake J-72	**Location**	300/J-72-6020-12245/0
Sample Type	Thin section/SEM grain mount from a core sample	**Depth (m)**	10246.00ft/3122.98m
Stratigraphic Unit	Nahanni Formation	**Reservoir Quality**	Poor
Classification	Dolostone	**Stain type**	½ Dual carbonate stain

MINERALOGY

	Total Bulk mineralogy					
Thin Section Point counting (%)	Calcite	Dolomite	Anhydrite	Quartz	Pyrite	Clays & organics
	-	95	-	3	1	1
	Framework, Matrix, Cement, and Replacement					
	Carbonate clasts	Bioclasts	Detrital grains	Matrix	Pore filling cement	Replacement
	-	-	-	1	3	96

ADDITIONAL FEATURES and OTHER COMMENTS

Depositional	At the time of deposition, the sample was most likely massive. Formation of low amplitude stylolites and fracturing of the sediment typically happens during burial diagenesis (mechanical and chemical compaction).
Textures	Dolomite within this sample predominately displays replacement or alteration textures. 'Saddle' or baroque dolomite is represented by subhedral coarse dolomite that displays stepped or curved crystal faces, while sweeping or undulatory extinction can be viewed under cross polarized light.
Framework (Carbonate clasts, Bioclasts)	Dolomitization and recrystallization fabrics have overprinted any original framework clasts/bioclasts within this sample.
Detrital Grains & Other Non-Carbonate Grains	There are no detrital grains in this sample.
Matrix	Minor organic matter, probable bitumen, and possible clays (1%) locally occlude pores. Patchy dolomicrite/very fine crystalline dolomite was also noted in trace amounts.
Pore Filling Cements	Authigenic quartz cement occurs in minor amounts (3%). A subvertical closed fracture is infilled by dolomite and quartz cements. Patchy polycrystalline quartz cement and well-formed euhedral quartz overgrowths were also observed.
Replacement Minerals	In addition to saddle dolomite (95%), which dominates the sample, minor pyrite (1%) replacement is also noted.
Porosity	The pore system consists of partially open sub-horizontal micro-fractures, in addition to trace isolated intercrystalline pores.

Annotated microphotographs with descriptions for the thin section and SEM samples are provided below.

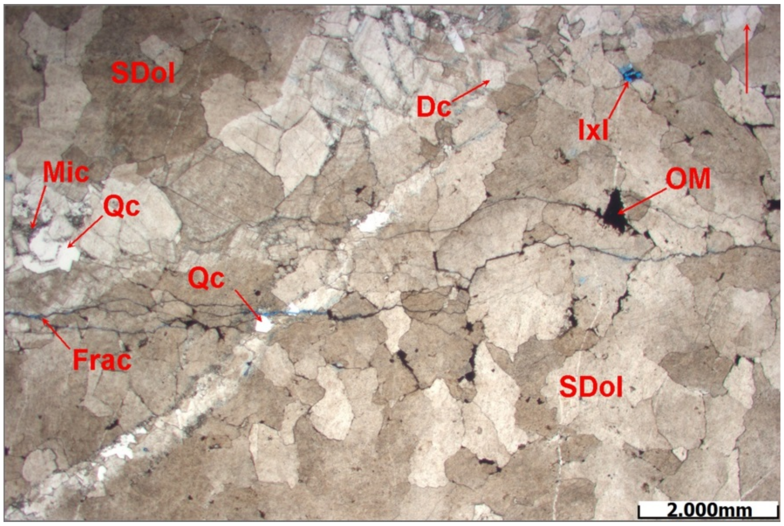

Figure 10.1. Sample T2, 10246.00ft/3122.98m. Overview image of the dolostone. Trace dolomite cement (Dc) likely formed as a later diagenetic phase and occurs as euhedral rhombs that overprint the dominant fabric of the saddle dolomite (SDol) which displays characteristic curved crystal faces. A subvertical closed fracture is infilled by dolomite and quartz (Qtz). Trace to minor amounts of dolomicrite/very fine crystalline dolomite (Mic) has a patchy distribution and is often noted in proximity to well-formed secondary quartz. Organic material (OM) locally occludes intercrystalline pores and also lines some crystal faces and portions of visible horizontal fractures. Trace intercrystalline porosity (Ixl) has been preserved. **x12.5 ppl**

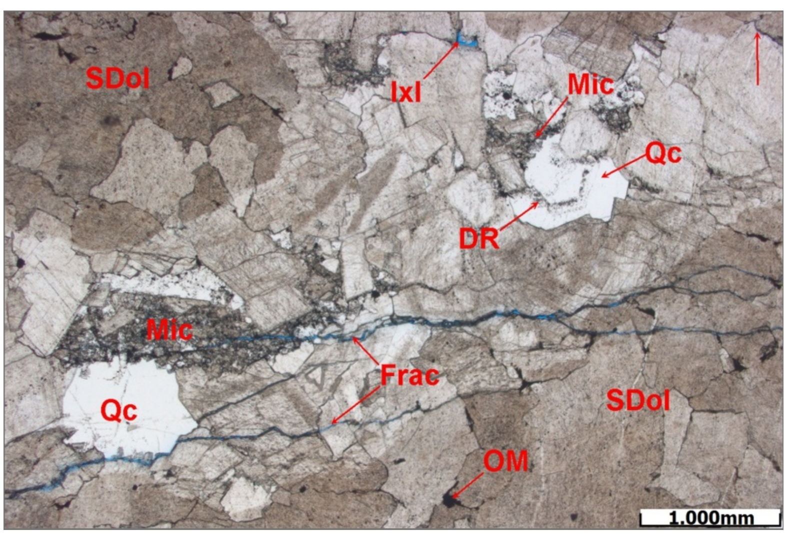

Figure 10.2. Sample T2, 10246.00ft/3122.98m. Low magnification image highlighting features of secondary quartz (Qc). The presence of a 'dust rim' (DR), or layer of minute inclusions, shows interrupted and continued growth. Available silica may have been provided by the replacement of clay minerals by carbonate, as patches of dolomicrite/very fine crystalline dolomite (Mic) are noted in close proximity. SDol: saddle dolomite; Ixl: intercrystalline porosity; Frac: fracture; OM: organic matter. **x25 ppl**

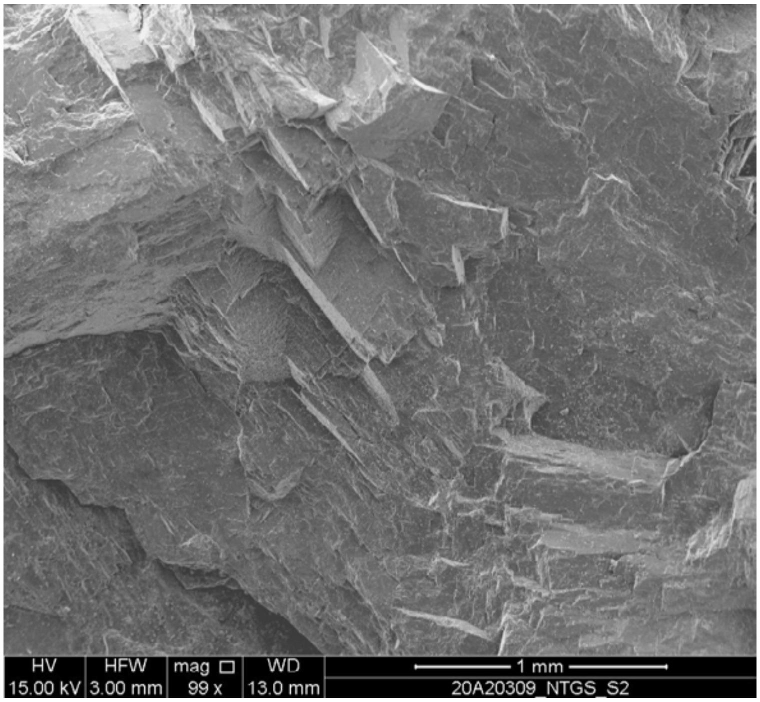

SEM Figure 10.3. Sample S2, 10246.00ft/3122.98m. Low magnification overview of the coarse to very coarse crystalline dolostone. Only trace isolated angular micropores were observed and are highlighted within the subsequent images associated with this sample (**Figures 10.6-10.9**). **x99**

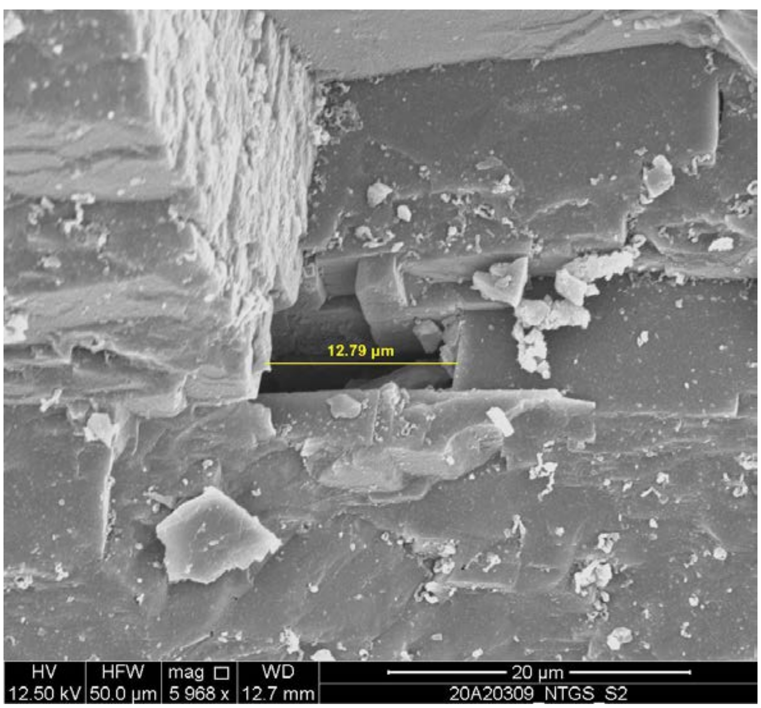

SEM Figure 10.4. Sample S2, 10246.00ft/3122.98m. High magnification image showing an open pore measuring ~13µm along the longest axis. **x5968**

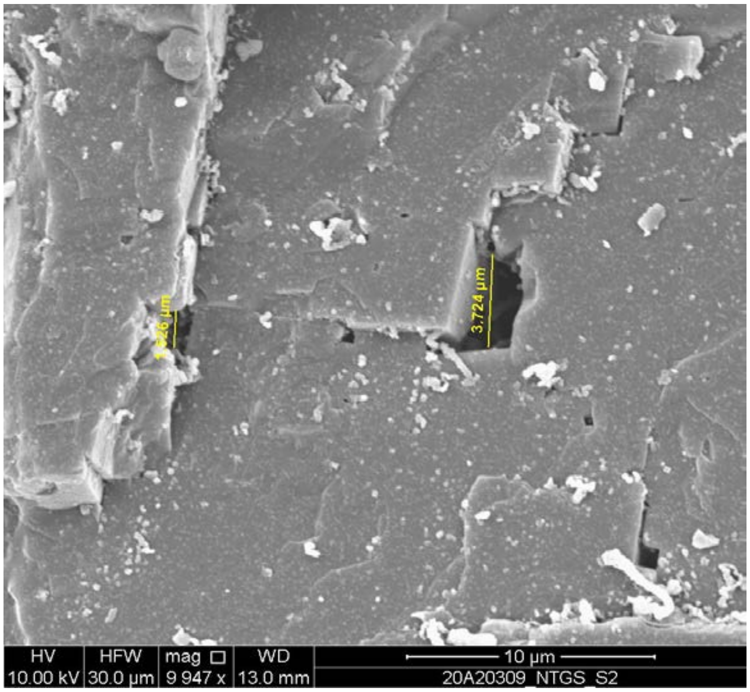

SEM Figure 10.5. Sample S2, 10246.00ft/3122.98m. Scattered micropores measuring <5µm. The angular shape of the pores reflects the blocky crystal shape of the dolomite. **x9947**

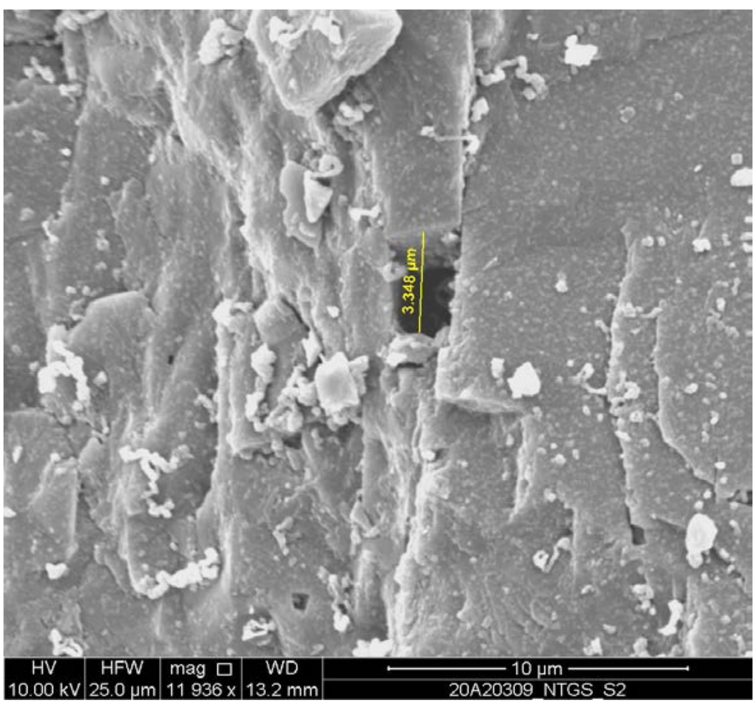

SEM Figure 10.6. Sample S2, 10246.00ft/3122.98m. Alternate image of an open micropore measuring ~3µm. **x11936**

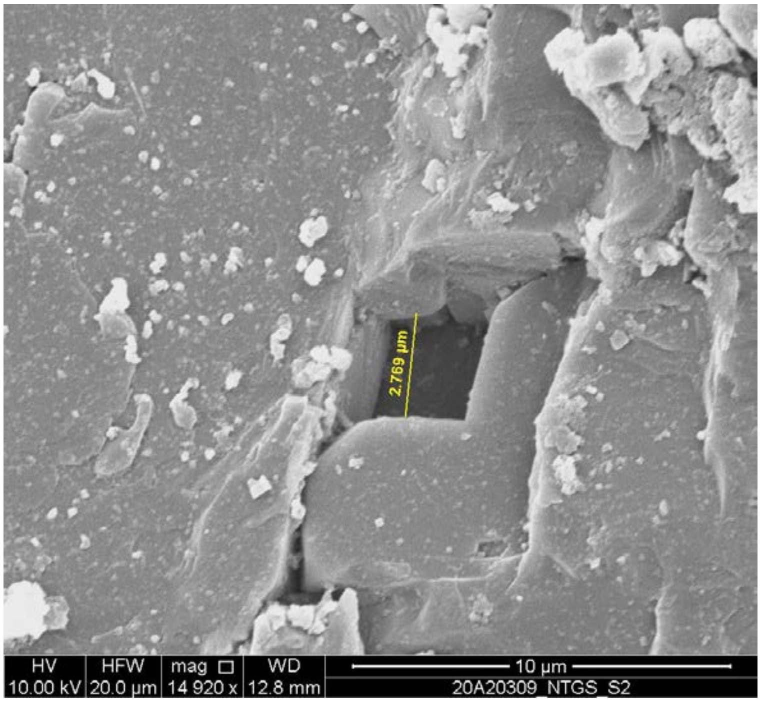

SEM Figure 10.7. Sample S2, 10246.00ft/3122.98m. High magnification image of an intercrystalline micropore measuring ~3µm. EDX analysis of the loosely adhered particles on the sample surface suggests these are dolomite particles produced during sample preparation. **x14920**

Sample T1/S1/X1, 10262.70ft/3128.07m

Well Name	Texaco Bovie Lake J-72	**Location**	300/J-72-6020-12245/0
Sample Type	Thin section/SEM grain mount from a core sample	**Depth (m)**	10262.70ft/3128.07m
Stratigraphic Unit	Nahanni Formation	**Reservoir Quality**	Moderate
Classification	Dolostone	**Stain type**	½ Dual carbonate stain

MINERALOGY

	Total Bulk mineralogy					
Thin Section Point counting (%)	Calcite	Dolomite	Anhydrite	Quartz/Cht	Pyrite	Clays & organics
	-	92	-	5	TR	3
	Framework, Matrix, Cement, and Replacement					
	Carbonate clasts	Bioclasts	Detrital grains	Matrix	Pore filling cement	Replacement
	-	-	-	3	5	92

ADDITIONAL FEATURES and OTHER COMMENTS

Depositional	At the time of deposition, the sample was most likely massive. Generation of low amplitude stylolites and fracturing of the sediment typically occurs during burial diagenesis (mechanical and chemical compaction). The presence of isolated pressure-solution stylolites and closed cemented sub-vertical fractures likely subsequently formed as a result of folding or compressional stresses. Saddle dolomite within the sample is a common product of late-stage diagenesis and hydrothermal activity.
Textures	Dolomite within this sample predominately displays replacement or alteration textures. ‘Saddle’ or baroque dolomite is represented by subhedral coarse dolomite that displays stepped or curved crystal faces, while sweeping or undulatory extinction can be viewed under cross polarized light.
Framework (Carbonate clasts, Bioclasts)	Dolomitization and recrystallization fabrics have overprinted any original framework clasts/bioclasts within this sample.
Detrital Grains & Other Non-Carbonate Grains	Detrital grains were not observed in this sample.
Matrix	Minor organic matter, probable bitumen, and possible clays (3%) locally occlude pores and occur as inclusions within secondary quartz cement.
Pore Filling Cements	Minor euhedral quartz cement (5%) locally occludes vuggy pore spaces, while some microvugs are lined with fine crystalline dolomite rhombs.
Replacement Minerals	Trace pyrite is associated with the localized replacement of pore-filling/pore-lining organic matter.
Porosity	The pore system consists of minor micro-vuggy porosity (2%) in addition to isolated intercrystalline pores (1%). Some vuggy porosity has been occluded by organic matter and/or pyrite, plus secondary quartz cement. Trace micro-intercrystalline porosity and micro-fractures are also present.

Annotated microphotographs with descriptions for the thin section and SEM samples are provided below.

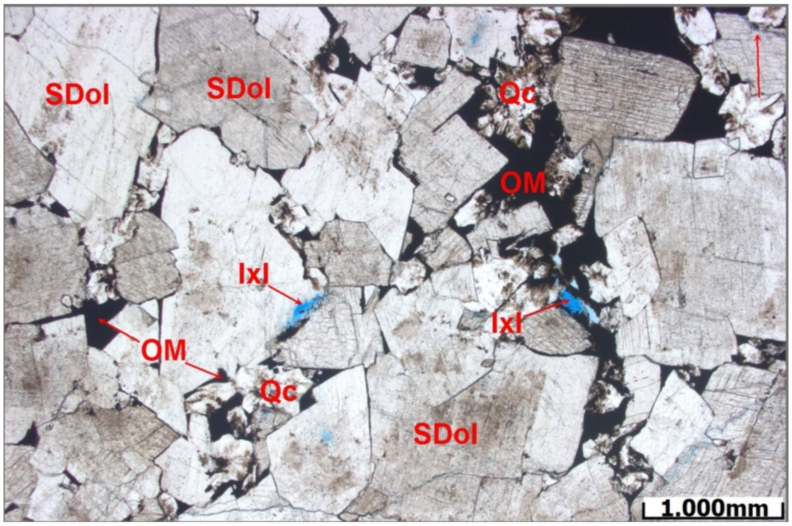

Figure 11.1. Sample T1, 10262.70ft/3128.07m. Low magnification overview image of the dolostone. Dolomite within this sample displays petrographic features that are consistent with saddle dolomite (SDol), which includes curved crystal faces and sweeping extinction. Moderate amounts of porosity occur in this sample. The pore system is characterized by minor microvuggy (mV) and intercrystalline (Ixl) porosity. Micro-vugs have been partly occluded by secondary fibrous quartz cement (Qc) and organic matter (OM – probable bitumen). Trace amounts of open fracture porosity and micro-intercrystalline porosity also occur within this sample. **x25 ppl**

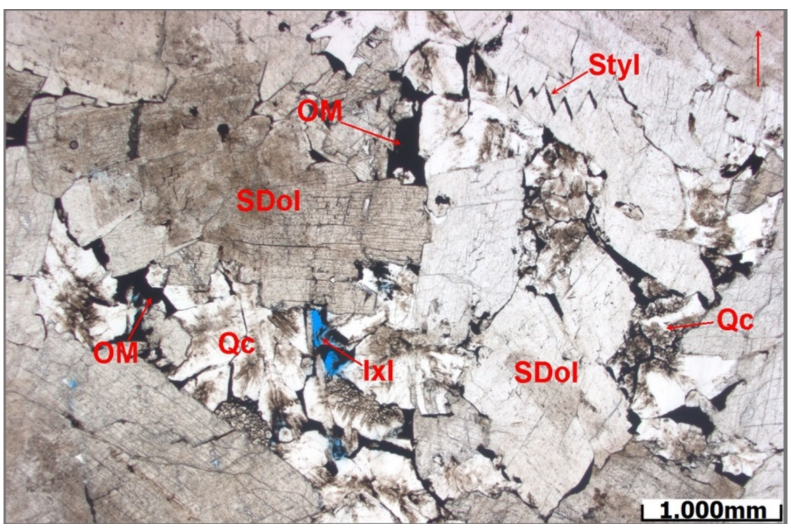

Figure 11.2. Sample T1, 10262.70ft/3128.07m. Alternate low magnification overview image showing similar features to **Figure 11.1**, in addition to a jagged stylolite (Styl) which represents isolated pressure-solution (chemical compaction) that may have occurred during burial diagensis or subsequent tectonic events. **x25 ppl**

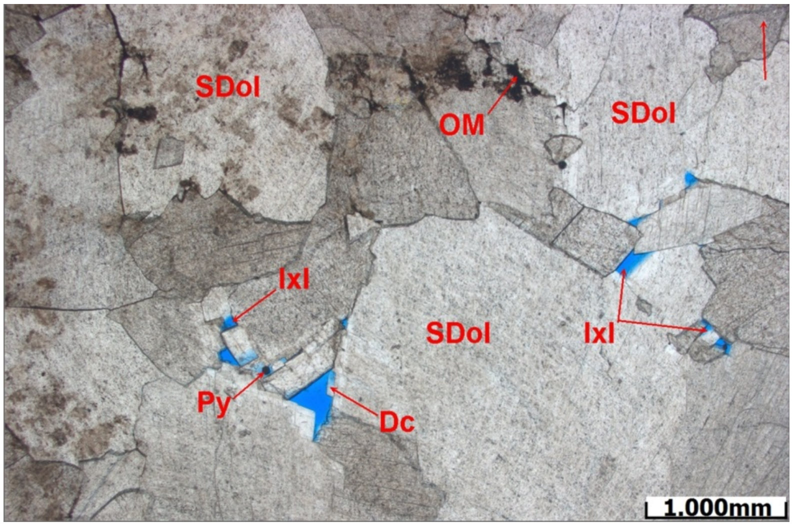

Figure 11.3. Sample T1, 10262.70ft/3128.07m. Alternate low magnification overview image highlighting intercrystalline porosity (Ixl). Relatively late phase dolomite cement (Dc) or overgrowths locally reduce pore volumes. Patchy discolouration of saddle dolomite (SDol) may be due to fluid inclusions or hydrocarbon staining. Py: pyrite. OM: organic matter.

x25 ppl

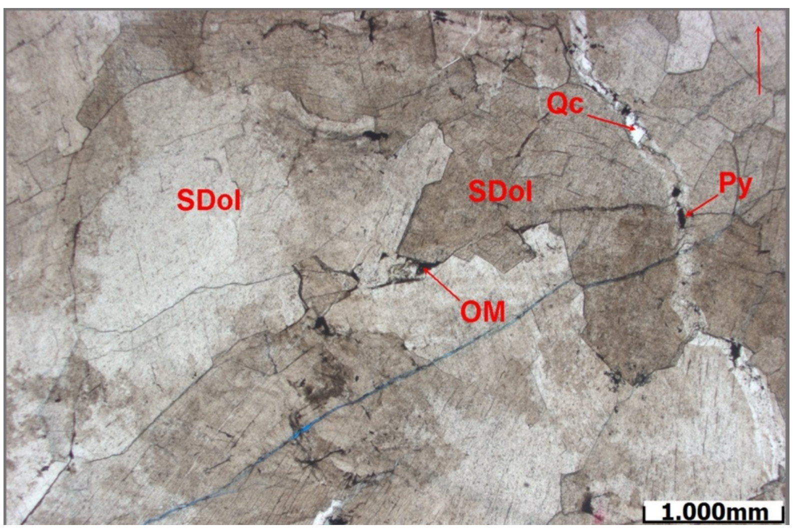

Figure 11.4. Sample T1, 10262.70ft/3128.07m. Alternate low magnification overview image of very coarse saddle dolomite (SDol). The right-hand side of the image shows a healed sub-vertical fracture along which apparent leaching of dolomite has occurred. Qc: quartz cement; Py: pyrite; OM: pore occluding organic matter.

x25 ppl

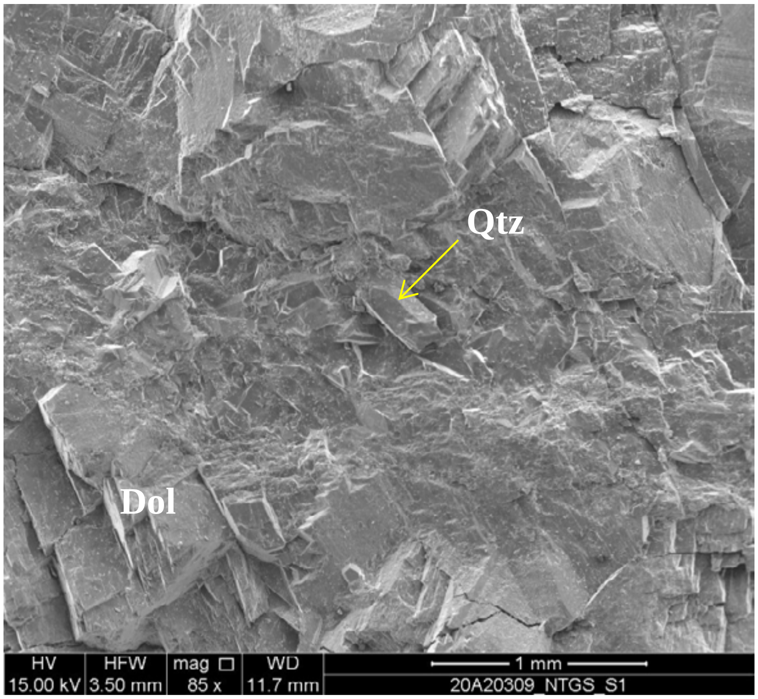

SEM Figure 11.5. Sample S1, 10262.70ft/3128.07m. Low magnification overview of the dolostone. The SEM micromount appears to have broken along a vuggy pore which is partially lined by euhedral authigenic quartz (Qtz) Dol: dolomite. **x85**

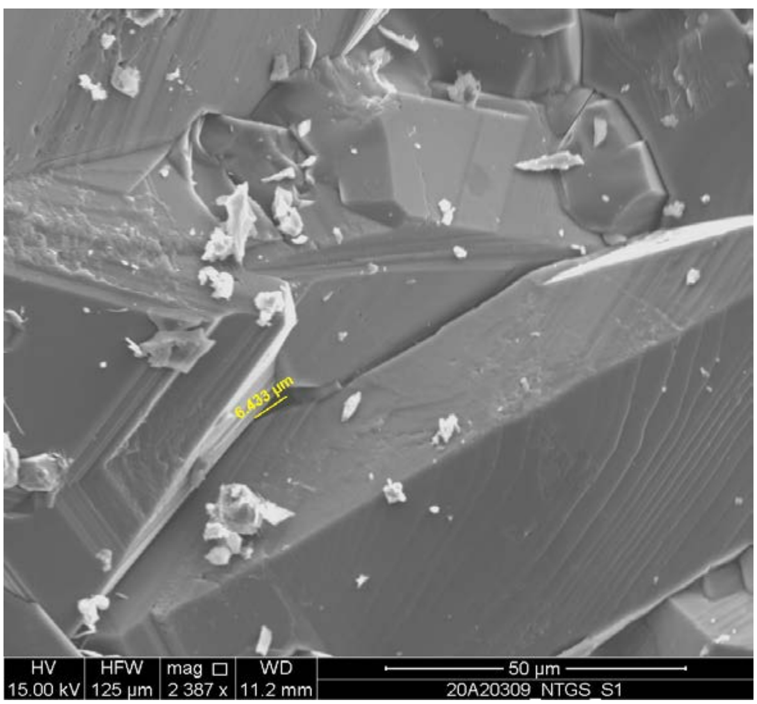

SEM Figure 11.6. Sample S1, 10262.70ft/3128.07m. High magnification image of a micropore associated with authigenic quartz which displays zoned crystal growth. **x2387**

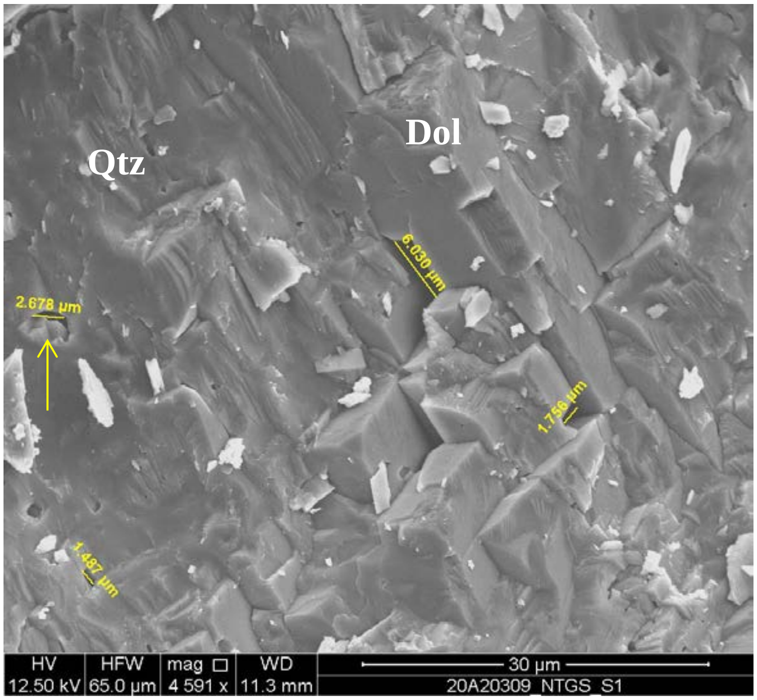

SEM Figure 11.7. Sample S1, 10262.70ft/3128.07m. SEM photomicrograph of the crystal boundary between quartz (Qtz) and dolomite (Dol). A rounded inclusion within the quartz (far left) shows subsequent crystal growth of rhombic dolomite crystals (yellow arrow). Micropores (<5µm) associated with the dolomite appear angular. **x4591**

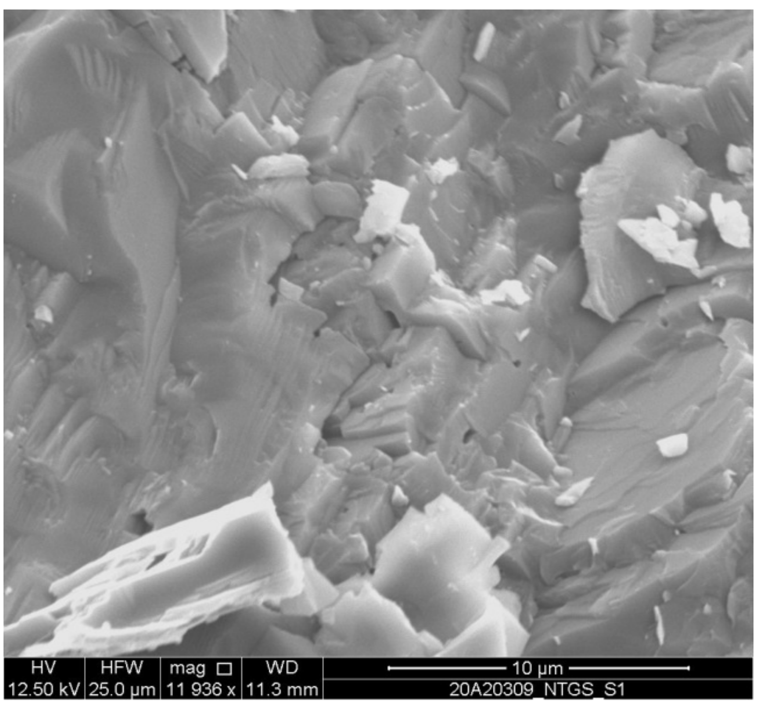

SEM Figure 11.8. Sample S1, 10262.70ft/3128.07m. High magnification view showing the presence of numerous submicron scattered pores. **x11936**

SUMMARY OF PORE SYSTEM, MAIN POROSITY CONTROLS AND RESERVOIR QUALITY

Porosity, permeability and overall reservoir quality of the observed samples from the study location can be function of various controls that includes depositional controls of grain size, sorting and mineralogy, and the diagenetic controls of compaction, dissolution and cementation.

Dolostone Samples T1 (10262.70ft) to T5 (10134.00ft)

Reservoir quality for these five samples ranges from poor to moderate and is mainly controlled by replacement texture (saddle dolomite) and the precipitation of secondary quartz cement. Compaction and pressure/solution (stylolites) are evident in these dolostones. Low amplitude stylolites are generally horizontal, while relatively high amplitude stylolites, in addition to cemented and partially open fracture systems, are generally subvertical to vertical.

Reservoir quality is considered to be poor for samples T3 (10191.50ft), T2 (10246.00ft) and T4 (10164.40ft) as they generally display only trace amounts of open fracture and intercrystalline porosity, while sample T2 also displays minor amounts of isolated microvuggy porosity (1%). Samples T1 (10262.70ft) and T5 (10134.00ft) are estimated to have moderate reservoir quality. In addition to trace to minor amounts of open fracture (trace to 1%) and intercrystalline (1%) porosity, these dolostones also display minor microvuggy porosity (2% to 5%); however, pore spaces in sample T1 have been predominately occluded by quartz cement and organic matter (probable bitumen). Please see the Petrographic Summary (Table 1B) in the appendix for details regarding mineralogy, texture and porosity.

Limestone Samples T6 (9799.00ft) to T9 (9745.75ft)

Visible porosity includes trace open fracture porosity in sample T8 (9761.50ft); therefore, overall reservoir quality is considered to be poor for these samples. The reservoir quality appears to be mainly controlled by depositional environment (i.e. abundance and distribution of micritic matrix and micritic framework grains), and to a lesser extent, by diagenetic events (compaction, precipitation of the framework sustaining cements). Stylolites, and cemented microfactures, are generally vertical to subvertical within these samples.

Intraparticle porosity and micro-fractures are locally filled with trace to minor amounts of calcite spar (trace to 2%) and pyrite (1% - T9 only). Trace dolomite cement also occludes intraparticle porosity in sample T8 (9761.50ft). Trace to minor amounts (trace to 2%) of pyrite replacement (carbonate grains, bioclast and matrix), along with minor calcite (2% to 5% - T6 and T7) and chert (2% - T9) replacement is also noted. Please see the Petrographic Summary (Table 1B) in the appendix for details regarding mineralogy, texture and porosity.

Shale Samples T10 (9627.60ft) to T11 (9609.75ft)

The two silty shale samples are massive to weakly laminated. Laminae are characterized by the parallel alignment of platy micas and elongate chert lenses. Subangular to subrounded framework grains are well sorted and range in size from clay-sized particles to very fine silt. Minor to moderate amounts of chert and dolomite, plus trace pyrite, locally replace matrix clays and minute framework grains. Dolomite is noted as very fine sub- to euhedral rhombs. Pyrite occurs as scattered irregular blebs or framboids. These sample lack visible porosity; therefore, overall reservoir quality is considered to be very poor. Please see the Petrographic Summary (Table 1B) in the appendix for details regarding mineralogy, texture and porosity.

The following table summarize the most important factors that control the reservoir quality of the eleven samples recovered from TEXACO BOVIE LAKE J-72 300/J-72-6020-12245/0 location.

Sample ID	Depth (ft)	Total Micrite /Matrix (%)	Total Cement (%)	Total Porosity (%)						Main Porosity controlling factors (*)	RQ(*)
				IP	Int.	Ixl	Mv	Fr	M		
Location: Texaco Bovie Lake J-72 300/J-72-6020-12245/0											
11	9609.75	68	20	-	-	-	-	-	-	C; Dc	VP
10	9627.60	62	29	-	-	-	-	-	-	C; Dc	VP
9	9745.75	15	3	-	-	-	-	-	-	Mic; Cc; Com	P
8	9761.50	80	1	-	-	-	-	TR	-	Mic; C; Py	P
7	9785.00	45	-	-	-	-	-	-	-	Mic; Cc; Com	P
6	9799.00	47	2	-	-	-	-	-	-	Mic; Cc; Com	P
5	10134.00	3	9	-	-	1	5	1	-	SDol; Qc; Py	M
4	10164.40	6	1	-	-	TR	-	TR	-	SDol; C; Dc; Qc; Com	P
3	10191.50	3	3	-	-	TR	-	TR	TR	SDol; Cc; C; Qc	P
2	10246.00	1	3	-	-	TR	TR	1	-	SDol; Qc; C; Mic	P
1	10262.70	3	5	-	-	1	2	TR	TR	SDol; Qc; C	M

Porosity value (%): **IP** – interparticle porosity; **Int** – intraparticle; **Ixl** – intercrystalline; **Mv** – micro-vuggy; **Fr** – fracture porosity; **M** – micro-intercrystalline porosity
Main Porosity controlling factors: **Com –** compaction**;** M**ic** – micrite (calcite or dolomite); **Ms** – micro- and/or pseudospar; **SDol** - saddle dolomite; **Cc** – calcite cement (druse and spar); **Dc** – dolomite cement**; Qc -** quartz cement; **C** – clays and organics; **Ov** – quartz overgrowths; **Py** – pyrite (replacement and/or cement); **F** – fabric: [**CC** – concavo-convex orthochem contacts; **S –** sutured orthochem contacts]
RQ (*) - reservoir quality: **VP –** very poor; **P –** poor; **M –** moderate; **G** - good

Reservoir problems for the samples recovered from the Nahanni Formation at the Texaco Bovie Lake J-72 300/J-72-6020-12245/0 location, may include the following: **(1)** Heterogeneity of the pore system, plus overall poor interconnectivity between pores could restrict the flow of hydrocarbons, **(2)** hydrochloric acid (HCl) treatment of this reservoir has the potential to loosen carbonate fines (dolo-micrite and calcite micrite) that could migrate and block pore throats, plus cause fabric collapse, **(3)** Sensitivity of calcium carbonate to hydrofluoric acid (HF) in regard to precipitation of calcium fluoride scales.

RFERENCES

Folk, R. L. (1974), Petrology of Sedimentary Rocks. Hemphills, Austin, Texas, USA.

Scholle, P.A. and Ulmer-Scholle, D.S. 2006. A Color Guide to the Petrography of Carbonate Rocks: Grains, Textures, Porosity, Diagenesis. AAPG Memoir 77. American Association of Petroleum Geologists, Tulsa, O.K.

Tucker, M. E. (1998). Sedimentary Petrology: An Introduction to the Origin of Sedimentary Rocks. Second Edition, Blackwell Science Ltd., Malden, Massachusetts.

Ulmer-Scholle, D.S., Scholle, P.A., Schieber, J. and Raine, R.J. 2014. A Color Guide to the Petrography of Sandstones, Siltstones, Shales and Associated Rocks. AAPG Memoir 109. American Association of Petroleum Geologists, Tulsa, O.K.

Welton, J.E. 2003. SEM Petrology Atlas. Methods in Exploration Series No. 4. American Association of Petroleum Geologists, Tulsa, O.K.

DATA TABLES

TABLE 1A
Petrographic Summary of Two Samples recovered from the Nahanni Formation at the Texaco Bovie Lake J-72 300/J-72-6020-12245/0 Location

Sample ID Depth (ft) Rock Type		T11 9609.75 Silty Sh	T10 9627.60 Silty Sh				
Quartz	*Monocrystalline*	7	6				
	Polycrystalline	-	-				
	Total	**7**	**6**				
Feldspar	*Potassium Feldspar*	-	-				
	Plagioclase	-	-				
	Total (or Fld not classified)	**TR**	**TR**				
Rock Fragments	*Chert*	-	-				
	Sedimentary Rock Fragments	-	-				
	Volcanic Rock Fragments	-	-				
	Metamorphic Rock Fragments	-	-				
	Plutonic Rock Fragments	-	-				
	Detrital Calcite	-	-				
	Detrital Dolomite	-	-				
	Total	**0**	**0**				
Accessories	*Mica*	5	3				
	Heavy Minerals	-	-				
	Glauconite	-	-				
	Carbonaceous detritus	-	-				
	Coated grains	-	-				
	Phosphate	-	-				
	Bioclast fragments	-	-				
	Total	**5**	**3**				
Matrix	*Detrital matrix(clay,silt,organics)*	68	62				
	Micrite (dolomite and calcite)	-	-				
	Total	**68**	**62**				
Authigenic Clays	*Kaolinite*	-	-				
	Illite	-	-				
	Chlorite	-	-				
	Smectite	-	-				
	Unidentified	-	-				
	Total	**0**	**0**				
Cements/ Replacement	*Chert*	14	2				
	Feldspar	-	-				
	Calcite	-	3				
	Ferroan Calcite	-	-				
	Dolomite	6	24				
	Ferroan Dolomite	-	-				
	Barite	-	-				
	Siderite	-	-				
	Pyrite	TR	TR				
	Residual Hydrocarbon/Bitumen	-	-				
	Total	**20**	**29**				
Total Rock Volume (%)		**100**	**100**				
Structures		Lm	Lm				
Textures	*Grain Size Average*	Clay	Clay				
	Grain Size Range	Clay-fSlt	Clay-fSlt				
	Sorting	W	W				
	Roundness	SA-SR	SA-SR				
Diagenesis	*Compaction*	X	X				
	Grain Fabric	M	M				
	Cementation	PCem	PCem				
	Dissolution	-	-				
Visible Porosity	*Intergranular*	-	-				
	Dissolution (unclassified)	-	-				
	Grain Dissolution	-	-				
	Cement Dissolution	-	-				
	Total Visible Porosity (%)	**0**	**0**				
Petrophysical Results	*Core Porosity (%)*	**N/A**	**N/A**				
	Gas Permeability (mD)	**N/A**	**N/A**				
Reservoir Quality		**VP**	**VP**				

Structures: **Mss**-massive, **Lm**-laminae; **Xlm**-cross laminae; **Xb**-cross bedded; **Bd**-bedded; **Bt**-bioturbated

Compaction: **X**-slightly; **XX**-moderately; **XXX**-highly

Grain Fabric: **G**-grain supported; **M**-matrix supported; **C**-cement supported; **P**-point contacts; **F**-flat contacts; **CC**-concavo-convex contacts; **S**-sutured contacts

Cementation: **Cem**-completely cemented; **NCem**-non-cemented; **PCem**-partly cemented

Dissolution: **Cor**-corroded surfaces; **GD**-grain dissolution; **GR**-grain replacement; **CCD**-complete cement dissolution; **SCD**-selective cement dissolution

Table 1B
Petrographic Summary of Eleven Samples recovered from the Nahanni Formation at the Texaco Bovie Lake J-72 300/J-72-6020-12245/0 Location

Sample ID		**T9**	**T8**	**T7**	**T6**	**T5**	**T4**
Depth (ft)		**9745.75**	**9761.50**	**9785.00**	**9799.00**	**10134.00**	**10164.40**
Rock Type		**LS**	**LS**	**LS**	**LS**	**DS**	**DS**
Mineralogy	*Calcite*	92	95	84	94	-	-
	Dolomite	-	-	-	-	87	93
	Anhydrite	-	-	-	-	-	-
	Quartz	-	-	-	TR	7	1
	Chert	2	-	-	-	-	-
	Pyrite and Heavy Minerals	1	2	1	1	3	TR
	Phosphate	-	-	-	-	-	-
	Clays & organics	5	3	15	5	3	6
Total Rock Volume (%)		**100**	**100**	**100**	**100**	**100**	**100**
Carbonate Clasts	*Peloids*	25	-	-	15	-	-
	Ooids	-	-	-	-	-	-
	Intraclasts/Oncolintes	-	-	-	-	3	-
	Total:	**25**	**0**	**0**	**15**	**3**	**0**
Bioclasts/Fauna	*Mollusks*	10	3	8	1	-	-
	Foraminifers	-	-	-	TR	-	-
	Brachiopod (shell & spines)	TR	5	3	-	-	-
	Bryozoa	TR	TR	-	3	-	-
	Corals	TR	1	-	-	-	-
	Sponge Spicules	-	TR	15	10	-	-
	Echinoderms/Crinoids	20	7	-	1	-	-
	Gastropods	-	-	1	-	-	-
	Ostracodes	-	1	-	TR	-	-
	Stromatoporoid	20	TR	5	10	-	-
	Unidentified	5	TR	20	5	-	-
	Total:	**55**	**17**	**52**	**30**	**0**	**0**
Detrital Grains and Other Non-Carbonate Grains	*Quartz*	-	-	-	TR	-	-
	Chert	-	-	-	-	-	-
	Heavy Mineral	-	-	-	-	-	-
	Total:	**0**	**0**	**0**	**TR**	**0**	**0**
Matrix	*Micrite (calcite or dolomite)*	10	77	30	42	-	-
	Micro- and pseudospar	-	-	-	-	-	-
	Clays & organics	5	3	15	5	3	6
	Sutured allochems	-	-	-	-	-	-
	Total:	**15**	**80**	**45**	**47**	**3**	**6**
Pore Filling Cement	*Calcite Spar*	2	1	TR	2	-	TR
	Calcite druse	-	-	-	-	-	-
	Dolomite	-	TR	-	-	-	1
	Ferroan Dolomite	-	-	-	-	-	-
	Quartz/Chert	-	-	-	-	7	1
	Pyrite	1	-	-	-	**2**	-
	Anhydrite	-	-	-	-	-	-
	Total:	**3**	**1**	**0**	**2**	**9**	**2**
Replacement	*Calcite*	-	-	2	5	-	-
	Dolomite	-	-	-	-	84	92
	Anhydrite	-	-	-	-	-	-
	Quartz/Chert	2	-	-	-	-	-
	Pyrite	TR	2	1	1	1	TR
	Total:	**2**	**2**	**3**	**6**	**85**	**92**
Total Rock Volume (%)		**100**	**100**	**100**	**100**	**100**	**100**
Crystal Texture (Matrix)		Anh	Anh	Anh	Anh	-	-
Crystal Texture (Cement)		Sub-Eu	Sub-Eu	Sub-Eu	Sub-Eu	Sub-Eu	Sub-Eu
Crystal Size (Dolomite)		-	-	-	-	Fxl-VCxl	Fxl-VCxl
Structure/Fabric		Frac	Frac	Styl; Frac	Styl: Frac	Styl; Frac	Styl; Frac
Ratio Matrix/Clasts (approximate)		1:6	5:1	7:3	1:1	-	-
Original Texture		PS	WS	PS	WS-PS	-	-
Porosity (%)	*Interparticle*	-	-	-	-	-	-
	Intraparticle	-	-	-	-	-	-
	Intercrystalline	-	-	-	-	1	TR
	Fracture	-	TR	-	-	1	TR
	Micro-Vuggy	-	-	-	-	5	-
	Micro- intercrystalline pores	-	-	-	-	-	-
	Total TS Porosity (%)	**0**	**TR**	**0**	**0**	**7**	**TR**
Petrophysical Results	*Core Porosity (%)*	**N/A**	**N/A**	**N/A**	**N/A**	**N/A**	**N/A**
	Core Permeability (mD)	**N/A**	**N/A**	**N/A**	**N/A**	**N/A**	**N/A**
Reservoir Quality		**P**	**P**	**P**	**P**	**M**	**P**

Table 1B (continued)
Petrographic Summary of Eleven Samples recovered from the Nahanni Formation at the Texaco Bovie Lake J-72 300/J-72-6020-12245/0 Location

Sample ID		**T3**	**T2**	**T1**			
Depth (ft)		**10191.50**	**10246.00**	**10262.70**			
Rock Type		**DS**	**DS**	**DS**			
Mineralogy	*Calcite*	3	-	-			
	Dolomite	94	95	92			
	Anhydrite	-	-	-			
	Quartz	TR	3	5			
	Chert	-	-	-			
	Pyrite and Heavy Minerals	-	1	TR			
	Phosphate	-	-	-			
	Clays & organics	3	1	3			
Total Rock Volume (%)		**100**	**100**	**100**			
Carbonate Clasts	*Peloids*	-	-	-			
	Ooids	-	-	-			
	Intraclasts/Oncolintes	-	-	-			
	Total:	**0**	**0**	**0**			
Bioclasts/Fauna	*Mollusks*	-	-	-			
	Foraminifers	-	-	-			
	Brachiopod (shell & spines)	-	-	-			
	Bryozoa	-	-	-			
	Corals	-	-	-			
	Sponge Spicules	-	-	-			
	Echinoderms/Crinoids	-	-	-			
	Gastropods	-	-	-			
	Ostracodes	-	-	-			
	Stromatoporoid	-	-	-			
	Unidentified	-	-	-			
	Total:	**0**	**0**	**0**			
Detrital Grains	*Quartz*	TR	-	-			
	Chert	-	-	-			
	Heavy Mineral	-	-	-			
	Total:	**TR**	**0**	**0**			
Matrix	*Micrite (calcite or dolomite)*	-	TR	-			
	Micro- and pseudospar	-	-	-			
	Clays & organics	3	1	3			
	Sutured allochems	-	-	-			
	Total:	**3**	**1**	**3**			
Pore Filling Cement	*Calcite Spar*	3	-	-			
	Calcite druse	-	-	-			
	Dolomite	-	-	TR			
	Ferroan Dolomite	-	-	-			
	Quartz/Chert	TR	3	5			
	Pyrite	-	-	-			
	Anhydrite	-	-	-			
	Total:	**3**	**3**	**5**			
Replacement	*Calcite*	-	-	-			
	Dolomite	94	95	92			
	Anhydrite	-	-	-			
	Quartz/Chert	-	-	-			
	Pyrite	-	1	TR			
	Total:	**94**	**96**	**92**			
Total Rock Volume (%)		**100**	**100**	**100**			
Crystal Texture (Matrix)		-	-	-			
Crystal Texture (Cement)		Sub	Sub-Eu	Sub-Eu			
Crystal Size (Dolomite)		Fxl-VCxl	Vfxl-VCxl	Fxl-VCxl			
Structure/Fabric		Frac; Styl	Styl; Frac	Styl; Frac			
Ratio Matrix/Clasts (approximate)		-	-	-			
Original Texture		-	-	-			
Porosity	*Interparticle*	-	-	-			
	Intraparticle	-	-	-			
	Intercrystalline	TR	TR	1			
	Fracture	TR	1	TR			
	Micro-Vuggy	-	TR	2			
	Micro- intercrystalline pores	TR	-	TR			
	Total TS Porosity (%)	**TR**	**1**	**3**			
Petrophysical Results	*Core Porosity (%)*	**N/A**	**N/A**	**N/A**			
	Gas Permeability (mD)	**N/A**	**N/A**	**N/A**			
Reservoir Quality		**P**	**P**	**M**			

LIST OF ABBREVIATIONS (CARBONATES)

SKELETAL GRAINS

Bry	-	BRYOZOAN
Ech	-	ECHINODERMS
Bra	-	BRACHIOPODS
Os	-	OSTRACODS
Cal	-	CALCISPHERES
Moll	-	MOLLUSKS
Plcy	-	PELECYPODS
Biv	-	BIVALVES
For	-	FORAMINIFERA
Strom	-	STROMATOPOROIDS
Cor	-	CORALS
Ga	-	GASTROPODS
Biocl	-	BIOCLASTS

OTHER GRAINS

Pel	-	PELOIDS
Ooi	-	OOIDS

ORIGINAL TEXTURE

GS	-	GRAINSTONE
PS	-	PACKSTONE
WS	-	WACKESTONE
MS	-	MUDSTONE
FS	-	FLOATSTONE
RS	-	RUDSTONE

CRYSTAL TEXTURE

Euh	-	EUHEDRAL
Sub	-	SUBHEDRAL
Anh	-	ANHEDRAL

CRYSTAL SIZE

Cxl	-	COARSE CRYSTALLINE
Mxl	-	MEDIUM CRYSTALLINE
Fxl	-	FINE CRYSTALLINE
Vfxl	-	VERY FINE CRYSTALLINE

CEMENT TYPES

Syn	-	SYNTAXIAL OVERGROWTHS
Blo	-	BLOCKY
Poik	-	POIKILOTOPIC
Dru	-	DRUSY
SD	-	SADDLE DOLOMITE
Lath	-	ANHYDRITE LATHS
Grm	-	GROUNDMASS
Iso	-	ISOPACHOUS RIMS
Spa	-	SPARITE

POROSITY TYPES

Mixl	-	MICRO-INTERCRYSTALLINE
Ixl	-	INTERCRYSTALLINE
Mo	-	BIOMOLDIC
mV	-	MICROVUGGY
mF	-	MICROFRACTURE
IG	-	INTERGRANULAR
IP	-	INTERPARTICLE
INTRP	-	INTRAPARTICLE

QUALITY

G	-	GOOD
M	-	MODERATE
P	-	POOR

Well Name: **Paramount et al. Liard M-25**
Well ID: **300/M-25-6030-12330/0**
NT WID # **N1867**

Table 2: Results of quantitative mineral analysis (relative weight %) of X-ray diffraction data for 3 (three) samples using Rietveld method

Geology ID	Depth (ft)	Depth (m)	Core & Box #	NTGS Sample Type & #	**Calcite**	**Dolomite**	**Quartz**	**Plagioclase feldspar**	**Pyrite**	**Total**
1	11024.6063	3360.30	2 & 4 of 5 R	X34 , P6	2.1	95.2	1.8	0.8	0.1	100
2	11138.45144	3395.00	2 & 3 of 5 L	X33, P5	0.4	96.1	2.9	0.6		100
3	11327.09974	3452.50	2 & 1 of 5 L	X32, P3	0.4	97.7	1.4	0.5		100

AGAT Laboratories